River Catchments to Coastal Seas: N_2O and CH_4 Variability and Insights for Ecosystem Restoration

by

Jasmin Dorinda Urwick

A thesis submitted in partial fulfilment of the degree of
Doctor of Philosophy

School of Environmental Sciences
University of East Anglia

June 2025

In collaboration with

Plymouth Marine Laboratory

Abstract

Limiting greenhouse gas emissions is of global importance to address the climate and biodiversity crises. Aquatic ecosystems include some of the world's most threatened habitats, making them a priority for ecological restoration efforts. They are also a significant source of methane and nitrous oxide, the second and third most potent greenhouse gases. Ecosystem managers now face the challenge of balancing the need for habitat restoration and biodiversity recovery with limiting exacerbations to emissions of greenhouse gases. In this thesis I broadly set out to investigate the variability of methane and nitrous oxide found in the surface waters of rivers, estuaries and coastal waters, and to understand how ecosystem restoration through nature-based solutions stands to influence this variability. I first review the major biological pathways of methane and nitrous oxide and identify knowledge gaps preventing a clear understanding of the effects of nature-based solutions on greenhouse gas emissions (Chapter 1). Next, I examine the methods used to estimate air-water fluxes of greenhouse gases by comparing several commonly used empirical models to estimate gas transfer velocity (Chapter 2), which informed the use of these models during a river-to-coast investigation of the River Tamar to identify opportunities for nature-based solutions (Chapter 3). This leads on to a detailed case study of an intertidal wetland restoration project in the Tamar Estuary, where I investigated the contribution of the wetland to methane and nitrous oxide export to the connected estuary (Chapter 4). This thesis adds to the growing body of knowledge that accounting for methane and nitrous oxide complicates the effectiveness of nature-based solutions to climate change mitigation. This work concludes with a call for increased guidance and evidence-driven target setting to ensure ecosystem managers are adequately supported in the spatial planning of nature-based solutions whilst simultaneously working towards global biodiversity and climate change commitments.

Contents

List of Figures

List of Tables

Acknowledgements

They say it takes a village to raise a PhD student. In my case, I have Britain's Ocean City of Plymouth, a few small Canadian mountain towns, and an incredible support network across the world to thank for encouraging me throughout my PhD.

I'd first like to thank my supervisory team; Prof. Andy Rees, Prof. Jan Kaiser, Dr. Vassilis Kitidis and Garry Armstrong. Thank you all for your trust and guidance throughout this project and for sharing with me your expertise. I would particularly like to acknowledge the incredible support of my primary supervisor, Prof. Andy Rees, and Ruth Airs, who prioritised my wellbeing above all else so that I could continue to tell this story. I am a better scientist for it and am immensely grateful for their support.

Thank you to Dr. Sarah Breimann for inspiring me with creative solutions in the lab and making me smile even on the toughest days. Thank you to Ian Brown for sharing his data and letting me pinch his N_2O standards. To the LOCATE and AgZero+ field crew; Sarah, Glen, Ian, Vas, Andy, Malc, Bethany, Lucinda. I have the fondest memories of the Tamar thanks to you all, including being caked in mud at Calstock Wetland, enjoying the views across the Tamar valley on Hinterland days, and exploring the Tamar Estuary. Thank you to Aser Mata and Will Jay for teaching me to fly drones and enlightening me on the possibilities of spatial data.

To the incredible student community at PML; Shauna, Ollie, Guy, Hayley, Simone, Emily, Charlotte, Lily Anna, Natalie, Chris, George and Hannah. Thank you for making me laugh over many needed cups of tea and inspiring me with your own passions for protecting the magical waters we've had the opportunity to work in. Ollie, thank you for being there during challenging lab days and sharing in the joy of working with carbon and nitrogen. Shauna, thank you for being there for PhD and general life advice, even when I moved halfway across the world.

Thank you to the Quest team for taking me out to the Western Channel Observatory. That is a privilege I will never take for granted. Thank you to the common dolphins who consistently made an appearance and to the salty sea air that helped me ruminate over many scientific conundrums.

To the wider community of brilliant scientists at PML who shared their work with me and offered advice when I needed it. I gained so much inspiration from you all. Thank you to everyone who invited me to play volleyball in the sunshine. I would particularly like to share my gratitude to a very missed colleague, Prof. Paul Somerfield, who was one of the first scientists I met at PML. He always offered words of kindness, as well as helping me be less afraid of stats. I feel very fortunate to have known him.

To the swim community of Firestone Bay, it is hard to put into words how grateful I am for you all. Thank you for the sunrise swims before long days in the lab and fieldwork. Thank you for listening to my dilemmas and offering words of wisdom that I will carry with me forever. Heather, Cords, thank you for making Plymouth mean what it does to me. What a gift it was to end up swimming in the same waters as you.

To my ecology OGs, Jen, Grace and Cam, for being wonderful humans whose friendship I am very grateful for. To the incredible community of Fernie, who have welcomed me with open arms and taught me so much about the climate change impacts on mountain communities. To everyone who gave me a break from thesis writing by inviting me out to go birdwatching, biking or hiking - thank you!

And, of course, thank you to my family. To my Mum and my Dad for gifting me with a curious mind and for being my first teachers about the awe and wonders to be found in nature. To Wendle, for making sure I took good care of myself and never gave up on what made me happy. To my sisters, Rosanna and Sapphire, for always lifting me up and celebrating every obstacle overcome. To my brothers-in-law, Cyril and James, for being there whenever I needed them. To my nephews, Fabian and Theodore, for reminding me of the future we are fighting for. To my Bethany, for inspiring me and challenging me to never limit my ambitions ever since we were 11

years old. And finally, but certainly not least, Matt. Thank you for reminding me of what was most important, for teaching me new perspectives on life, filling my days with adventure, welcoming me into your beautiful family, and supporting me to be brave in all walks of life. Your love and friendship have made me believe anything is possible.

Funding and collaborators

This work was supported by the Natural Environment Research Council (NERC) and the ARIES Doctoral Training Partnership [grant number NE/S007334/1], Plymouth Marine Laboratory and the University of East Anglia. I am grateful for the support and training provided by Sercon Ltd. through the NERC CASE Studentship Award. This work was also made possible through the LOCATE (NERC Award: NE/N018087/1) and AgZero+ projects (NERC Award: NE/W005050/1). I would like to thank the Plymouth Marine Science & Education Foundation (PlyMSEF) for awarding me Grant-in-Aid which supported invaluable learning opportunities during my PhD.

Data contributions

Sample analyses for dissolved nitrous oxide (N_2O) and methane (CH_4) were conducted by Ian Brown and analyses for nutrients were conducted by E. Malcolm S. Woodward at Plymouth Marine Laboratory. I gratefully acknowledge their contributions to this thesis.

“The final chapter is ours to write. We know what we need to do.
What happens next is up to us.”
- *David Attenborough*

Chapter 1: Introduction

1.1 A brief introduction to greenhouse gas emission reduction targets

The future of the planet will be determined by our ability to turn the tide on the climate and biodiversity crises. Global temperatures are expected to exceed an increase of 1.5 °C by 2035, with the effects of this warming already being experienced disproportionately around the world (Calvin *et al.,* 2023). Urgent action is needed to reduce greenhouse gas (GHG) emissions if we are to prevent global warming beyond 2.5 °C by 2100 and avoid crossing thresholds of positive climate feedback loops (Armstrong McKay *et al.,* 2022). After carbon dioxide (CO_2), methane (CH_4) and nitrous oxide (N_2O) are the second and third most potent GHGs with a respective lifespan of 9 ± 0.9 years and 116 ± 9 years (Prather *et al.,* 2015, 2012). Despite their comparatively shorter lifespans, the global warming potentials (GWP) of CH_4 and N_2O were most recently estimated to be 27 and 273 times higher than CO_2, respectively, over a 100-year time horizon (Calvin *et al.,* 2023). Atmospheric concentrations of CH_4 and N_2O have maintained an increasing trend since monitoring began (Lan *et al.,* 2025), except for brief stabilisation periods of CH_4 growth rates in the early 1990s (Dlugokencky *et al.,* 1998) and the 2000s (Nisbet *et al.,* 2016) (Figure 1.1). In addition to their contributions to global climate change, the increasing concentrations of both gases also present substantial threats to human health. Rising CH_4 concentrations lead to reduced oxidation capacity of the atmosphere and increased tropospheric ozone concentrations through the reaction with hydroxyl radicals, overall increasing the presence of atmospheric pollutants (Saunois *et al.,* 2024a; Zhao *et al.,* 2019). N_2O is a major contributor to the depletion of the stratospheric ozone layer, increasing risk of skin damage through increased UV radiation exposure (Ravishankara *et al.,* 2009). However, our growing understanding of these gases has presented opportunities to slow increasing global mean surface temperatures through targeted solutions to reduce CH_4 and N_2O emissions, securing the

possibility of a world rich in biodiversity and protecting future generations from the impacts of climate change.

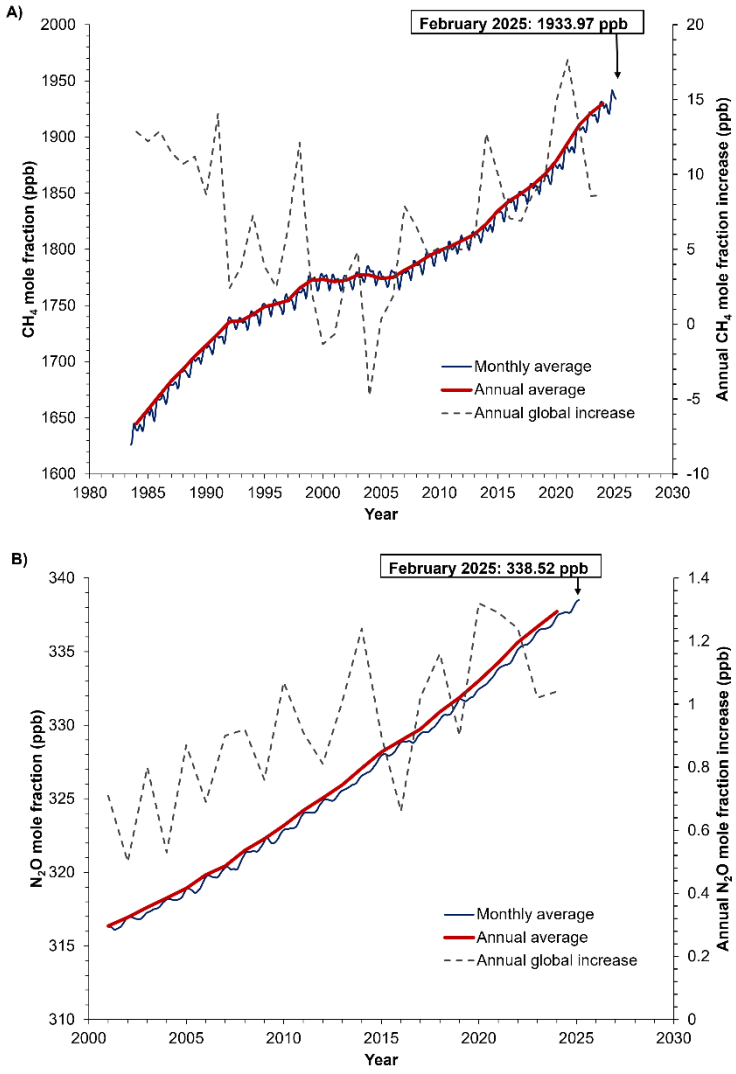

Figure 1.1. Globally averaged annual and monthly mean atmospheric methane (A) and nitrous oxide (B) abundance determined from marine surface sites by the Global Monitoring Division of NOAA's Earth System Research Laboratory time-series starting in 1983. Atmospheric concentrations are expressed as parts per billion (ppb). Data source: Lan *et al.,* (2022)

Emissions of CH_4 and N_2O are governed by complex microbial processes which could be limited by the availability of carbon (C), nitrogen (N), phosphorus (P) or oxygen (O). These processes are explained in detail later in this chapter. The atmospheric increase of both gases has been attributed to the increased burning of fossil fuels since the industrial revolution in the late 18th Century, and more recently to habitat degradation and land reclamation for agricultural purposes, and perturbations to nutrient cycles through applications of manure and synthetic fertilisers (Davidson, 2009; Magazzino *et al.,* 2024; Saunois *et al.,* 2020a; W. Tian *et al.,* 2019). Until recently, most scientific and political attention, and therefore environmental management practices, has been focused on CO_2 emissions, with concepts such as 'carbon footprint' becoming an incentive for reducing public and private sector CO_2 emissions. However, owing to the wealth of knowledge shared largely through the International Panel on Climate Change (IPCC) Reports, the importance of CH_4 and N_2O emissions, including those from natural sources, are now becoming more widely recognised both in scientific literature and policy (Figure 1.2).

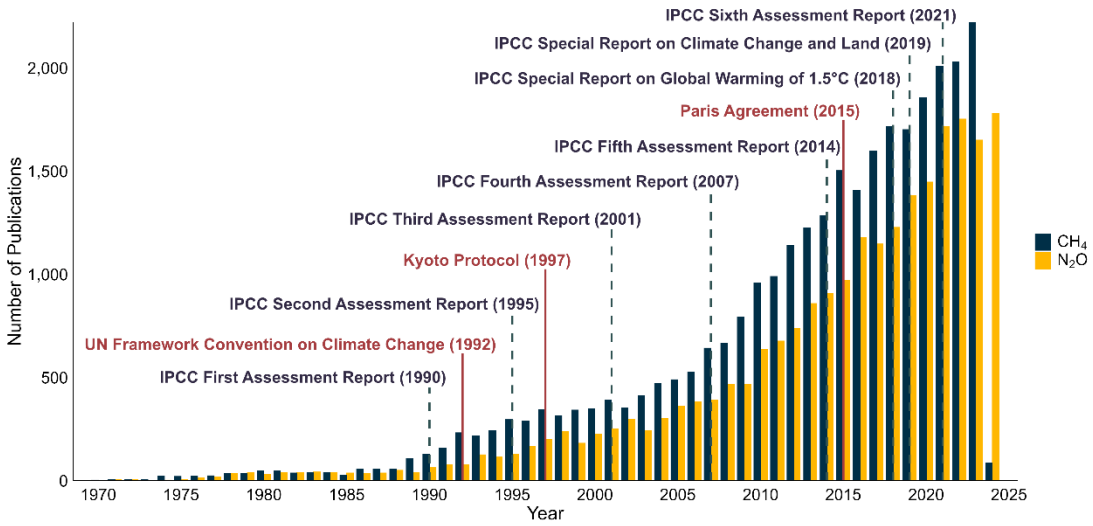

Figure 1.2 Number of publications related to nitrous oxide (N_2O) and methane (CH_4) in aquatic ecosystems per year between 1970 and 2024. Results from search on Web of Science. Search criteria provided in Appendix A. Blue dashed lines indicate dates of key global IPCC reports and red lines indicate key international agreements

In 1990, the IPCC published the First Assessment Report (FAR), presenting the most up to date scientific evidence and global understanding of climate change at the time. This report summarised the influence of human activities on the climate, urging the scientific community to increase efforts towards quantifying emissions of GHG. The FAR was the first major catalyst for global cooperation and political strategies to tackle climate change. It was shortly followed by the United Nations (UN) Framework Convention on Climate Change in 1992, which was further implemented by the Kyoto Protocol in 1997 and the Paris Agreement in 2015. Specific guidelines on reporting GHG inventories have also been published, including the '2013 Supplement to the 2006 IPCC Guidelines for National Greenhouse Gas Inventories: Wetlands' and the '2019 Refinement to the 2006 IPCC Guidelines for National Greenhouse Gas Inventories'. These international agreements and reports have informed formalised global commitments to country-specific GHG emission reduction targets towards Net-Zero, and near-term strategies known as Nationally Determined Contributions (NDCs) (Smith *et al.,* 2024). In the UK's case, the NDCs aim to reduce all GHG emissions by at least 81 % by 2035 compared to levels in 1990 (UK Government, 2025). At the time of writing this thesis, the UK has 10 years remaining to meet this target, however most existing strategies are generally considered insufficient to achieve this due to lags between research and its application via evidence-based targeted mitigation measures (Anderson *et al.,* 2019; Smith *et al.,* 2024).

1.2 Balancing climate change mitigation with ecological restoration

Alongside reducing GHG emissions, we are also challenged with restoring lost global biodiversity. Advances in long-term environmental monitoring, satellite imagery and remote sensing capabilities has allowed for impressive, and deeply concerning, quantifications of global and regional biodiversity decline caused by the exploitation of natural resources and the extent of habitat replaced by expansive transport networks, energy production, urbanisation and agriculture (Fluet-Chouinard *et al.,* 2023; Liu

et al., 2025). Aquatic ecosystems are particularly vulnerable to human activities and the increasing occurrence of extreme weather due to climate change (Belletti *et al.,* 2020; Bidlack *et al.,* 2021; Murray *et al.,* 2022). The Intergovernmental Science-Policy Platform on Biodiversity and Ecosystem Services (IPBES) Global Assessment 2019 Report published alarming statistics including 75 % of the world's available freshwater sources are devoted to crop and livestock production, 80 % of global wastewater is released into the environment untreated, and only 13 % of the wetlands present in 1700 remained in 2000 (Díaz *et al.,* 2019). At a regional scale, the UK State of Nature 2023 Report highlighted that in the last decade, the UK has failed to improve beyond 36 % of lakes, rivers and estuaries meeting good ecological status (GES) under the Water Framework Directive (WFD) and less than 50 % of UK saltmarsh is in good ecological condition (Burns *et al.,* 2023).

In December 2022, the Convention on Biological Diversity (CBD) COP15 Summit presented the Kunming-Montreal Global Biodiversity Framework, which sets out 23 global biodiversity targets to be achieved by 2030. This includes restoring 30 % of all degraded ecosystems (Target 2), conserving 30 % of land, water and seas (Target 3), and minimizing the impacts of climate change on biodiversity and building resilience (Target 8) (Convention on Biological Diversity, 2022). These targets are further bolstered by specific actions required by the United Nations (UN) Sustainable Development Goals (SDGs), namely Climate Action (Goal 13), Life Below Water (Goal 14) and Life on Land (Goal 15) (Brooks *et al.,* 2015). In the UK, progress towards these targets are being driven by the Nature Recovery Network, underpinned by the Environment Act 2021 and Environmental Improvement Plan 2023, which commits to restoring or creating 140,000 hectares of wildlife-rich habitat outside of protected sites by 2028 compared to 2022, and restoring 75 % of terrestrial and freshwater protected sites to favourable condition by 2042 (UK Gov, 2024).

To complicate matters, aquatic ecosystems are also an important source of CH_4 and N_2O (Saunois *et al.,* 2024a; Tian *et al.,* 2024). Our management, and restoration, of them must therefore carefully avoid tipping the fine balance between aquatic systems acting as a GHG source or a GHG sink. However, there is a long way to go to implement specific management guidelines or environmental frameworks which address this issue. Within reports on climate change, biodiversity and the UK NDCs, there is seldom recognition of the complex interdependencies between ecosystem health, habitat restoration, and emissions of GHG from natural sources. Whilst the IPBES report does highlight a data deficiency on the impacts of increasing CO_2 upon marine ecosystem functioning, there is no mention of CH_4 or N_2O. The UK State of Nature Report quotes a reduction in agricultural soil N_2O emissions in a case study of biodiversity restoration and refers to C sequestration benefits of saltmarsh restoration, but there is no mention of the impacts on N_2O or CH_4 emissions. Traditional approaches to environmental management and policy require improvement to better integrate terrestrial and aquatic management practices if we are to balance GHG reduction and biodiversity objectives. We must take opportunities to translate the latest scientific advances in GHG budgeting into major reports which are influencing conservation targets and strategies. Without this, we could potentially under- or overestimate the effectiveness of nature recovery towards slowing climate change.

1.3 Nature-based Solutions (NbS) to climate change

In the last two decades there has been a rapid adoption of nature-based solutions (NbS) and ecosystem-based approaches to both halt biodiversity declines and achieve Net-Zero emission targets, although there is debate over the effectiveness of NbS in providing long-term climate benefits (Fankhauser *et al.,* 2022; Girardin *et al.,* 2021). NbS often involve the restoration or creation of lost habitats to reinstate depleted or entirely lost ecosystem services (ES) (Nesshöver *et al.,* 2017; Williams *et al.,* 2020). In 2021, two major reports on NbS to climate change in the UK were compiled

to identify best management practices for reducing GHG emissions from natural sources (Stafford *et al.,* 2021; Thom and Doar, 2021). Both reports provide valuable insights to management measures that can be adopted to simultaneously restore biodiversity and halt GHG emissions that are exacerbated by human activity. Focusing on aquatic ecosystems, these NbS may include the restoration or rewetting of wetlands, such as peatlands (Evans *et al.,* 2021) and saltmarshes (Cadier *et al.,* 2023; Temmink *et al.,* 2022), planting of seagrass meadows (Needelman *et al.,* 2018), and reintroduction of species referred to as ecosystem engineers, such as European beaver (*Castor fiber*) (Brazier *et al.,* 2021; Puttock *et al.,* 2021). Restoring ecosystem functioning and alleviating environmental stressors from human activities can prevent aquatic ecosystems from deteriorating to the point they become large emitters of GHG (Evans *et al.,* 2021; Zou *et al.,* 2022). For example, Stutter *et al.,* (2018) explore the potential of reconnecting rivers with wetlands and riparian forests to achieve stoichiometric rebalancing, whereby C:N:P ratios are altered by changing the transport of organic C, to prevent eutrophication, improve water quality and restore overall aquatic ecosystem health. Plankton and microbial community shifts following lake restoration have also been shown to eventually reduce GHG emissions associated with eutrophication due to a reduced abundance of organic matter decomposers and an increased abundance of autotrophs (He *et al.,* 2025). However, a lack of in-situ measurements of GHGs in natural systems, particularly in rivers and restored wetlands, limit our full understanding of how long-term changes in climate, land use, human populations and restoration schemes may alter the N_2O and CH_4 from each habitat type.

1.4 The uncertainty of natural capital and carbon credits

Detailed evaluations of the earth's ES have been completed to understand the importance of ecological integrity and habitat connectivity to climate change resilience, such as the Millennium Ecosystem Assessment (2005) and the UK National Ecosystem Assessment (2011). This has supported

political and financial incentives termed ‘natural capital’ or ‘carbon credits’ which aim to attract private investment in nature recovery (Costanza *et al.,* 1997; Smith *et al.,* 2022). However, as GHG budgeting from natural sources improves, there is increasing variability within reported emissions of CH_4 and N_2O following NbS interventions, calling into question the effectiveness of natural capital and carbon crediting schemes in tackling climate change (Bastviken *et al.,* 2011; Rosentreter *et al.,* 2021a; Zou *et al.,* 2022). From the perspective of restoration ecology, it is increasingly evident that there may be a trade-off between NbS measures which best support biodiversity recovery and those which will most effectively reduce GHG emissions, particularly in the case of wetland restoration (Rosentreter *et al.,* 2021a). There is an important emerging conversation about the risk of relying heavily on NbS to restore the provision of ES whilst working towards Net Zero, with large uncertainties over the longevity of C storage and the potential benefits offset by enhanced CH_4 and N_2O emissions following ecological restoration (Rosentreter *et al.,* 2021a). As we gather more evidence, there is a need to better integrate the agendas between biodiversity restoration and climate change mitigation to avoid misrepresenting the contribution of carbon crediting or natural capital schemes towards meeting Net Zero (Arias-Ortiz *et al.,* 2021).

1.5 Introducing the Land to Ocean Aquatic Continuum (LOAC)

The Land to Ocean Aquatic Continuum (LOAC) refers to the hydrologically and biogeochemically connected series of aquatic systems, linking terrestrial and marine ecosystems (Figure 1.3) (Beusen *et al.,* 2022; Regnier *et al.,* 2022; Wurtsbaugh *et al.,* 2019; Xenopoulos *et al.,* 2017). Improvements to knowledge sharing across scientific disciplines have enabled substantial strides towards a holistic approach to ecosystem management across the LOAC, with freshwater studies providing important insights for coastal and marine systems (Hessen and Kaartvedt, 2014; Xenopoulos *et al.,* 2017). However, a remaining challenge is to address how human development has drastically altered the hydrological connectivity of

habitats along the LOAC. A global assessment of 12 million km of rivers found only 23 % had capacity to flow uninterrupted to the ocean (Grill *et al.,* 2019). Belletti *et al.,* (2020) warn about the severe impacts caused by even relatively small barriers (> 2 m in height) to natural river flow regimes after identifying at least 1.2 million instream barriers in rivers across 36 European countries. In England, over 65 % of floodplains are devoted to intensive agriculture, representing the loss of ecologically important fen, marsh, swamp and bog wetland habitats (Entwistle *et al.,* 2019).

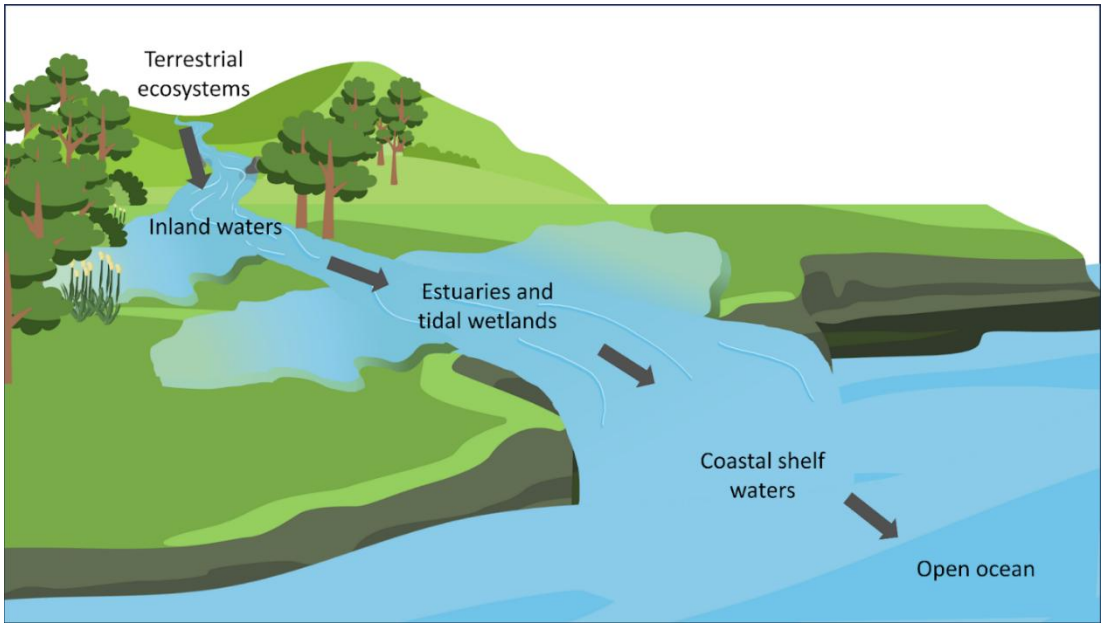

Figure 1.3. Schematic illustrating the connectivity of aquatic ecosystems along the Land to Ocean Aquatic Continuum (LOAC)

Rivers serve as the direct link between terrestrial and marine habitats. Changes to the transfer and transformation of organic matter and nutrients between lakes, streams, rivers, wetlands, estuaries, coastal waters and oceans can therefore have drastic consequences to biogeochemical cycling of GHG at scales from local to global magnitude (Poff *et al.,* 1997; Pringle, 2003). Human perturbations to the exchange of C and nutrients across the LOAC have been estimated to increase the lateral C flux from land to ocean

by 1.0 Pg C yr^{-1} since the pre-industrial era (Regnier *et al.,* 2013). By considering the aquatic continuum as one and characterising the interactions between freshwater and coastal systems, improvements have been made in understanding the transformation of organic material into CO_2 and better constraining the outgassing of GHG from surface waters (Drake *et al.,* 2018; Mwanake *et al.,* 2023a; Ward *et al.,* 2017). For example, Marcé *et al.,* (2019) identify potentially underrepresented fluxes of atmospheric C from inland waters which experience dry phases, such as ephemeral or intermittent streams and seasonally dry reservoirs, noting the importance of abstraction and water level management to CO_2 emissions. Huggett *et al.,* (2021a, 2021b) demonstrate that river flows as low as 2.5 m^3 s^{-1} increase the flushing times of shallow estuaries and increase their vulnerability to water quality deterioration by allowing the accumulation of nutrients and plankton communities, leading to an increased susceptibility to GHG producing phenomena such as eutrophication. These findings need to be considered when developing aquatic ecosystems management plans and identifying opportunities for NbS which balance restoring biodiversity and mitigating GHG emissions. Meeting the climate and biodiversity targets defined by international agreements, legislation and policy frameworks will require a robust transdisciplinary understanding of the complexities between biogeochemical cycling of GHG and ecological integrity along the LOAC. The remainder of this chapter will introduce the major biological pathways of CH_4 and N_2O cycling in aquatic ecosystems, focusing on rivers, wetlands, estuaries and coastal waters. The literature reviewed enables a better understanding of the role of NbS in tackling issues of water quality, nutrient management, biodiversity restoration and subsequently emissions of CH_4 and N_2O from aquatic ecosystems. The remaining structure of this thesis is defined in section 1.8.

1.6 Methane pathways

Responsible for 23 % of warming induced by long-lived GHGs, CH_4 reduces the oxidising capacity of the atmosphere and increases tropospheric ozone concentrations by reacting with hydroxyl radicals (Tian *et al.,* 2019). Sources of atmospheric CH_4 can be placed into three main categories: biogenic, thermogenic and pyrogenic (Figure 1.4). Here we will focus on biogenic sources. The discovery of a unique group of anaerobic archaebacteria named methanogens led to significant advances in the understanding of CH_4 production pathways. Methanogens are found in anoxic conditions such as aquatic sediments, waterlogged soils, the gastrointestinal tract of animals and sewage systems, and can withstand extremes in temperature, hypersalinity and pH (Capelle, 2016; Cicerone and Oremland, 1988; O'Neill, 1998). Methanogens, and therefore the production of CH_4 through methanogenesis, relies on complex microbial interactions to provide available substrates to feed on, such as methylamines, dimethysulphide and methanol. These interactions can be competitive or symbiotic and play a key role in the development of aquatic ecosystems. Considering the anoxic conditions favoured by methanogens, the presence of CH_4 in oxic environments has been a key interest of research. Feeding experiments have shown that anaerobic microniches within the digestive tracts of zooplankton feeding on phytoplankton provide ideal conditions for methanogen activity and can make a significant contribution to the CH_4 concentrations found in oxic oceanic subsurface waters (de Angelis and Lee, 1994). CH_4 producing bacteria have also been shown to be present in the gastrointestinal tract of some marine fish species (Oremland, 1979).

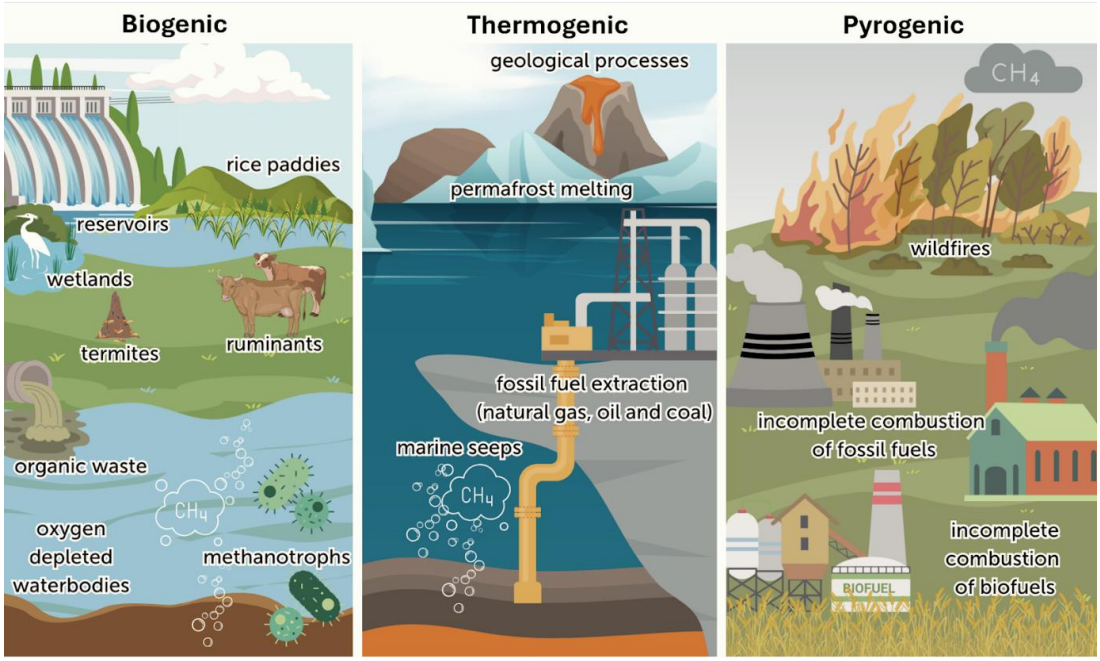

Figure 1.4. Schematic showing the methane sources broadly grouped into three categories: biogenic (microbial), thermogenic, and pyrogenic based on descriptions by the NOAA Global Monitoring Laboratory

An estimated 85 % of atmospheric CH_4 molecules are removed by oxidation in the troposphere during a reaction with the hydroxyl radical HO*, eventually leading to the production of CO_2 and H_2O (Cicerone and Oremland, 1988; O'Neill, 1998). The oxidation of CH_4 involves five key intermediates (CH_3, CH_3O_2, CH_3O, CH_2O, and HCO) and is affected by the presence of O(1D), Cl, NO, NO_2, HO_2, and O_2 (Dlugokencky *et al.,* 1994). In soils and sediments, CH_4 is removed by methanotrophs, a group of microbes which can use CH_4 as a source of C and energy to produce CO_2 and H_2O in oxic conditions (aerobic methanotrophy) and utilise CH_4 as an electron acceptor in anoxic conditions (anaerobic methane oxidation (AMO)) (Yang *et al.,* 2021). By tracing isotopic enrichment of ^{13}C, Gauci *et al.,* (2024) found methanotrophic bacteria on tree surfaces in the Amazonian floodplains are also important for atmospheric CH_4 oxidation, particularly during extreme dry seasons. Methanotrophs therefore play a major role in mitigating CH_4 sources in a range of habitat types, though there remains uncertainty in precise estimates of how much methanotrophy mitigates CH_4 production from methanogenesis. Even after CH_4 has been removed from

the atmosphere, a radiative effect continues through the production of CO_2 and H_2O which are both GHG. Increasing concentrations of CH_4 and other pollutants also increases the competition for HO* which reduces the oxidative capacity of the atmosphere and hinders its ability to process other pollutants (O'Neill, 1998).

Global anthropogenic emissions of CH_4 for the 2010 – 2019 decade are estimated at 369 Tg CH_4 yr^{-1} (Saunois *et al.,* 2024b), but, as shown in Figure 1.1, the growth rate in CH_4 emissions has not been constant. Between the industrial revolution and the 1970s, Etheridge *et al.,* (1992) reported an increase in CH_4 emission rates of 14 ppb yr^{-1}, with the exception of years 1920-1945 when growth rates stabilised at approximately 5 ppb yr^{-1}. Dlugokencky *et al.,* (1998) reported another stable period with little to no increase in CH_4 emissions between 1984 to 1996. However, CH_4 emissions began rising again in 2007 with a particularly strong growth in 2014 of 12.5 ± 0.4 ppb across all latitudes, especially in the equatorial belt (Nisbet *et al.,* 2016). Saunois *et al.,* (2020b) presented an estimated mean annual total emission between 2008 – 2017 29 Tg CH_4 yr^{-1} larger than the previous decade (2009- 2012) and 24 Tg CH_4 yr^{-1} larger than 2003-2012. It has been suggested that due to its relatively short lifespan, reducing emissions of CH_4 can have rapid results in limiting global warming and preventing adverse effects of climate change (Shindell *et al.,* 2012).

Whilst the instability of atmospheric CH_4 concentrations and growth rates has presented challenges in reviewing the global budget, more recent publications have improved estimates with the inclusion of complex biogeochemical cycling in both natural ecosystem processes and human activities (Saunois *et al.,* 2024a). However, large uncertainties persist in the temporal and seasonal variation in CH_4 sources and sinks. Saunois *et al.,* (2024a) report relative uncertainties of 20 % - 35 % for anthropogenic emissions (agriculture, waste and burning of fossil fuels), 50 % for biomass burning and natural wetlands, and as high as 100 % for other natural

sources such as inland waters and geological sources. Approximately 40 % of global CH_4 emissions are from natural sources, but work remains to fully understand how ecosystem management can influence the microbial processes which govern CH_4 cycling and the relative contributions of aquatic ecosystems to the global C budget.

1.6.1 Methane in rivers, wetlands and estuaries

The most recent budgeting exercise reported that of the global total natural and indirect sources of CH_4 (305 [108-44] Tg yr^{-1}) between 2000 to 2009, 50 % were from wetlands (153 [116 – 189] Tg yr^{-1}), and 36 % from inland waters (112 [49 – 202] Tg yr^{-1}), minus double counting (-23 [-9 to -36] Tg yr^{-1}) (Saunois *et al.,* 2024a). There has been a high degree of variability in CH_4 emissions reported in rivers and estuaries over recent decades. Stanley *et al.,* (2015) report most fluvial systems to be supersaturated with CH_4, with an annual global emission of 26.8 Tg yr^{-1} equivalent to 15 % of wetland and 40 % lake fluxes. This contrasts with the study by Bastviken *et al.,* (2011) which estimates freshwater CH_4 emissions at 103 Tg yr^{-1} based on data from 474 freshwater ecosystems, highlighting the uncertainty in CH_4 emission rates and the importance of considering systems with varying environmental factors and stoichiometric characterisations. There are also disparities in how aquatic ecosystems are categorised, making comparisons between reports challenging.

Environmental factors are reported to strongly influence the contribution of a waterbody to CH_4 emissions. Bange *et al.,* (2019b) found an inverse relationship with rainfall and CH_4 concentrations in rivers in northwest Borneo, suggesting CH_4 oxidation combined with increased river flow were responsible for a decrease in CH_4 concentrations. This could also be explained by an increased dilution or flushing of a CH_4 source from river sediments or terrestrial inputs under high river flow conditions. In contrast, changes to the rates of sedimentation and reduced river flows due to river

obstructions such as dams have been suggested to increase freshwater emission rates by 7% (Maeck *et al.,* 2013). This effect can also be observed from continuous measurements of surface water CH_4 concentrations of the German Elbe River, ranging from 40 – 1,456 nmol CH_4 L^{-1}, with hotspots occurring at weirs and harbours (Bussmann *et al.,* 2022). These results highlight the need for further continuous measurements along river and estuarine environments to provide accurate spatial representations of CH_4 variability, particularly to understand how future planned obstructions to natural river flows, or the removal of them, may change future emission scenarios (Bednařík *et al.,* 2017; DelSontro *et al.,* 2016).

Dissolved CH_4 concentrations in estuaries are largely dominated by riverine inputs and conservative mixing, with records of non-conservative mixing due to methanotrophs and outgassing to the atmosphere (Abril *et al.,* 2007; Abril and Iversen, 2002; Upstill-Goddard and Barnes, 2016). Upstill-Goddard and Barnes (2016) reported total CH_4 emissions for estuaries in the UK and Europe at 5.8 ± 5.8 x 10^9 g yr^{-1} and 2.7± 6.8 x 10^{10} g yr^{-1} respectively, with maximal CH_4 concentrations found in the low salinity Turbidity Maximum Zone (TMZ) of some estuaries considered. This agrees with previous research into the same estuaries by Upstill-Goddard *et al.,* (2000) where highest concentrations of CH_4 (~190 – 670 nmol L^{-1}) correlated with low salinities in the TMZ.

Wetlands such as intertidal saltmarsh play an important role in cycling C received from terrestrial and freshwater inputs and can act as a large contributor to CH_4 emissions (Ho *et al.,* 2024; Saunois *et al.,* 2024a). The complex variability and interaction between physical parameters such as temperature, dissolved oxygen and salinity over tidal cycles in estuaries and coastal wetlands cause seasonal and diurnal cycles in CH_4 production linked to soil salinity, vegetation growth, decomposition of organic matter (Jiang *et al.,* 2012; Rosentreter *et al.,* 2023). Salinity plays a particularly important role on the ecological community structure of methanogens and

methanotrophs by effecting ion availability. Under high salinity, an abundance of ions favours nitrate (NO_3^-), sulphate (SO_4^{2-}), and iron (Fe^{3+}) reducing microbes allowing them to outcompete methanogens for labile C substrates and hydrogen ions (La *et al.,* 2022; Sivan *et al.,* 2016; Soued *et al.,* 2024). Salinity has also been shown to suppress CH_4 concentrations by changing nutrient and dissolved organic carbon (DOC) availability linked to solute accumulation, leading to inhibited methanogenesis (Soued *et al.,* 2024). Vegetation structure can also impact CH_4 production. Tong *et al.,* (2010) found a saltmarsh dominated by common reed (*Phragmites australis*) in the Min River estuary, south-east China, was a net source of CH_4 (32.59 CH_4 m^{-2} yr^{-1}) with considerable monthly variation and linked to the tidal cycle.

1.6.2 Methane in coastal waters and shelf seas

Saunois *et al.,* (2024) report that of the global total natural and indirect sources of CH_4 between 2000 – 2009, 4 % (12 [6-20] Tg yr^{-1}) were from coastal and oceanic sources. European coastal waters alone have been reported to contribute 0.35 – 0.75 Tg C yr^{-1} to global oceanic CH_4 emissions (Bange, 2006). In comparison, storage of CH_4 in deep marine sediments and the small differences between gross production (methanogenesis) and gross consumption (methanotrophy) acts to prevent large emissions of CH_4 from the open ocean to the atmosphere. However, high CH_4 surface saturations have been reported in the shelf and central deep basins of the Arctic Ocean (Kitidis *et al.,* 2010; Rees *et al.,* 2022), suggesting it is a source of atmospheric CH_4 due to methanogenesis in sediments, gas hydrates and diffusion from geological dissolution in shelf areas, with potential for increased emissions with climate change related to increases in temperature, increased river melt inputs and reductions in ice cover (Shakhova *et al.,* 2019, 2010).

1.7 Nitrous oxide pathways

The production of N_2O is controlled by a series of microbial reduction and oxidative transformations of N species in soils, sediments and water (Figure 1.5). These processes are limited by a large range of factors including changes in oxygen, temperature, acidity, biological activity or availability of organic C, ammonium, nitrate, iron and P (Bange *et al.,* 2019b; Gruber and Galloway, 2008; Stein and Klotz, 2016). Direct anthropogenic production of N_2O includes biomass burning and combustion in industrial processes (Tian *et al.,* 2024). The breakdown of atmospheric N_2O takes place via stratospheric UV photolysis and the reaction with excited oxygen atoms O(1D) to create NOx (Minschwaner and Siskind, 1993). Studies into the production pathways of N_2O have partly been driven by efforts to increase the efficiency of agricultural systems and reduce N losses during the application of N-based fertilisers, and the adoption of wastewater treatment techniques such as OLAND (Oxygen-Limited Autotrophic Nitrification-Denitrification) and ANAMMOX (anaerobic ammonium oxidation) to encourage biological degradation of chemicals (Verstraete and Philips, 1998; Zhu *et al.,* 2013)

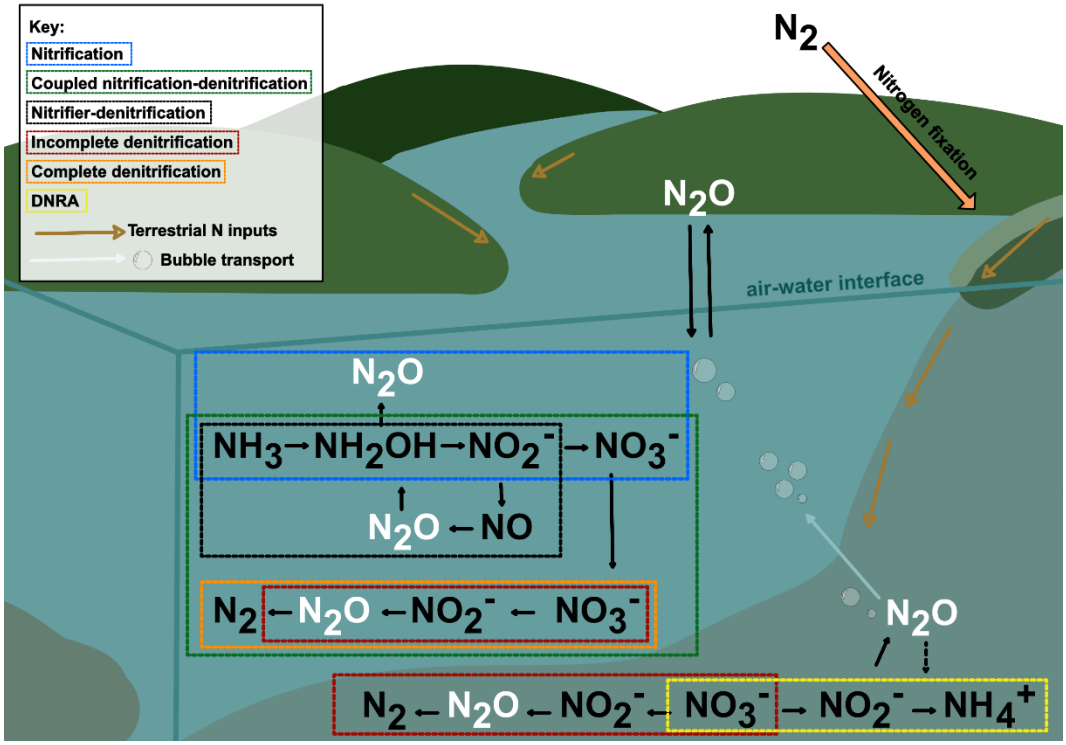

Figure 1.5. Major N_2O pathways in aquatic sediments and surface waters. Adapted from Webb *et al.,* (2019).

Incomplete denitrification is understood to be the dominant N_2O production pathway. During this process, NO_3^- is reduced to nitrite (NO_2^-) before being returned to the atmosphere in the gaseous form of N_2, with NO and N_2O released as intermediates under low oxygen conditions and in the presence of the denitrifying enzyme nitrite reductase (Tian *et al.,* 2020; Zhang *et al.,* 2020). The second common N_2O pathway is nitrification, where ammonia-oxidising bacteria (AOB) and ammonia-oxidising archaea (AOA) convert ammonium (NH_4^+) into NO_2^- and then NO_3^- (Casciotti *et al.,* 2011). Yoshida and Alexander (1970) observed a fraction of N was lost in the gaseous form of N_2O during the oxidation of NH_4^+ to NO_2^- by the nitrifying bacteria *Nitrosomonas europaea*. Farquharson (2016) reports 0.03 % - 1 % of N associated with nitrification in agricultural soils is released as N_2O, with NH_4^+ and pH acting as key controlling factors. This increasing body of evidence has suggested nitrification is a particularly important contributor to N_2O inventories in sediments and aquatic ecosystems (Tian *et al.,* 2024).

In soils, nitrifier-denitrification (ammonia (NH_3) oxidised to NO_2^- then to NO, N_2O and N_2) carried out by AOB is thought to be a significant contributor to the loss of NH_4^+ in the form of NO and N_2O, particularly under low oxygen conditions and following high NO_2^- additions from fertilizers (Storch *et al.,* 2023; Wrage-Mönnig *et al.,* 2018). A 'hybrid formation' has also been reported where AOA utilise N from both NO_2^- and NH_4^+ to produce N_2O (Trimmer *et al.,* 2016). This has been suggested as an important source of oceanic N_2O (Ji and Ward, 2017) which could be enhanced under low dissolved oxygen concentrations (Kelly *et al.,* 2024) and therefore could be an increasingly important source of N_2O in oxygen depleted waters. Advances in the use of isotopes continue to unveil more complex interactions leading to the production of N_2O.

Approximately 60% of N_2O emissions are from natural sources including soils, rivers, estuaries and oceans, with a 30% increase in global human-induced emissions over a 40-year period largely due to N additions for crop production (Tian *et al.,* 2024). The IPCC inventory methods include estimates of indirect N_2O emissions caused by the transport of terrestrial nitrogen into aquatic habitats such as rivers, estuaries or wetlands. This occurs as leached or nitrogen carried by runoff enters groundwater or surface waters which is then converted into N_2O through nitrification or denitrification. The 2013 Wetland Supplement to the 2006 IPCC guidelines further improved the characterization of wetland and aquatic environments, encouraging an approach which considers indirect N_2O emissions from water a result of land-based nitrogen losses downstream. Between 2007-16, the IPCC reported that agricultural production of crop and livestock within the farm gate alone indirectly produced 8.0 ± 2.5 Tg N_2O yr^{-1} (Shukla *et al.,* 2019). Quantifications of natural sources of N_2O have shown terrestrial environments act as major contributors to emissions across the LOAC due to artificially fertilised agricultural soils entering inland waters (Bouwman *et al.,* 2013; Tian *et al.,* 2024). Significant correlations found

between NO_2^-, NO_3^-, NH_4^+ and N_2O concentrations in aquatic ecosystems suggest estuaries are also a significant source of N_2O emissions (Barnes and Upstill-Goddard, 2011; Dong *et al.,* 2005; Law *et al.,* 1992). The complexity of N_2O production and consumption pathways, together with large spatial and temporal variability in N_2O emissions, create challenges in determining whether an aquatic ecosystem acts as a source or sink of this GHG (Tian *et al.,* 2024), justifying the need for temporally and spatially extensive monitoring of N_2O across the LOAC.

1.7.1 Nitrous oxide in rivers, wetlands and estuaries

Of the total natural emissions of N_2O (1.8 [1.0 – 3.0] Tg N yr^{-1}) between 1980 - 2020, inland waters, estuaries and coastal vegetation account for 0.1 Tg yr^{-1} (Tian *et al.,* 2024). The connectivity between these ecosystems has large implications for their relative contributions to N_2O emissions. Kroeze and Seitzinger (1998) reported that global exports of dissolved inorganic nitrogen (DIN) from rivers to estuaries were 20.8 Tg N yr^{-1}, of which 75% were from anthropogenic sources such as fertiliser and sewage effluent. This same study estimated that 1% of these anthropogenic N inputs to watersheds are lost as N_2O from rivers and estuaries at a rate of 1.2 Tg N yr^{-1}, making rivers and estuaries accountable for ~25% of global anthropogenic N_2O emissions, which at the time of study were in the range of 4 - 5 Tg N yr^{-1} (Kroeze and Seitzinger, 1998). Improvements to N modelling have since reported DIN export to coastal waters of between 18.9 - 25 Tg N yr^{-1}, with future increases or reductions of this number largely attributed to regional efficiency of fertiliser applications (Dumont *et al.,* 2005; Mayorga *et al.,* 2010; Seitzinger *et al.,* 2010). More recent studies have shown that rivers are increasingly important hotspots of N_2O, with 50 % of global emissions attributed to streams less than 10 m wide (Marzadri *et al.,* 2021). These studies uncover uncertainties in river nutrient loading over the next 25 years but highlight that rivers and estuaries could become increasingly important sources of global N_2O emissions if active solutions to reduce surplus biologically available N are not implemented.

The factors controlling N_2O pathways are influenced by site specific climatic conditions and surrounding land-use and land cover (Que *et al.,* 2023; Upadhyay *et al.,* 2023). N_2O production in rivers is dominantly driven by nitrification, though denitrification can also play a role depending on site specific DIN and DOM loadings, water quality, water residence times and river hydromorphology (Beaulieu *et al.,* 2011; Marzadri *et al.,* 2021). In estuaries, nitrification is the main pathway for production (Maavara *et al.,* 2019). In wetlands, the rich availability of organic matter (OM) and anoxic conditions often favours the anaerobic microbial process of denitrification, which has been harnessed in constructed wetlands to remove excess NO_3^- for water quality improvements (Martínez-Espinosa *et al.,* 2021).

It should also be noted there is often a geographic bias towards studies being carried out in catchments with existing conservation and water quality issues often related to urbanisation or agricultural practices, and therefore the data used to inform N_2O models may not accurately represent biogeochemical pathways in pristine ecosystems (Borges *et al.,* 2018; Logozzo *et al.,* 2025). Bias towards timing of sampling can also effect global quantification of dominant N_2O biogeochemical pathways in aquatic ecosystems, causing a lack of spatial heterogeneity of measurements and limiting observations of extreme hydrological events or diel cycles (Woodrow and White, 2023), particularly when site accessibility is limited.

1.7.2 Nitrous oxide in coastal waters and open shelf seas

Bange (2006) reported European shelf waters contribute up to 26% of global oceanic N_2O emissions, with future emissions from coastal areas likely to be determined by the degree of eutrophication. Oceanic N_2O production can occur through microbial nitrification, partial denitrification and, under low oxygen conditions, nitrifier-denitrification, though there is discrepancy over the contribution of each process to global N_2O emissions (Bange, 2006;

Grundle *et al.,* 2017). Syakila and Kroeze (2011) estimated natural ocean emissions of N_2O to be 3.5 Tg N yr^{-1}, with an additional 1 Tg N yr^{-1} due to anthropogenic sources of atmospheric N deposition as a result of increasing NOx emissions. Compared to freshwater, concentrations and emissions of N_2O in oceanic waters are more limited by nutrient availability, mixing and upwelling processes which affect phytoplankton growth, with ocean-atmosphere exchange playing the dominant role in surface concentrations (Wanninkhof, 2014; Zhang *et al.,* 2020).

In recent years there have been increasing investigations into N fixation (diazotrophy) in marine and coastal waters which has furthered scientific understanding of N_2O reduction in these environments. Rees *et al.,* (2009) show evidence of N fixation (upper limit of 20 nmol N L^{-1} d^{-1}) in the mesotrophic waters of the Western English Channel (WEC) acting to meet requirements of phytoplankton during summer conditions of thermal stratification and nutrient limitation. Further reconsideration of limitations on the N cycle, coupled with findings of waters sub-saturated with N_2O, have led to discoveries of biological mechanisms in which N_2O is consumed during N fixation. Cornejo-D'Ottone *et al.,* (2015) carried out in-situ experiments in surface waters labelled with $15N_2O$ which highlighted active biological fixation (0.43 – 87.34 nmol L^{-1} d^{-1}) with highest rates associated with the Sub Antarctic Water Mass (SAAW). Biological N_2O fixation/consumption has been reported in several waterbodies including the Atlantic (Rees *et al.,* 2021), Southern Ocean (Cornejo-D'Ottone *et al.,* 2015)and Nordic Seas (Bange *et al.,* 2019a). The presence of N_2O reductase genes *nosZ* has been highlighted in the South-Eastern Indian Ocean, suggesting canonical denitrification (N_2O used as an electron acceptor in lieu of dissolved O_2) was responsible for sub-saturated N_2O concentrations (Farías *et al.,* 2013; Raes *et al.,* 2016). However, Rees *et al.,* (2021) show evidence of N_2O removal under fully oxygenated conditions in the presence of bacteria with novel atypical *nosZ* gene sequences important for the reduction of N_2O to N_2, suggesting canonical denitrification does not always require anoxic conditions.

1.8 Thesis outline

Understanding of CH_4 and N_2O cycling pathways is continuously evolving with the development of new scientific monitoring equipment and access to previously underrepresented freshwater and marine systems. The challenge now is to ensure that understanding is being effectively translated into management practices which will ensure long-term climate benefits. Increasing collaboration between the fields of biogeochemistry, restoration ecology, and biodiversity conservation, while maximising engagement with policy- and decision-makers, is vital to ensure continued progress towards GHG emission reduction targets.

The overarching aim of this thesis is to better understand the potential impact of restoring aquatic ecosystems on the production and transport of N_2O and CH_4 across the LOAC. The concentrations of both gases discussed throughout this thesis were collected during the Land-Ocean Carbon Transfer (LOCATE) (locate.ac.uk) and AgZero+ (agzeroplus.org.uk) projects, which are large monitoring programmes taking place across the UK to improve understanding of land management practices on carbon and GHG cycling processes. Measurements taken from routine monitoring at Station L4 by the Western Channel Observatory (WCO) (westernchannelobservatory.org.uk) are also included in the analysis to present the full spectrum between freshwater, estuarine, coastal and shelf sea waters (Brown and Rees, *in prep*). This thesis contains 3 research chapters, outlined below, followed by a final discussion and outlook.

Chapter 2 introduces a total of 11 empirical models commonly used to estimate the gas transfer velocity (k) of N_2O and CH_4 when calculating emissions from river and estuary surface waters. These models are applied to measurements of dissolved N_2O and CH_4 concentrations taken along a freshwater to estuary axial transect of the River Tamar and River Dart. The results inform the use of these models in Chapter 3.

Chapter 3 will introduce the Tamar catchment in more detail, presenting the results from an extensive monitoring programme which took place between 2019 and 2020 along a transect from near the source of the Tamar to its coastal waters. Estimates of N_2O and CH_4 flux from surface waters to the atmosphere are used to identify targeted NbS to reduce natural sources of GHG.

Chapter 4 continues exploring hydrological connectivity by zooming into the Calstock Intertidal Wetland, an example of a NbS in the Tamar with the objectives of reconnecting the river with its floodplain to alleviate flood risk and enhancing biodiversity and carbon storage of the local area. Measurements of N_2O and CH_4 and other relevant variables took place from the initial creation of the wetland. Results are discussed to evaluate the impact of wetland restoration on estuarine and coastal emissions of N_2O and CH_4.

Chapter 5 summarises the thesis findings through a general discussion and conclusion, identifying key takeaways for decision makers in ecosystem restoration.

Chapter 2: A comparison of empirical models of gas transfer velocity for estimating N_2O and CH_4 air-water fluxes

Abstract

To understand the relative contributions of aquatic ecosystems to atmospheric concentrations of greenhouse gases (GHG), it is first necessary to select a method for estimating air-water fluxes. This chapter explores the use of empirical models for estimating gas transfer velocity (k) to assist with calculating air-water fluxes of nitrous oxide (N_2O) and methane (CH_4) from river and estuary surface waters. Commonly used models were applied to measurements of dissolved concentrations of N_2O and CH_4 sampled from river and estuary locations in the River Tamar and River Dart in southwest England. It was found that river models present considerable variability in estimates of k, ranging by a magnitude of 5 in the Tamar and by 20 in the Dart. This finding was not surprising as it agreed with previous applications of river-based empirical models and highlighted the sensitivity of gas flux estimations to hydrological variables. This was therefore carefully considered in the approach to estimating of air-water fluxes of GHG from river surface waters. Windspeed-based models typically applied to estuary and coastal waters presented far less variability and overall showed better agreement. By including river models to calculate air-water fluxes from freshwaters, the overall calculation of GHG emissions from the estuaries were larger than previously reported. This demonstrated the importance of considering the hydrological drivers of GHG emissions and their export from rivers into estuary surface waters. The understanding gained from this exercise was used to inform the use of empirical models in Chapter 3, where a full river-to-coast investigation of N_2O and CH_4 fluxes is applied to the Tamar Catchment.

2.1 Introduction

Aquatic ecosystems, such as inland waters, estuaries, and wetlands, are responsible for approximately 60% of natural nitrous oxide (N_2O) sources and 80% of natural methane (CH_4) sources (Saunois *et al.,* 2024a; Tian *et al.,* 2024). Ecological and hydrological processes play an important role in the exchange of these greenhouse gases (GHG) between surface waters and the atmosphere (Tian *et al.,* 2019). However, accurately quantifying natural emissions of N_2O and CH_4 remains a challenge. Air-water gas exchange is dependent on the dissolved concentration of the gas, the atmospheric concentration, and the rate at which the gas moves across the air-water interface, known as the piston or gas transfer velocity (*k*) (Jähne and Haußecker, 1998; Raymond and Cole, 2001). The dominant factors driving *k* in surface waters are illustrated in Figure 2.1. In river environments, *k* is driven by complex hydrological interactions between river channel slope, depth, discharge, and velocity which leads to bubble production and turbulent mixing at the air-water interface (Alin *et al.,* 2011; Hall Jr. and Ulseth, 2020; Raymond *et al.,* 2012). It has been shown that these interactions are highly site specific with even small changes leading to large variations in *k* and the resulting calculated GHG emissions (DelSontro *et al.,* 2016; Raymond *et al.,* 2012; Wallin *et al.,* 2011). In steeper flowing waters, such as high-energy mountain streams, the consideration of bubble entrainment can also enhance *k* by several orders of magnitude, particularly when there are instream features such as cascades or waterfalls leading to large hydraulic jumps (Cirpka *et al.,* 1993). However, the sensitivity of bubble entrainment to site-specific flow conditions complicates the application of bubble models to other studies (Klaus *et al.,* 2022). Gas exchange in estuaries on the other hand is dominantly driven by windspeed and, though strong tidal influences can also lead to site specific variability in estimated *k*, there is overall less disagreement over the model parameterizations controlling gas exchange in estuarine and coastal systems (Wanninkhof *et al.,* 2009)

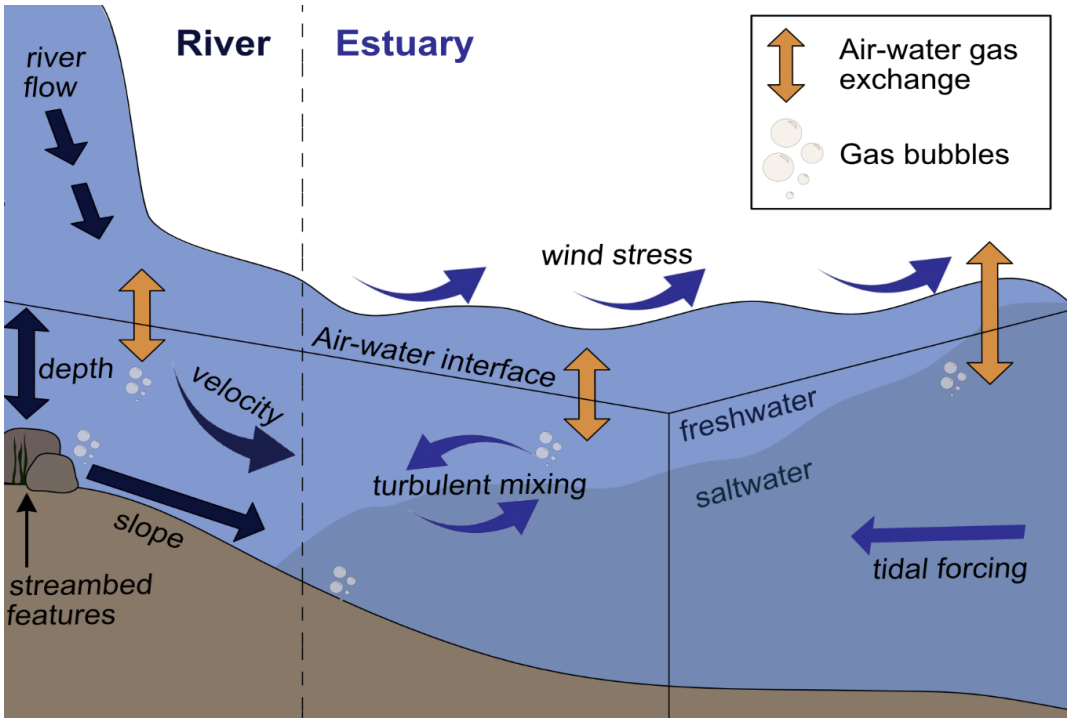

Figure 2.1. Diagram showing the dominant factors controlling air-water gas exchange in river and estuary surface waters

The emissions of GHG from aquatic ecosystems scales several orders of magnitudes, making comparisons between locations along a water continuum difficult, particularly when there is high discrepancy between methods specific to different aquatic habitat types (Billett and Moore, 2008; DelSontro *et al.,* 2016; Jonsson *et al.,* 2008; Lorke *et al.,* 2019; Nightingale *et al.,* 2000). Nevertheless, there is an increasingly urgent need to quantify the relative contributions of aquatic ecosystems to reliably inform GHG budgets, climate change forecasting and impactful mitigation practices.

Whilst direct measurements of *k* produce results with considerably lower standard errors, they rely on time-consuming discrete gas measurements which is not always feasible during a river-to-coast study. Alternatively, empirical models of *k*, informed by gas tracer experiments and direct measurements of gas exchange between surface waters and the atmosphere, enable estimates of GHG emissions at a larger catchment scale (Raymond and Cole, 2001; Wanninkhof, 2014). Whilst it is

acknowledged these models can lead to significantly larger errors, they have in part satisfied the immediate need for a better understanding of the role of surrounding land use practices and water management frameworks in controlling emissions of GHG from aquatic ecosystems (Logozzo *et al.,* 2025; Rosentreter *et al.,* 2021b).

This study takes place in the Tamar and Dart estuaries in southwest England. The purpose of this investigation is to compare several empirical models commonly used to estimate *k* in assessments of N_2O and CH_4 emissions from river and estuary surface waters. The results of this study provide an understanding of the limitations in reporting on GHG emissions from aquatic ecosystems in this way and informs the application of these models in a river-to-coast transect of the Tamar in Chapter 3.

2.2 Methods

2.2.1 Study location

This study investigates data from Pickard *et al.,* (2022), focusing on the River Tamar and River Dart in southwest England which were sampled during four freshwater-to-estuary axial transects along a practical salinity gradient of 0 – 35 in April and July 2017 and January and April 2018 (Figure 2.2, Table S2.1) (Tye *et al.,* 2020). This timeframe allows a seasonal comparison between GHG emissions in spring (2 x April), summer (July) and winter (January).

The Tamar catchment is located between the county borders of Devon and Cornwall in southwest England. The Tamar catchment drains a total area of 1800 km^2 dominated by agricultural land use with small areas of woodland and is influenced by the weather systems created over moorland landscapes of the Bodmin Moors and Dartmoor (Morton *et al.,* 2024). The

catchment suffers from diffusive pollution of nutrients caused by nitrogen (N) and phosphorus (P) runoff from agricultural fertiliser usage (Uncles *et al.,* 2002), and metal legacy pollutants from historic mining activity (Price, 2002), which combined with issues of water abstraction have resulted in a moderate ecological status under Water Framework Directive (WFD) assessments (Environment Agency, 2025a). The main River Tamar flows south for 98 km towards the coastal waters of Plymouth Sound and eventually mixing with the Western English Channel (WEC) (McEvoy *et al.,* 2023). The Tamar is a gently sloping river (0.2%) with a moderate annual average flow rate of 22.9 $m^3 s^{-1}$ and is characterised by its reactive flash floods during storm events (National River Flow Archive, 2025a). These waters drain into the Tamar Estuary, a well-mixed drowned river valley, or ria, where a strong tidal influence can lead to saline intrusion upstream until the tidal limit of Gunnislake Weir approximately 30 km upstream (Uncles and Stephens, 2010). Low river flow events can also lead to stratification in these upper estuary regions (Uncles and Stephens, 1993). The tidal amplitude of the estuary is approximately 5 m during spring tides and 2 m during neap tides (Yang *et al.,* 2016).

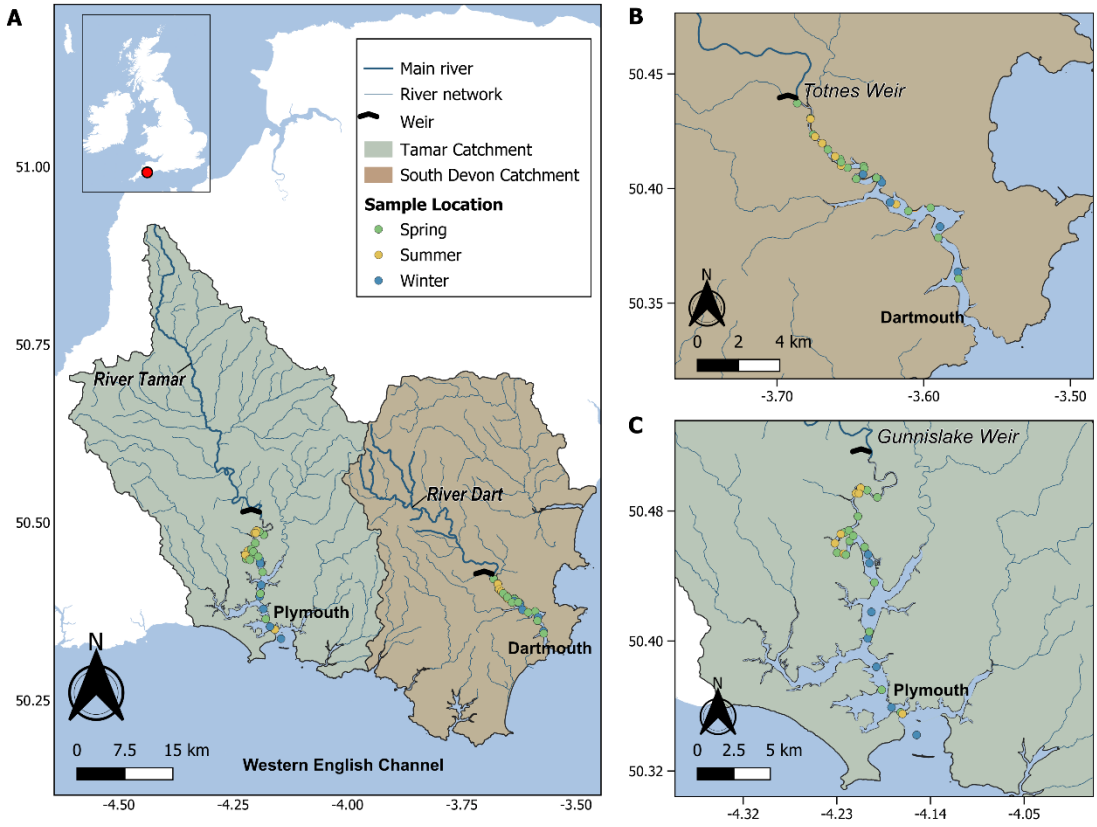

Figure 2.2. Map showing the location of A) Tamar and South Devon Management Catchments defined by the Environment Agency in southwest England, highlighting the main River Tamar and River Dart and the locations of sampled sites in the Tamar and Dart Estuaries. B) Magnified positions of Dart Estuary sampled positions C) Magnified positions of Tamar Estuary sampled positions.

The River Dart and Estuary sit within the South Devon Management Catchment, neighbouring the Tamar Catchment in southwest England. The River Dart drains a comparatively smaller area of 475 km^2, with two main sources on Dartmoor, the East Dart and West Dart. The Dart is more heavily influenced by moorland and grassland habitats in its upper catchment before reaching agricultural and urban areas in the lower reaches (Morton *et al.,* 2024). The Dart has less historical issues of pollution from mining activity, but its water quality has suffered similarly from localised agricultural inputs of N and P, vulnerability to sedimentation and acidification (Evans *et al.,* 2001; Schuwerack *et al.,* 2007), and changes to its natural hydrological

regime through artificial barriers or water abstraction. The Dart also therefore has an overall moderate ecological WFD status (Environment Agency, 2025b). The main body of the River Dart flows south for 39 km until reaching its coastal waters in Dartmouth, again eventually mixing with the WEC (Environment Agency, 2025b). The Dart is a slightly steeper river (slope 0.8%) compared to the Tamar, with a higher flashy response to rainfall and storm events though a lower average annual flow of 11.5 m^3s^{-1} (National River Flow Archive, 2025b). The Dart Estuary, also a ria, has a narrower and more sheltered geomorphology compared to the Tamar, with an artificial tidal limit at Totnes Weir, approximately 20 km upstream of Dartmouth. The tidal amplitude has a mean range of 4.3 m on spring tides and 1.8 on neap tides (Campos *et al.,* 2011).

Table 2.1. Summary of main River Tamar and River Dart characteristics (Source: Environment Agency Catchment Data Explorer)

	River Tamar	**River Dart**
Length	80 km	39 km
Catchment Drainage Area	1800 km^2	475 km^2
Slope	0.2 %	0.8 %
Average annual discharge	22.9 m^3 s^{-1}	11.5 m^3 s^{-1}
Average annual mean rainfall	1319 mm yr^{-1}	1984 mm yr^{-1}
WFD Ecological Status	Moderate	Moderate

2.2.2 Sample Collection

Freshwater samples were collected from mid-channel where accessible from a bridge or riverbank and estuary samples were collected based on a target practical salinity range of 0 to 35 from a rigid inflatable boat (RIB). The location of estuary samples therefore varied with salinity. Salinity, water temperature and pH were measured using a multiparameter YSI sonde (YSI PRO30) placed directly into the estuary water or into a bucket of sampled freshwater. River and estuary samples were collected from the surface (<

30 cm) using a thrice-rinsed bucket before being decanted into the appropriate container. For N_2O and CH_4, this was a 500 ml borosilicate glass bottle, which was allowed to overflow to remove gas bubbles and poisoned with 100 µl saturated mercuric chloride solution before sealing with a glass stopper.

Table 2.2 Summary of hydrological and hydrochemical conditions sampled in the Tamar and Dart Estuaries. *S* = river slope, *Q* = river discharge, *D* = river depth, W = river width, *V* = river velocity (calculated as $V = Q / (D*W)$), U_{10} = windspeed

River	Date	Station	Salinity	Temp (°C)	*S* (%)	*Q* (m^3s^{-1})	*D* (m)	*V* ($m\ s^{-1}$)	U_{10} ($m\ s^{-1}$)
Tamar	2017-04-24	FW	0	10.5	0.05	6.28	0.45	0.351	3.75
		1	1.82	13.2					
		2	4.7	13.3					
		3	9.83	13.5					
		4	15.1	13.6					
		4A	19.3	13.6					
		5	25	13.5					
		6	29.3	13.5					
		7	34.2	11.9					
	2017-07-24	FW	0	15.3	0.05	8.35	0.54	0.390	5.41
		2	2.1	18.6					
		3	5.5	18.8					
		4	10.8	18.8					
		5	15	18.9					
		5A	20.8	21.8					
		6	24.8	21.5					

		6A	29.2	21.5					
	2018-01-21	FW	0	9.4	0.05	97.63	1.63	1.494	6.36
		2	2	9.2					
		3	4.9	9.6					
		4	10.6	9.4					
		5	15	9.4					
		5A	19.9	9.5					
		6	24.4	9.6					
		6A	30.3	10					
	2018-04-16	FW	0	10.7	0.05	21.44	0.89	0.603	6.87
		2	2	11.5					
		3	4.8	12.9					
		4	10.5	13.8					
		5	15.4	13.3					
		5A	20.4	10.3					
		6	26.1	10.3					
		6A	29.7	10.3					
Dart	2017-04-26	FW	0	10.5	0.4	3.61	0.42	0.287	3.68
		1	2.7	9.6					
		2	5	10.5					

		3	10.6	11.2					
		4	14.5	11.4					
		4A	19.1	11.3					
		5	23.9	11.4					
		6	31.9	11.5					
	2017-07-19	FW	0	18.2	0.4	3.87	0.42	0.309	4.93
		2	1.7	19.3					
		3	5.2	20.1					
		4	10.4	20.7					
		5	15	21.1					
		5A	19	21					
		6	25.5	21.1					
		6A	31.5	19.9					
	2018-01-21	FW	0	13.7	0.4	31.05	0.95	1.088	6.36
		2	1.3	13.4					
		3	3.7	13.5					
		4	10.5	13.9					
		5	16	14.2					
		5A	21.1	14.3					
		6	26.9	14.7					

	2018-04-17	FW	0	11.1	0.4	25.85	0.79	1.091	11.14
		2	1.6	12.7					
		3	4.2	13					
		4	11.6	12					
		5	16.1	11.4					
		5A	19.9	10.4					
		6	27.7	9.9					
		6A	32.7	9.6					

2.2.3 Dissolved Gas Concentrations

Samples were analysed in triplicate by single-phase equilibration gas chromatography using electron capture detection for N_2O and flame ionisation detection for CH_4 similar to the methods described by Upstill-Goddard *et al.,* (1996). Samples were calibrated with three certified standards (Air Products Ltd.; mixing ratios 317.4, 406.4, 496.7 ppb N_2O and 1.009, 2.058, 3.04 ppm CH_4 in synthetic air; calibrated against NOAA primaries). Aqueous CH_4 and N_2O concentrations were calculated from the solubility tables of Wiesenburg and Guinasso (1979) and Weiss and Price (1980) respectively.

2.2.4 Empirical models of *k* and gas flux calculations

Because *k* was not measured directly during the collection of water samples, commonly applied empirical models were selected by reviewing literature reporting on N_2O and CH_4 emissions from similar temperate rivers and estuary environments. It is acknowledged that models of gas transfer in rivers and estuaries are uncertain compared to direct measurements, however it is viewed that these results offer the best available insight to GHG emissions where direct measurements of *k* are unavailable. The empirical models compared in this study are detailed in Table 2.2.

The diffusive flux of N_2O and CH_4 from surface waters to the atmosphere are calculated using Equation 2.1:

$$f_{GHG} = k_{GHG} * (C_w - C_{eq}) \qquad \text{(Eq 2.1)}$$

where f_{GHG} is the diffusive gas flux at the air-water interface, k_{GHG} is the gas transfer velocity of the relevant gas, C_w is the measured concentration of the dissolved gas in the water, and C_{eq} is the equilibrium concentration of gas in the water based on solubilities calculated with atmospheric partial

pressure and Henry's Law (Weiss and Price, 1980; Wiesenburg and Guinasso, 1979). All *k* models and gas flux calculations were performed using functions written in RStudio Version 2024.12.0.

Estimates of *k* in freshwater locations were obtained using a model described by Borges *et al.,* (2004) (B04), and 7 models described by Raymond *et al.,* (2012) (R1 – R7). The Borges *et al.,* (2004) model calculates *k* as a function of river depth (*D*) and velocity (*V*), whilst the 7 models from Raymond *et al.,* (2012) introduce additional parameters such as river slope (*S*) and discharge (*Q*). By comparing these 8 models I aim to assess variability in the estimated *k* caused by different physical river parameters driving gas exchange at the water surface. As river *D*, *Q*, and *V* were not measured directly during sample collection, values were obtained from records published by the National River Flow Archive at stations Gunnislake (Tamar) (National River Flow Archive, 2025a) and Austins Bridge (Dart) (National River Flow Archive, 2025b). River *S* was measured along a 500 m section of the river (250 upstream and 250 downstream of the sampled location) following the guidelines of the River Habitat Survey (Environment Agency, 2022), using shapefiles obtained from the Environment Agency Catchment Data Explorer (https://environment.data.gov.uk/catchment-planning/) with the Elevation Profile tool in QGIS (Geographic Information System), version 3.32.3. All river models were normalised to a Schmidt number (Sc) of 600, a dimensionless number which represents the kinematic viscosity of a gas, according to the coefficients expressed in Wanninkhof (2014). This is used to describe the change in the rate of gas exchange at different temperatures.

Wind-dependent models developed by Clark *et al.,* (1995) (C95), Nightingale *et al.,* (2000) (N00) and Wanninkhof (2014) (W14) were compared in estimating *k* in estuary locations. Each of these models are driven by windspeed which was obtained from (Rame Head NCI, (www.nci-ramehead.org.uk) and normalised to 10 metres above sea level (U_{10}) using

the ‘wind.scale.base’ function in the ‘LakeMetabolizer’ R package (Winslow *et al.,* 2016). Estuary models were normalised to a Sc of 600, except for W14 which uses a higher Sc of 660, which translates to a slower diffusive rate, relevant to the Sc of CO_2 at seawater temperatures (Wanninkhof, 2014).

Table 2.3. Models to estimate gas transfer velocity (k_{ghg}) based on average daily wind speed measured at Rame Head ($U_{10,}$ in m s^{-1}), daily average river discharge (Q in m^3 s^{-1}) and river depth (D in m), river velocity (V in m s^{-1}, calculated as $V = Q / (D*W)$, river slope (S), and Froude number ($Fr = V/(gD)^{0.5}$). Values of k are normalised to a Schmidt number (Sc_{GHG}) to account for the different effects of water temperature and salinity on gas exchange relative to other gases of interest (Wanninkhof, 2014).

Model	**Author(s)**	**Unit**	**Model equation**
C95	Clark *et al.,* (1995)	cm h^{-1}	$k_{ghg} = (2.0 + (0.24 * U_{10})^2) * (Sc_{GHG} / 600)^{-0.5}$
N00	Nightingale *et al.,* (2000)	cm h^{-1}	$k_{ghg} = (0.222 * U_{10}^2 + 0.333 * U_{10}) * (Sc_{GHG} / 600)^{-0.5}$
W14	Wanninkhof (2014)	m d^{-1}	$k_{ghg} = 0.24 \times 0.251 \times U_{10}^2 (Sc_{GHG} / 660)^{-0.5}$
B04	Borges *et al.,* (2004)	m d^{-1}	$k_{ghg} = 0.24 \times 17.19 \times (V / D)^{0.5} (Sc_{GHG} / 600)^{-0.5}$
R1	Raymond *et al.,* (2012)	m d^{-1}	$k_{ghg} = 5037 \times (SV)^{0.89} * D^{0.54} (Sc_{GHG} / 600)^{-0.5}$
R2	Raymond *et al.,* (2012)	m d^{-1}	$k_{ghg} = 5937 \times (1 - 2.54 \times Fr^2) (SV)^{0.89} D^{0.58} (Sc_{GHG} / 600)^{-0.5}$
R3	Raymond *et al.,* (2012)	m d^{-1}	$k_{ghg} = 1162 \times S^{0.77} V^{0.85} (Sc_{GHG} / 600)^{-0.5}$
R4	Raymond *et al.,* (2012)	m d^{-1}	$k_{ghg} = 951.5 \times (SV)^{0.76} (Sc_{GHG} / 600)^{-0.5}$
R5	Raymond *et al.,* (2012)	m d^{-1}	$k_{ghg} = (2841 \times (SV) + 2.02) (Sc_{GHG} / 600)^{-0.5}$
R6	Raymond *et al.,* (2012)	m d^{-1}	$k_{ghg} = 929 \times (SV)^{0.75} * Q^{0.011} (Sc_{GHG} / 600)^{-0.5}$
R7	Raymond *et al.,* (2012)	m d^{-1}	$k_{ghg} = 4725 \times (SV)^{0.86} Q^{-0.14} D^{0.66} (Sc_{GHG} / 600)^{-0.5}$

2.3 Results

2.3.1 Environmental conditions

Water temperatures along the axial transect ranged from 9.2 ºC to 21.8 ºC and windspeeds averaged 5.87 m s^{-1} across the four respective survey periods. Water *V* ranged from 0.35 m s^{-1} to 1.49 m s^{-1} on the Tamar and 0.287 m s^{-1} to 1.09 m s^{-1} on the Dart. Daily average *Q* ranged between 6.3 m^3 s^{-1} to 27.7 m^3 s^{-1} on the River Tamar and 3.6 m^3 s^{-1} to 25.8 m^3 s^{-1} on the River Dart, with lower flows recorded during the 2017 surveys compared to 2018 (Figure 2.3A).

2.3.2 Nitrous oxide dissolved concentrations

The concentration of N_2O in the River Tamar Estuary displays spatial and temporal variability along the salinity transect, ranging between 8.1 nmol L^{-1} and 27.5 nmol L^{-1} (Figure 2.3B). A N_2O maximum can be seen in the upper to mid-estuary (salinity 5-20), with highest concentrations occurring during spring conditions in April 2018 and lowest concentrations occurred when winter river flows were higher in January 2018. In the River Dart Estuary, N_2O concentrations ranged between 7.7 nmol L^{-1} to 30.1 nmol L^{-1} (Figure 2.3C) and were generally higher in the lower salinity ranges (0-5) and decreased towards higher salinities, the sharpest decline most notably in July 2017. Highest concentrations were measured in summer (July 2017) and lowest recorded in the winter (January 2018).

2.3.3 Methane dissolved concentrations

Concentrations of CH_4 in the River Tamar Estuary ranged between 3.9 nmol L^{-1} – 1040 nmol L^{-1} (Figure 2.3D). Results show a general decrease in CH_4 between lower and higher salinity values in the Tamar Estuary, except for a

steady increase throughout the estuary followed by a sharp decline at salinity 30 in July 2018. CH_4 concentrations in the Dart ranged between 9.9 nmol L^{-1} and 1004 nmol L^{-1} (Figure 2.3E) and show a relatively uniform trend of decreasing concentrations moving from low to high salinities, with CH_4 concentrations again highest in the summer and lowest in the winter.

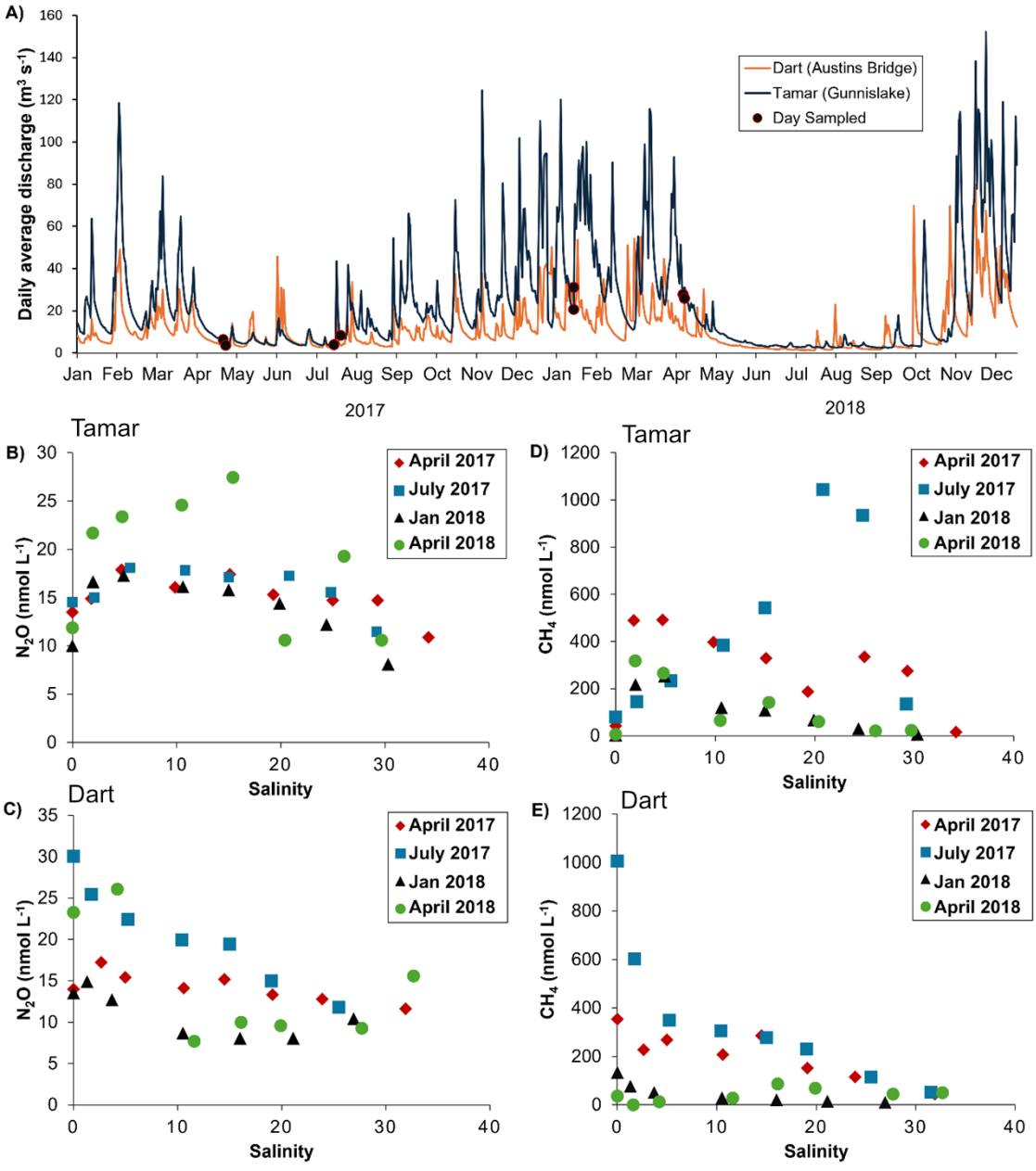

Figure 2.3. A) Sampled river discharge conditions. Dissolved concentrations of N_2O in the B) Tamar and C) Dart estuaries and dissolved concentrations of CH_4 in the D) Tamar and E) Dart estuaries.

2.3.4 Estimates of gas transfer velocity (*k*)

The estimated k_{CH4} and k_{N2O} from each model is shown for the respective freshwater samples from the River Dart and River Tamar in Figure 2.4. k_{CH4} values ranged between 0.9 to 7.5 m d^{-1} (median range 1.0 – 3.2 m d^{-1}) in the Tamar (Figure 2.4A) and between 1.2 to 32.3 m d^{-1} (median range 4.4 – 14.2 m d^{-1}) in the Dart (Figure 2.4B). k_{N2O} in the Tamar ranged from 0.9 to 7.3 m d^{-1} (median range 1.0 – 3.1 m d^{-1}) (Figure 2.4C) and 1.2 to 31.8 m d^{-1} (median range 4.3 – 14.0 m d^{-1}) in the Dart (Figure 2.4D).

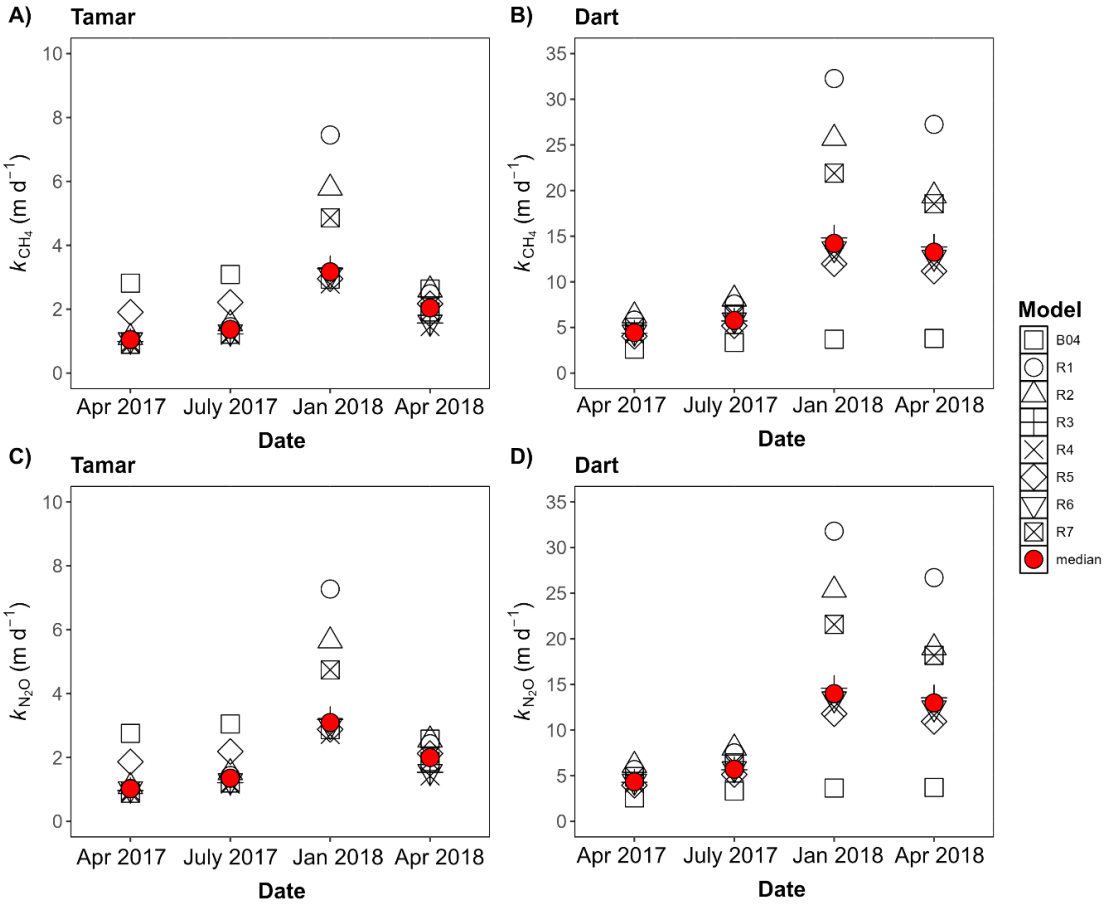

Figure 2.4. Comparison of k values using river parameter-based k models from Borges *et al.,* (2004) (B04) and Raymond *et al.,* (2012) (R1 – R7) applied to the freshwater locations of the Tamar and Dart. Median values are shown as red circles. A) k_{CH4} for the Tamar B) k_{CH4} for the Dart C) k_{N2O} for the Tamar D) k_{N2O} for the Dart.

The results from the B04 model show little seasonal variation and produced similar results for each sampling campaign (Tamar; k_{CH4} range 2.6 – 3.1 m d^{-1}, k_{N2O} range 2.6 – 3.0 m d^{-1}, Dart; k_{CH4} range 2.6 – 3.8 m d^{-1}, k_{N2O} range 2.6 – 3.7 m d^{-1}), compared to the other models. In the Tamar, B04 produced the largest values for the April and July 2017 surveys, and the smallest for the Dart in January and April 2018 but were similar to the other results for the rest of the surveys. The overall largest *k* values, and the greatest variation between the 8 river models, occurred in January 2018, ranging by a magnitude of 5 in the Tamar and by 20 in the Dart. This large variability is driven by the results of R1, R2 and R7, which are the only Raymond *et al.,* (2012) models to consider river D, demonstrating their sensitivity to seasonal changes in hydrological parameters controlling gas exchange. R3, R4, R5 and R6 showed closer agreement in each of the four surveys. The median reduces the large effect of these outliers on the estimated *k*, whilst retaining the seasonal effect of higher river flow conditions observed in January and April 2018.

Modelled *k* in the estuaries were much lower than that of the river site, and scale with windspeed in close agreement with one another (Figure 2.5). ranging between 0.6 m d^{-1} to 6.14 m d^{-1}. C95 showed higher results during low wind speeds compared to N00 and W14 but may slightly underestimate *k* in higher wind speeds as seen in the spring 2017 results. The results for k_{N2O} in the Dart showed the same pattern, ranging between 1.1 m d^{-1} to 59.0 m d^{-1} in the freshwater location and 0.6 m d^{-1} to 6.0 m d^{-1} in the estuary. The close agreement between estuary models ensure confidence with using the most applied and most recent of the three, described by Wanninkhof (2014). The results of Clark *et al.,* (1995) which stand out from the others is not entirely surprising as it was built upon site-specific dual-tracer gas release experiments, as opposed to the wind parameterisations of Wanninkhof (2014) and Nightingale *et al.,* (2000) which make them more widely applicable empirical windspeed-based models.

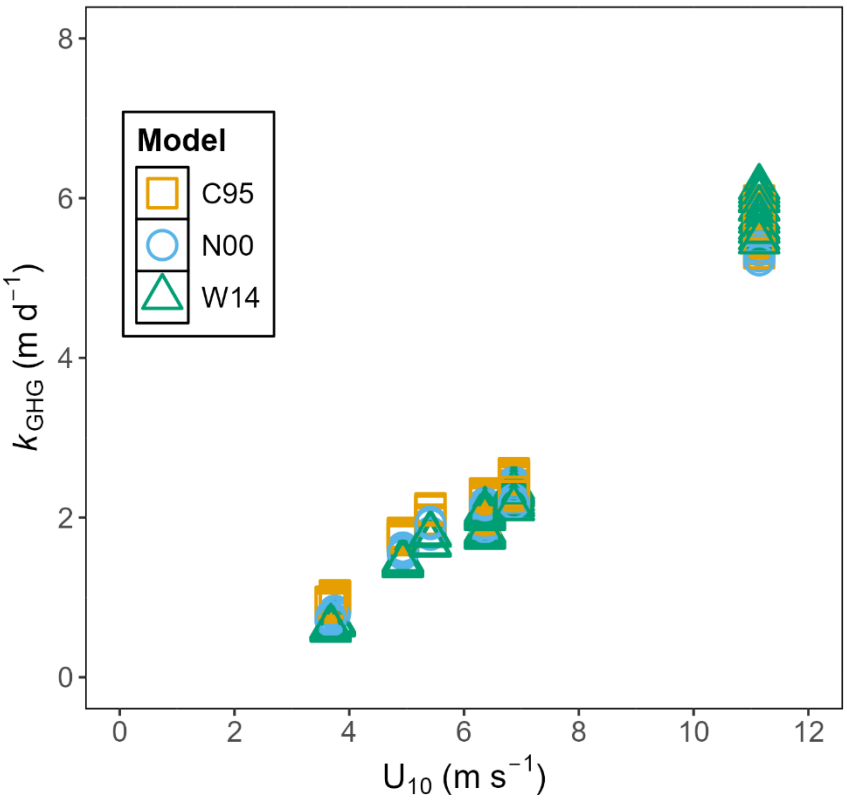

Figure 2.5. Predicted gas transfer velocity of estuary concentrations of N_2O and CH_4 (k_{GHG}) against wind speed (U_{10})

2.3.5 Calculated GHG fluxes

An ensemble approach was used to calculate gas fluxes in the river by using the median *k* value of all eight river models, with uncertainty quantified using the interquartile range (25th–75th percentiles) of the model-derived flux estimates. Gas fluxes in the estuary were calculated using the *k* values derived from the model W14 only. N_2O fluxes (f_{N2O}) mirror the spatial and temporal variability of dissolved concentrations in the surface waters. In the Tamar, the minimum f_{N2O} was -10.3 μmol m^{-2} d^{-1} at the freshwater location in January 2018 (Figure 2.6C) and the maximum was 38.9 μmol m^{-2} d^{-1} in the mid salinity region (15) during April 2018 (Figure 2.6). Overall, the Tamar generally acted as a source of N_2O to the atmosphere, with the average f_{N2O}

across the whole estuary transect at 8.2 ± 10.3 μmol m^{-2} d^{-1}. The Dart overall fell within a similar range of positive fluxes within estuary waters but had substantially larger freshwater fluxes of up to 139 μmol m^{-2} d^{-1} and a more negative flux of -22 μmol m^{-2} d^{-1} in the mid estuary around salinity 11, both of which occurred in April 2018 (Figure 2.6H). The average f_{N2O} across the estuary was 15.6 ± 36 μmol m^{-2} d^{-1}.

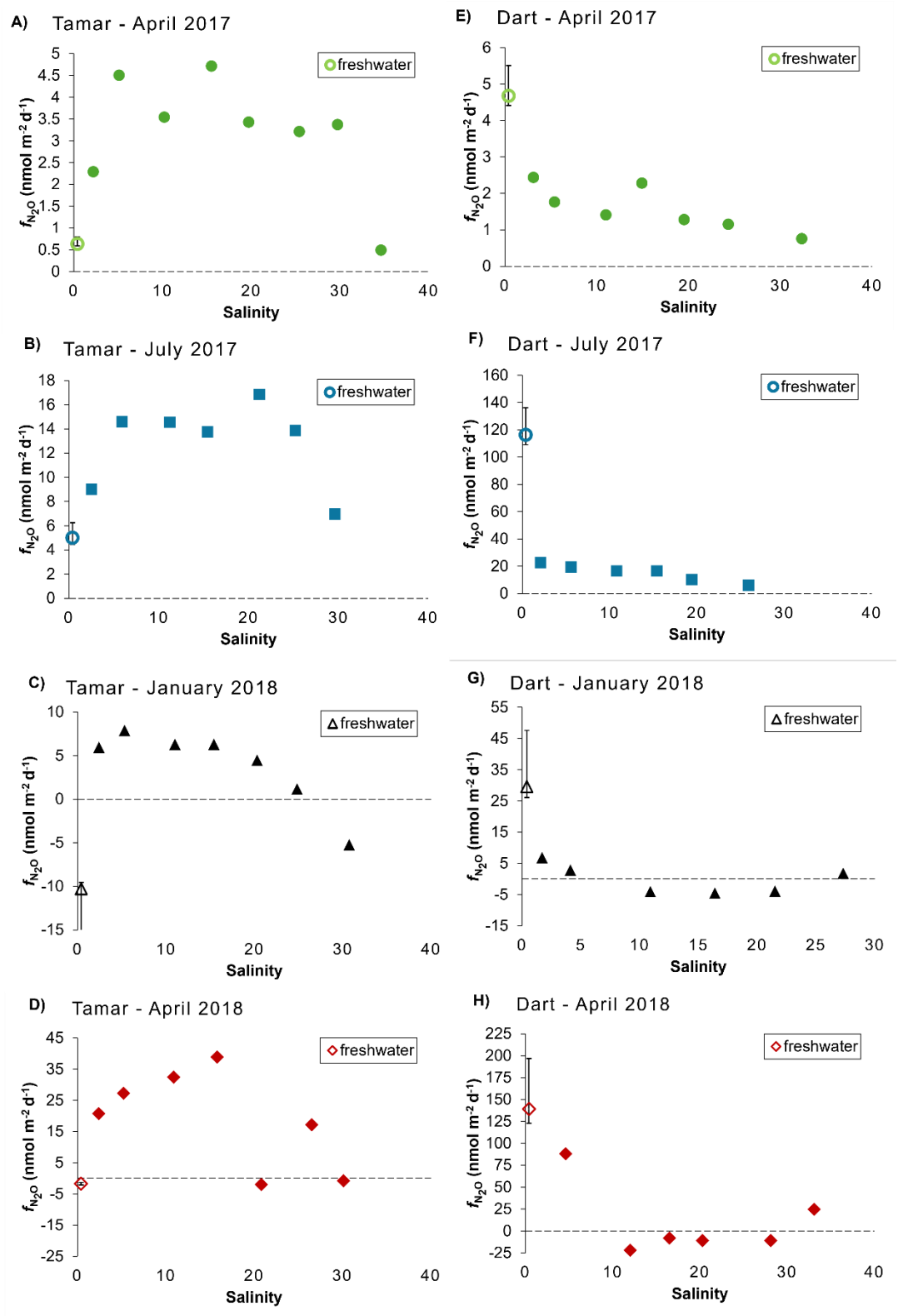

Figure 2.6. Results for calculated N_2O (fN_2O) flux along a salinity gradient in the Tamar (A-D) and Dart (E-H) between January 2017 to April 2018. Freshwater (salinity = 0) fluxes are estimated using an ensemble approach, with points derived from the median value of eight river gas exchange

velocity (*k*) models (B04 – R7); error bars show the interquartile range (25th – 75th percentiles) of model-derived flux estimates. Estuary (salinity = > 0) fluxes are calculated using the *k* values derived from W14 only. Models are described in Table 2.3. A dashed line signals 0 flux to ease visualisation of when each waterbody is acting as a source (above 0 line) or sink (below 0 line) of N_2O

The flux of CH_4 (f_{CH4}) in both the Tamar and Dart again reflect the spatial and temporal variation of dissolved concentrations. Both consistently acted as a source of CH_4 across the four surveys. In the Tamar f_{CH4} ranged from 0.3 µmol m^{-2} d^{-1} in January 2018 (Figure 2.7C) to 1880 µmol m^{-2} d^{-1} in July 2017 (Figure 2.7B). f_{CH4} generally started smaller in the freshwater location followed by a small spike in the upper reaches of the estuary (between salinity 5 to 10) before reducing again, except for July 2017 where f_{CH4} increased along the salinity gradient until a decline at salinity 25. Overall, the average f_{CH4} across the Tamar was 431 ± 424 µmol m^{-2} d^{-1}. The Dart showed larger f_{CH4} values, highest being in the freshwater zone, and ranged from 14.8 µmol m^{-2} d^{-1} in January 2018 (Figure 2.7G) to 5770 µmol m^{-2} d^{-1} in July 2017 (Figure 2.7F). The f_{CH4} values in the Dart were averaged 504 ± 1060 µmol m^{-2} d^{-1} across the estuary.

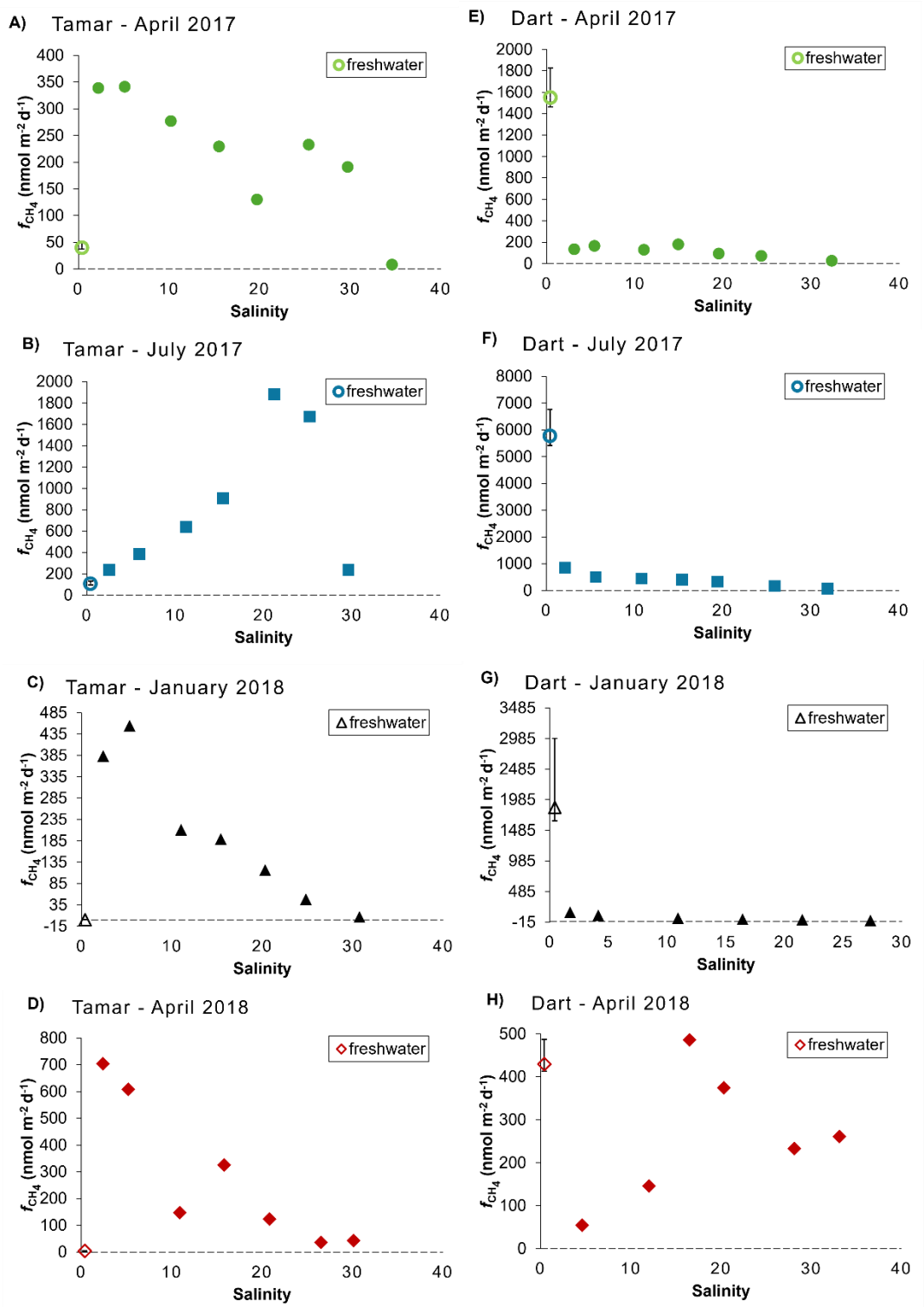

Figure 2.7. Results for calculated CH_4 (fCH_4) flux along a salinity gradient in the Tamar (A-D) and Dart (E-H) between January 2017 to April 2018. Freshwater (salinity = 0) fluxes are estimated using an ensemble approach, with points derived from the median value of eight river gas exchange velocity (k) models (B04 – R7); error bars show the interquartile range (25th

– 75th percentiles) of model-derived flux estimates. Estuary (salinity = > 0) fluxes are calculated using the *k* values derived from W14 only. Models are described in Table 2.3. A dashed line signals 0 flux to ease visualisation of when each waterbody is acting as a source (above 0 line) or sink (below 0 line) of CH_4

2.4 Discussion

2.4.1 Model effectiveness for estimating k_{GHG} and GHG fluxes

Rivers and estuaries are important sources of both N_2O and CH_4 (Saunois *et al.,* 2024a; Tian *et al.,* 2024). Therefore, selecting an accurate method to estimate *k* is of paramount scientific importance to provide reliable evidence towards effective GHG emission mitigation measures. As shown, there was considerable variability between the results of each river *k* model. This variability was largely driven by outliers from the results of R1, R2 and R7, which agrees with the findings of DelSontro *et al.,* (2016). The depth-dependent models from Raymond *et al.,* (2012) were developed based on a dataset with an average depth of 0.28 m. The average depths considered in this study were 0.64 in the Dart and 0.88 m in the Tamar, therefore these models should be appropriate for estimating *k* in these rivers. Using the median of multiple river-based gas transfer models provides a central estimate which reduces the influence of extreme predictions from individual models. However, this ensemble approach treats each model equally which may not accurately capture differences in their performance under specific river conditions. Some models may capture hydrodynamic processes better than others and combining them may smooth these differences. Despite this, taking a median value for the river models allows us to account for the dynamic effects of variable river parameters acting on *k* and provide a best estimate to support robust flux calculations, providing these results are interpreted as indicative rather than absolute values. This also allows for a reasonable comparison alongside the results from W14, presenting a robust

spatial assessment of N_2O and CH_4 fluxes from river to estuary and a representative total annual emission from the estuary.

Table 2.4 compares the results from this study to CH_4 and N_2O emissions reported by other studies, including the UK average. In this study, CH_4 flux densities were 2.87 g CH_4 m^{-2} yr^{-1} in the Dart and 2.02 g CH_4 m^{-2} yr^{-1} in the Tamar. These values are above the UK average of 1.6 g CH_4 m^{-2} yr^{-1}, suggesting enhanced CH_4 production in these systems driven by site-specific hydrological and biogeochemical conditions. The calculated CH_4 emissions for the Tamar are slightly higher than those reported by previous studies in the Tamar (Brown *et al.,* 2024; Upstill-Goddard and Barnes, 2016), which is expected due to the inclusion of the river-based models in the calculations that account for the site specific hydrological conditions affecting *k* across the river-estuary transition. In contrast, N_2O flux densities were 0.26 g N_2O m^{-2} yr^{-1} in the Dart and 0.13 g N_2O m^{-2} yr^{-1} in the Tamar, which are similar to densities reported in these estuaries by Barnes and Upstill-Goddard (2011) and below the UK average of 0.61 g N_2O m^{-2} yr^{-1}. Both CH_4 and N_2O flux densities are higher than estimates calculated from average dissolved gas concentrations multiplied by estuary area (Brown *et al.,* 2024), highlighting the importance of incorporating daily average fluxes and site-specific hydrodynamics to capture finer spatial and temporal variability.

Table 2.4. Reported CH_4 and N_2O emissions from the Tamar and Dart estuaries compared to the UK average

Location	**Annual emission (T CH_4 yr^{-1})**	**Flux density (g CH_4 m^{-2} yr^{-1})**	**Annual emission (T N_2O yr^{-1})**	**Flux density (g N_2O m^{-2} yr^{-1})**
UK estuary average (*)	**49.8**	**1.6**	**42.6**	**0.61**
Dart (1)	24.8	2.87	2.23	0.26
Dart (2)	8.40	0.98	0.880	0.1
Tamar (1)	80.2	2.02	5.30	0.13
Tamar (2)	47.0	1.19	3.90	0.1
Tamar (3,4)	62.0	1.8	5.80	0.13

(*) Average UK estuary emissions reported by Brown *et al.,* (2024)

(1) This study

(2) Brown *et al.,* (2024)

(3) Upstill-Goddard and Barnes (2016)

(4) Barnes and Upstill-Goddard (2011)

2.4.2 Spatial variability in GHG emissions along a salinity gradient

DelSontro *et al.,* (2016) demonstrate the use of *k* values to explore degassing along a river transect to determine the GHG transfer from one site to another. The *k* value represents the length of time it should take for a parcel of water to equilibrate with the atmosphere (Raymond *et al.,* 2012). By applying a similar approach here, we can consider the contribution of

river GHG concentrations to estuary fluxes. For example, the average *k* value in the Tamar was 1.9 m d^{-1}, meaning than 1.9 m of water should equilibrate with the atmosphere over 24 hours. The average depth of the sampled river location was 0.9 m, which is 46 % of the average *k*. Therefore, it should take approximately 11 hours (46 % of 24 hours) for the sampled section of river to degas to the atmosphere. By taking the average *Q* during the sampled period (33.4 m^3 s^{-1}) and estimating the volume of water that would need to flow 8 km from the river station to the first sampled position in the estuary (8 km x 40 m width x 0.9 m depth), it would take 140 minutes for the water to pass from the river to the beginning of the sampled estuary transect. Applying the same methods in the Dart, it would take approximately 2 hours for the water to equilibrate with the atmosphere based on an average *k* of 9.3 m d^{-1}, but only 26 minutes for the river water to reach the first sampled position in the estuary (0.64m average depth, 30 m width, 1.29 km distance, 16.1 m^3 s^{-1} average Q). Therefore, the N_2O and CH_4 in theory have sufficient time to be transported downstream from the river into the estuary without degassing to the atmosphere. This transport of N_2O and CH_4 could explain the accumulation of both gases in the Tamar Estuary if we were to assume no other sources. But the Dart displays higher river concentrations and fluxes compared to the estuary suggesting N_2O and CH_4 are lost through river-estuary mixing or biological consumption.

2.5 Conclusion

River emissions of N_2O and CH_4 vary more greatly depending on the applied empirical model used to estimate *k*, compared to estuarine estimates of gas fluxes where *k* models are in better agreement. This is due to the complexity of river variables interacting to drive the transfer of gases across the water surface into the atmosphere, whereas estuarine and coastal fluxes are dominantly driven by surface wind conditions. Therefore, it is advisable to take a median flux calculated from several river models to account for this

variability and provide a best estimate of river emissions of N_2O and CH_4. For estuary and coastal fluxes, the model described by Wanninkhof (2014) has been demonstrated to be an effective tool for calculating GHG emissions. Therefore, it is with confidence that Wanninkhof (2014) will be taken forward to estimate N_2O and CH_4 fluxes along an estuarine salinity gradient and ensure comparable results with other similar studies. By applying these methods to a river-to-coast catchment wide monitoring programme, it should be possible to identify hot spots of GHG emissions in freshwater and estuary waters which could inform a holistic approach to the spatial targeting of NbS to natural sources of N_2O and CH_4.

Chapter 3: Emissions of methane (CH_4) and nitrous oxide (N_2O) along a river-to-coast aquatic continuum and opportunities for nature-based solutions

Abstract:

This study presents observations of methane (CH_4) and nitrous oxide (N_2O) concentrations and estimates of their air-water fluxes through a river-to-coast investigation of the Tamar Catchment, southwest England. Dissolved concentrations ranged between 8 – 43 nmol N_2O L^{-1} and 39 – 510 nmol CH_4 L^{-1} in freshwaters; 9 – 22 nmol N_2O L^{-1} and 17 – 737 nmol CH_4 L^{-1} in the estuary; and 7 – 13 nmol N_2O L^{-1} and 1 – 12 nmol CH_4 L^{-1} in the coastal waters of the L4 station monitored by the Western Channel Observatory (WCO). Estimated emissions revealed that the agriculturally dominated upper headwaters of the Tamar Catchment act as hotspot of both N_2O and CH_4 (average 50.4 µmol N_2O m^{-2} d^{-1} ± 87.3; and 1906.4 µmol CH_4 m^{-2} d^{-1} ± 697.9). In total, the combined annual emissions of the River Tamar and Tamar Estuary were estimated to be 4.6 x 10^6 mol CH_4 yr^{-1} and 6.6 x 10^4 mol N_2O yr^{-1}. Scaling up to the total area of UK estuaries revealed the importance of these contributions compared to other UK sector greenhouse gas (GHG) emissions, which is not currently considered in UK Nationally Determined Contributions (NDC). This study reveals important spatiotemporal variability in N_2O and CH_4 emissions from surface waters. These findings can support evidence-based nature-based solutions (NbS) and other management interventions which target areas most vulnerable to becoming hotspots of GHG production.

3.1 Introduction

Aquatic ecosystems provide extensive ecosystem services (ES) to humanity, supporting biodiversity richness, providing habitat for economically and culturally important fisheries (Wood *et al.,* 2024), storing and slowing floodwater (Puttock *et al.,* 2021), retaining nutrients to alleviate pollution (Puttock *et al.,* 2018; Stutter *et al.,* 2018), and providing climate regulation (Zou *et al.,* 2022). This plethora of ES provided also subjects aquatic ecosystems to hubs of human development and modification, making them among the habitats most vulnerable to land use and the increasing severity of climate change, and are therefore a priority focus of ecological restoration (Liu *et al.,* 2025). However, the potential of these habitats to become increasing sources of GHG needs to be carefully considered in all stages of habitat restoration practices. The relative contribution of rivers, estuaries and coastal habitats to atmospheric GHG concentrations can be altered by the presence of human pressures in the form of environmental pollution through excess nutrient loading (Beaulieu *et al.,* 2019; Upadhyay *et al.,* 2023), modifications to river morphology (Borges *et al.,* 2018), changes to natural hydrological regimes and connectivity (Borges *et al.,* 2019; Wu *et al.,* 2021; Xing *et al.,* 2023), and indirect feedback effects of climate change driven variability in temperature, precipitation, drought and flooding (Dijkstra *et al.,* 2012; Khalil and Rasmussen, 1989).

As previously mentioned, Saunois *et al.,* (2024) report that of the global total natural and indirect sources of CH_4 (305 [108-44] Tg yr^{-1}) between 2000 to 2009, 50 % were from wetlands (153 [116 – 189]), 36 % from inland waters (112 [49 – 202]), minus double counting (-23 [-9 to -36]), and 4 % from coastal and oceanic sources (12 [6-20]). Of the total natural emissions of N_2O (1.8 [1.0 – 3.0] Tg N yr^{-1}) between 1980 - 2020, inland waters, estuaries and coastal vegetation account for 0.1 Tg yr^{-1} (Tian *et al.,* 2024). Management of the hydrological connectivity between habitats along the LOAC is increasingly recognised as important for GHG emissions, with

rivers acting as important C and dissolved inorganic nitrogen (DIN) delivery mechanisms to estuary and coastal ecosystems (Bouwman *et al.,* 2013; Drake *et al.,* 2018; Tye *et al.,* 2024). Over the last four decades, anthropogenic N_2O emissions from inland waters (rivers, lakes, and reservoirs), estuaries and coastal vegetation has increased from 0.1 Tg N yr^{-1} to 0.15 Tg N yr^{-1} due to N additions (Tian *et al.,* 2024). Anthropogenic causes of eutrophication and urban influences on organic matter and nutrient loading is estimated to contribute 30 % to stream and river CH_4 fluxes (Saunois *et al.,* 2024). Management practices of aquatic ecosystems therefore have the potential to reduce emissions of N_2O and CH_4, if targeted interventions are applied (Bhushan *et al.,* 2024; Yang *et al.,* 2020; Zou *et al.,* 2022).

However, challenges remain in accurately quantifying the relative contributions of each aquatic ecosystem type to atmospheric GHG concentrations and therefore limit our ability to identify opportunities to reduce human perturbations to emissions from natural sources. This is largely due to a lack of observations which capture the variability along a river to coast aquatic continuum, often limited by logistical constraints: the large spatial extent of a river system and difficulty accessing representative sections of a watershed's freshwater and saltwater zones (Xenopoulos *et al.,* 2017). This study aims to constrain this variability through a comprehensive monitoring programme of dissolved N_2O and CH_4 concentrations along a river to coast transect. These observations are used to estimate the relative contribution of the river, estuary and coastal waters to fluxes of N_2O and CH_4 to the atmosphere to inform the direction of targeted ecosystem management strategies for controlling natural sources of GHG.

3.2 Methods

3.2.1 Study location

As introduced in Chapter 2, the River Tamar flows south for 98 km from its source towards Plymouth in Southwest England, draining a total catchment area of 1800 km^2 at an average flow rate of 22.9 m^3s^{-1} (National River Flow Archive, 2025a) (Figure 3.1A). The upper catchment is described as responsive with rapid spikes in river flows after rainfall events due to its granite bedrock in the east and west of the catchment (Rawlins *et al.,* 2003). In the lower Tamar, sandstone and mudstone with silt and clay deposits increase towards the Tamar Estuary which is designated for its biodiversity and rich mudflat habitats (Uncles *et al.,* 2003). Much of the Tamar catchment is agricultural with urban sprawl increasing around the Tamar Estuary which borders the City of Plymouth (Morton *et al.,* 2024). The River Tamar meets the Tamar Estuary at an artificial barrier, Gunnislake weir, located 22 km inland. The tidal amplitudes are approximately 5 m during spring tides and 2 m during neap tides (Yang *et al.,* 2016). The Tamar's waters eventually mix with the western English Channel, the location of the long-term monitoring stations of the Western Channel Observatory (WCO) (McEvoy *et al.,* 2023). The current study primarily focuses on samples collected monthly from four freshwater stations along the main axis of the River Tamar between April 2019 to March 2020, and 7 surveys of the Tamar Estuary which took place in May, July, September, and November in 2019, and February and March in 2020. One extra survey took place in July during an intensive study. Mean measurements of seawater N_2O and CH_4 concentrations collected at Station L4 in the WCO between 2011 and 2018 are later considered to enable a comparison of estimated atmospheric fluxes of freshwater and estuary N_2O and CH_4 with coastal records. The locations of all sampling positions are displayed in Figure 3.1.

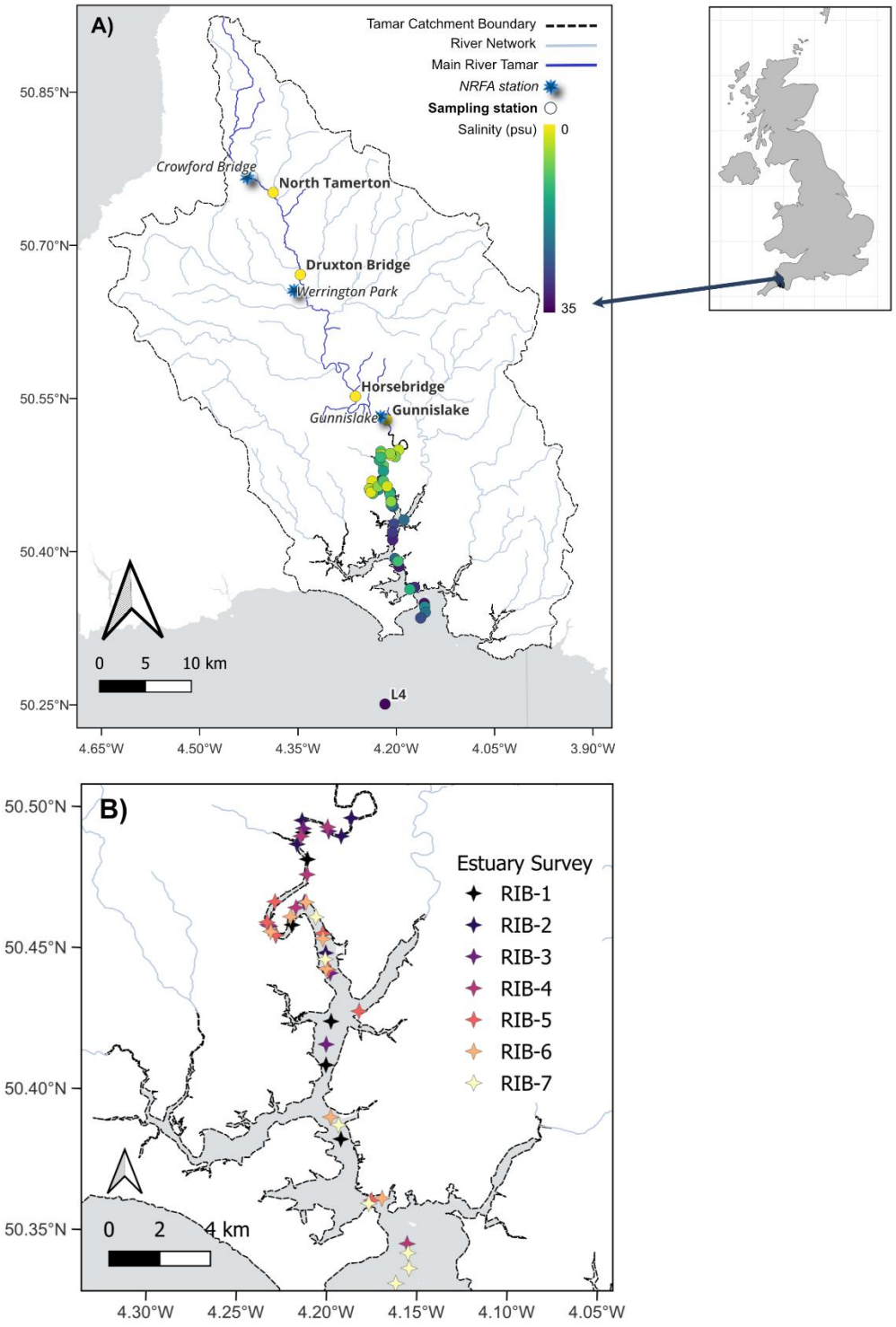

Figure 3.1. Overview of the Tamar Catchment location displaying A) NRFA river gauges and sampled positions along the water continuum coloured by salinity value, and B) sampled positions in the Tamar Estuary coloured by sampling campaign (RIB-1 to RIB-7).

3.2.2 Environmental parameters

River depth (*D* in m), discharge (*Q* in m^3 s^{-1}) and daily rainfall (mm) were obtained from records provided by Defra Hydrology Data Explorer (Environment Agency, www.environment.data.gov.uk/hydrology/explore) for the closest National River Flow Archive (NRFA) gauges upstream of the sampled locations on the main River Tamar; Crowford Bridge, Warrington Park and Gunnislake (Figure 3.1A). To attain a catchment representation of rainfall, the average of the three gauges was used. Daily, 3-day and 30-day average rainfall were explored to account for the effects of variable runoff conditions on river concentrations, and daily, 3-day and 10-day average *Q* was used to account for mixing effects of variable water residence times in the estuary. River width (*W*) was measured using Google Earth Pro and river velocity (*V* in m s^{-1}) was calculated using the formula $V = Q / (D * W)$. River slope (*S*) was measured using shapefiles obtained from the Environment Agency Catchment Data Explorer with the Elevation Profile tool in QGIS (Geographic Information System), version 3.32.3, along a 500 m stretch of the river (250 m upstream and downstream of the sample location) based on guidelines of the River Habitat Survey (Environment Agency, 2022). Each section of river sampled had a gentle *S* gradient (0.01 % to 0.35 %) (Figure 3.2). Average daily wind speed (m s^{-1}) and atmospheric pressure were calculated from measurements made by the Rame Head National Coastwatch Institution (NCI) station (Rame Head NCI, www.nci-ramehead.org.uk). Daily average atmospheric mixing ratios of N_2O and CH_4 used in flux emission estimations were accessed from the Mace Head station via the NOAA Global Monitoring Laboratory (NOAA, www.gml.noaa.gov).

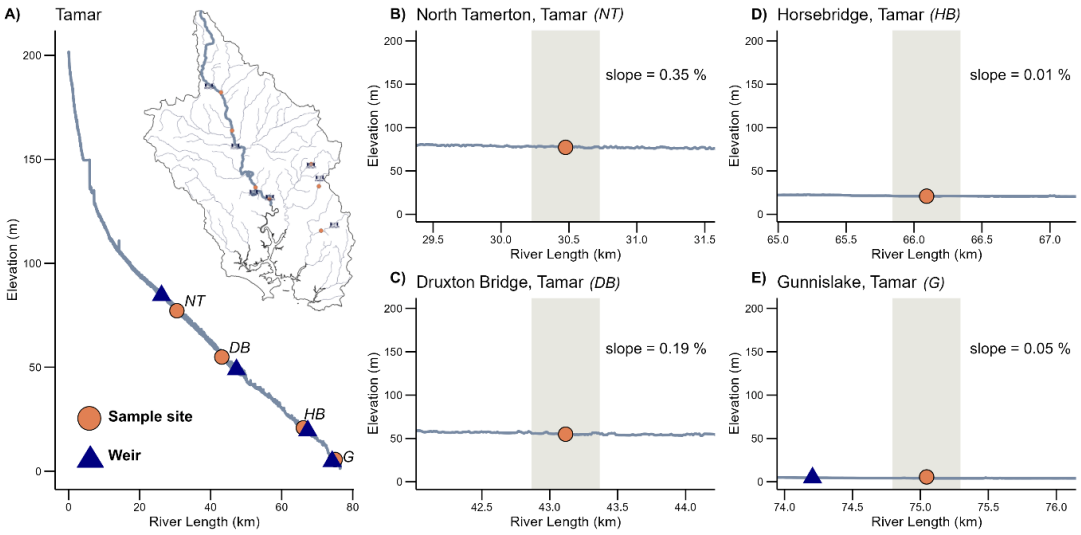

Figure 3.2. Elevation profiles of sampled sections of the River Tamar, showing position of sample sites (orange circles) and weirs (blue triangles). Sections have been magnified to better show slope of each section of river. Greyed out sections represent the 500 m stretch of river used to calculate % slope. A) main River Tamar, B) North Tamerton (*NT*) (S = 0.35 %), C) Druxton Bridge (*DB*) (S = 0.19 %), D) Horsebridge (*HB*) (S = 0.01 %) and E) Gunnislake (*G*) (S = 0.05 %).

3.2.3 Sample water collection

Two field teams were deployed in the catchment to cover the upper freshwater to the lower estuary waters of the Tamar on the same day. Freshwater samples were collected from mid-channel where accessible from a bridge or riverbank. Estuary samples were collected based on a target practical salinity range of 0 to 35 identified using a YSI sonde (YSI PRO30) from a rigid inflatable boat (RIB) (Figure 3.3). All estuary surveys were completed on a falling (ebb) tide, except one of the surveys in July (RIB-2) which took place on a rising (flood) tide and has been included in this study for comparison. In some cases, the first sample was taken closer to the high tide mark compared to others (Figure 3.4).

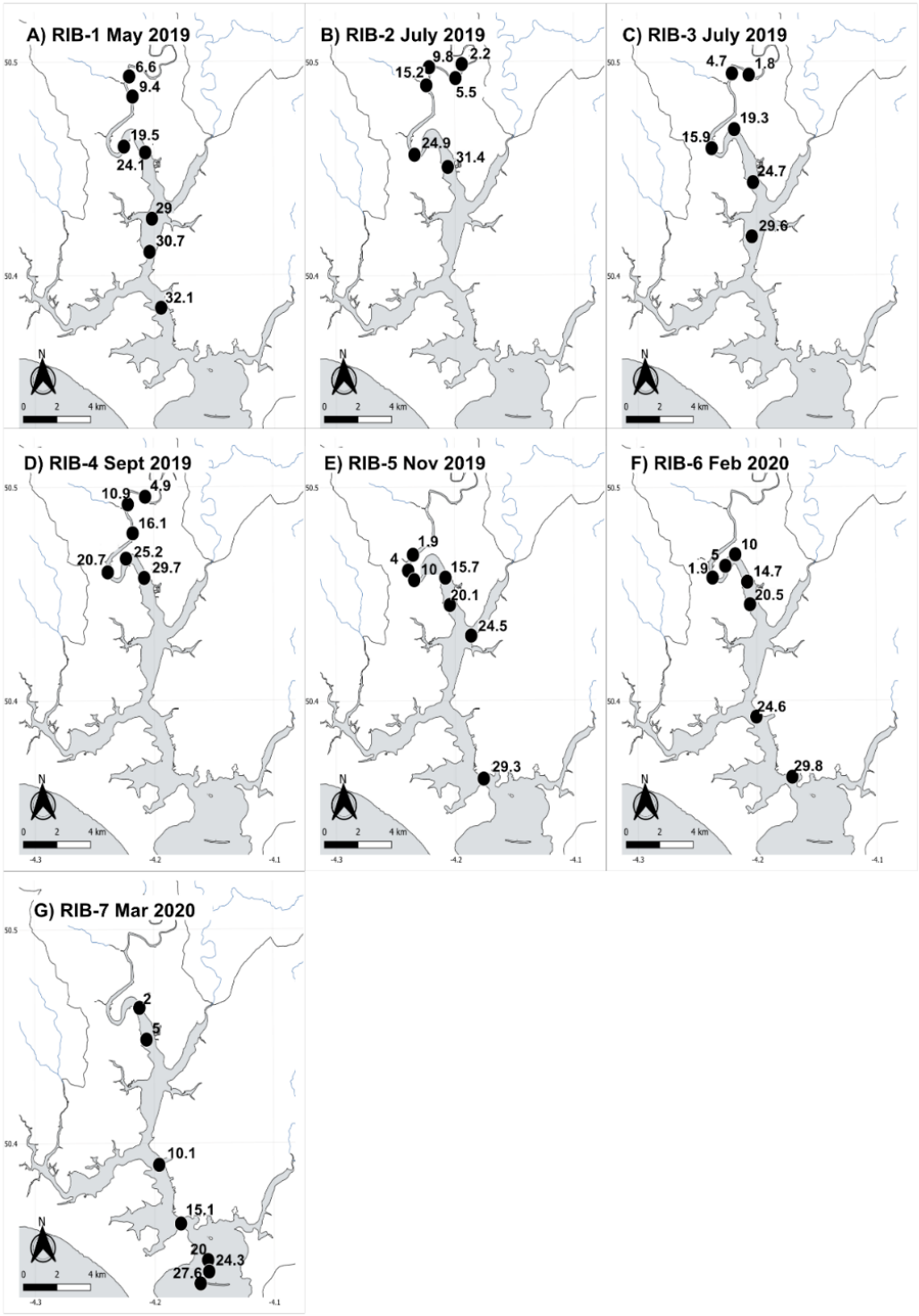

Figure 3.3 Salinity maps of surveys completed in the Tamar Estuary between May 2019 to March 2020

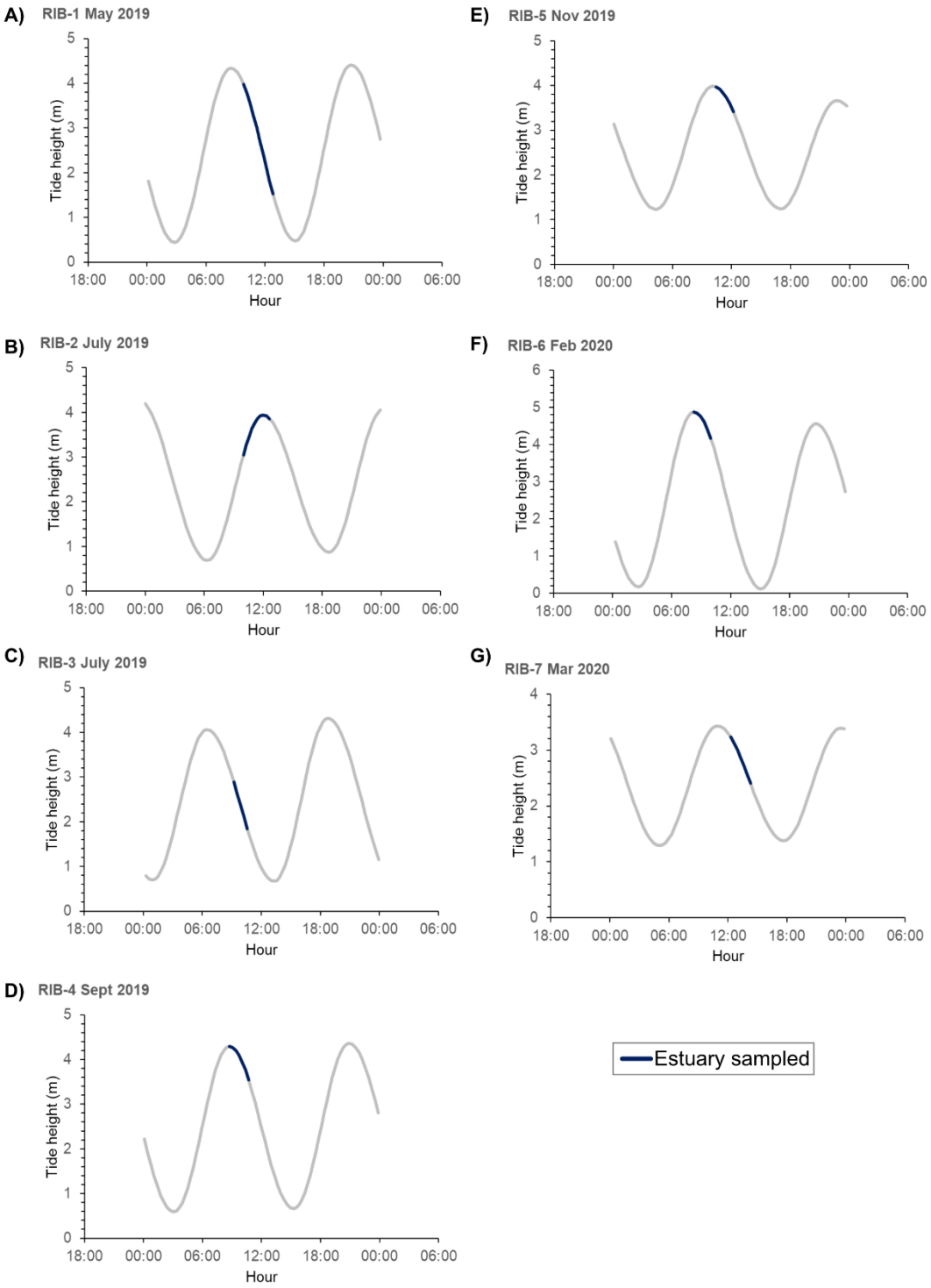

Figure 3.4 Tidal conditions at Devonport, Plymouth during surveys completed in the Tamar Estuary between May 2019 to March 2020

River and estuary samples were collected from the surface (within the upper 30 cm) using a thrice-rinsed bucket from which subsamples for individual analytes were taken. For N_2O and CH_4, this was a 500 ml borosilicate glass bottle, which was allowed to overflow to remove gas bubbles, and which was poisoned with 100 µl saturated mercuric chloride solution before sealing with a glass stopper. Seawater samples at L4 were collected from surface waters (~ 1m depth) using Niskin bottles via clean Tygon tubing following the deployment of a CTD Rosette on Research Vessel Plymouth Quest (Brown and Rees, *in prep*).

3.2.4 Water chemistry measurements

Water temperature and pH were measured using a multiparameter YSI sonde (Model PRO30) placed into a bucket of sampled freshwater or directly into the estuary water.

3.2.5 Dissolved gas concentrations analysis

Samples were analysed in triplicate by single-phase equilibration gas chromatography using electron capture detection for N_2O and flame ionisation detection for CH_4 similar to the methods described by Upstill-Goddard *et al.,* (1996). Samples were calibrated with three certified standards (Air Products Ltd.; mixing ratios 317.4, 406.4, 496.7 ppb N_2O and 1.009, 2.058, 3.04 ppm CH_4 in synthetic air; calibrated against NOAA primaries). Aqueous CH_4 and N_2O concentrations were calculated from the solubility tables of Wiesenburg and Guinasso (1979) and Weiss and Price (1980) respectively.

3.2.6 Dissolved nutrient concentrations analysis

Thrice-rinsed plastic sample bottles were filled from the sampling bucket or container and then transported back to the laboratory for filtering through a 0.45 µm cellulose acetate filter. Freshwater samples were analysed for nutrients at the Centre for Ecology and Hydrology using methods described by Tye *et al.,* (2020) and were below detection for ammonium and nitrite. Estuary and coastal samples were analysed at Plymouth Marine Laboratory and determined using methods described by described by Mantoura and Woodward (1983) for ammonium, Brewer and Riley (1967) for nitrate and nitrite combined, Graßhoff (1976) for nitrate only, Zhang and Chi (2002) for phosphate, and Kirkwood (1989) for silicate. Samples were handled with nitrile gloves to prevent contamination, particularly in coastal waters where nutrient concentrations are expected to be relatively low.

3.2.7 Coloured dissolved organic matter analysis

Thrice rinsed, 14 mL amber glass bottles were filled with filtrate (0.45 µm cellulose acetate) for spectrophotometric determination of chromophoric dissolved organic matter (CDOM) absorbance. Absorbance spectra were collected on a VWR UV3100 PC with a 10 mm quartz cuvette. Spectra were referenced against analytical grade water (Millipore, Milli-Q) and drift-corrected by subtracting the average absorbance between 680-700 nm. The decadic absorbance at 254 nm was used as a relative measure of CDOM absorbance here.

3.2.8 Estimating air-water diffusive flux of N_2O and CH_4

The diffusive flux of N_2O and CH_4 across the air-water boundary was calculated using Equation 2.1 as described in Chapter 2 section 2.2.4. The parameters influencing the gas transfer velocity k_{GHG} differ between river,

estuary and coastal systems depending on whether the turbulence is primarily induced by wind shear at the sea surface or bed shear at the bottom of the water column in rivers and sheltered, shallow estuaries (Raymond and Cole, 2001). Several empirical models have been developed to estimate k_{GHG} and are widely used in calculations of gas fluxes from aquatic ecosystems. Chapter 2 provided a comparison of models commonly applied in scientific literature and gives the equations and key parameters used for each model in Table 2.3.

In this study, estimates of k_{GHG} in freshwater locations were obtained using the median k_{GHG} values of all 8 river-based models compared in Chapter 2. The Borges *et al.,* (2004) (B04) model calculates k_{GHG} as a function of D and V, whilst the 7 models from Raymond *et al.,* (2012) (R1 – R7) include additional parameters such as S and Q. By taking the median value of these models, I aim to account for variability in the dominant hydrological river conditions driving gas exchange at the water surface at the time of sampling.

For estuary and coastal stations, k_{GHG} was estimated using the windspeed-based model described by Wanninkhof (2014) due to the little variability found between it and other models commonly used to estimate estuary GHG fluxes. The ratio of kinematic viscosity of water over the diffusivity of the gas was calculated according to Wanninkhof (2014) to produce Schmidt numbers (Sc_{GHG}) for each gas under the temperature and salinity conditions measured in the field.

3.2.9 Statistical analysis

A Shapiro-Wilk test was used to determine normality, followed by either a Kruskal-Wallis test or ANOVA to assess statistically significant spatial and seasonal differences in dissolved GHG concentrations measured along the

main River Tamar and Tamar Estuary. Data were binned into seasons defined as Spring (March – May), Summer (June – August), Autumn (September – November) and Winter (December – February). A Spearman's rank correlation was performed to assess relationships between environmental and biogeochemical variables and N_2O and CH_4 concentrations respectively in river and estuary locations. A principal component analysis (PCA) was applied to further identify key seasonal and spatial relationships between environmental and biogeochemical variables influencing observations of N_2O and CH_4 concentrations. All statistical tests were performed in R version 2024.12.0 using the 'Tidyverse' (Wickham *et al.,* 2019) and 'factoextra' R packages (Kassambara and Mundt, 2020).

3.3 Results

3.3.1 Environmental variability

During the sampling period, *Q* ranged between 0.08 $m^3 s^{-1}$ and 255 $m^3 s^{-1}$ across the three gauges considered along the main River Tamar (Figure 3.5A). Crowford Bridge and Werrington Park are in the upper part of the catchment and therefore receive a considerably smaller proportion of the catchment runoff. In contrast, Gunnislake drains an area of 917 km^2, roughly 50 % of the total catchment area. Lowest flows were therefore unsurprisingly recorded at the most upstream gauge, Crowford Bridge, in July 2019 and highest were recorded at the most downstream gauge, Gunnislake, in January 2020. A seasonal effect can be seen as a response to the total daily average rainfall, which ranged from 0 mm to 47 mm. This seasonal pattern generally reflects lower rainfall in spring and summer and higher rainfall during autumn and winter. River water temperatures ranged between 6.1 °C and 20.0 °C (Figure 3.5B and 3.5C), again showing a seasonal pattern with temperatures increasing in June to September and declining from October to March. Estuary temperatures displayed the same pattern, ranging between 6.4 °C to 22.9 °C.

3.3.2 Spatiotemporal variability of N_2O and CH_4

Mean dissolved concentrations of N_2O and CH_4 varied both temporally and spatially across the water continuum. River N_2O concentrations varied between 8.2 and 42 nmol L^{-1} (Figure 3.5B) and CH_4 between 38.8 and 510.4 nmol L^{-1} (Figure 3.5C). Spatially, N_2O and CH_4 concentrations most often decreased moving from the upstream to downstream sites. At all four river stations the highest N_2O concentrations were measured in October 2019, coinciding with an increase in both rainfall and *Q*, showing a markedly higher concentration in the upper reaches of the catchment compared to sites downstream. Whilst a Kruskal-Wallis test indicated no significant differences between N_2O concentrations among the sampled river stations (χ^2 = 1.86, *df* = 3, *p* = 0.6), there were significant differences between seasons (χ^2 = 24.93, *df* = 3, *p* = < 0.05). Specifically, N_2O measurements were significantly higher in autumn (September – November) (*Z* = 3.06, *p* = 0.01) and spring (March – May) (*Z* = 3.13. *p* = < 0.01) compared to summer (June – August), and significantly lower in summer compared those in winter (December – February) (*Z* = -4.7, *p* = < 0.01).

CH_4 concentrations showed greater variability between sites along the river, with higher concentrations observed at the upstream sites, North Tamerton and Druxton Bridge. Significant differences in measured CH_4 concentrations were found between sampled river stations (χ^2 = 19.93, *df* = 3, *p* = < 0.05). Post-hoc pairwise comparisons using Dunn's test with Bonferroni correction showed that the most upstream site, North Tamerton, had significantly higher concentrations than Horsebridge (*Z* = -3.07, *p* = < 0.05) and Gunnislake (*Z* = -4.22, *p* = < 0.05). No other significant differences were found between other stations or seasons (*p* = >0.05).

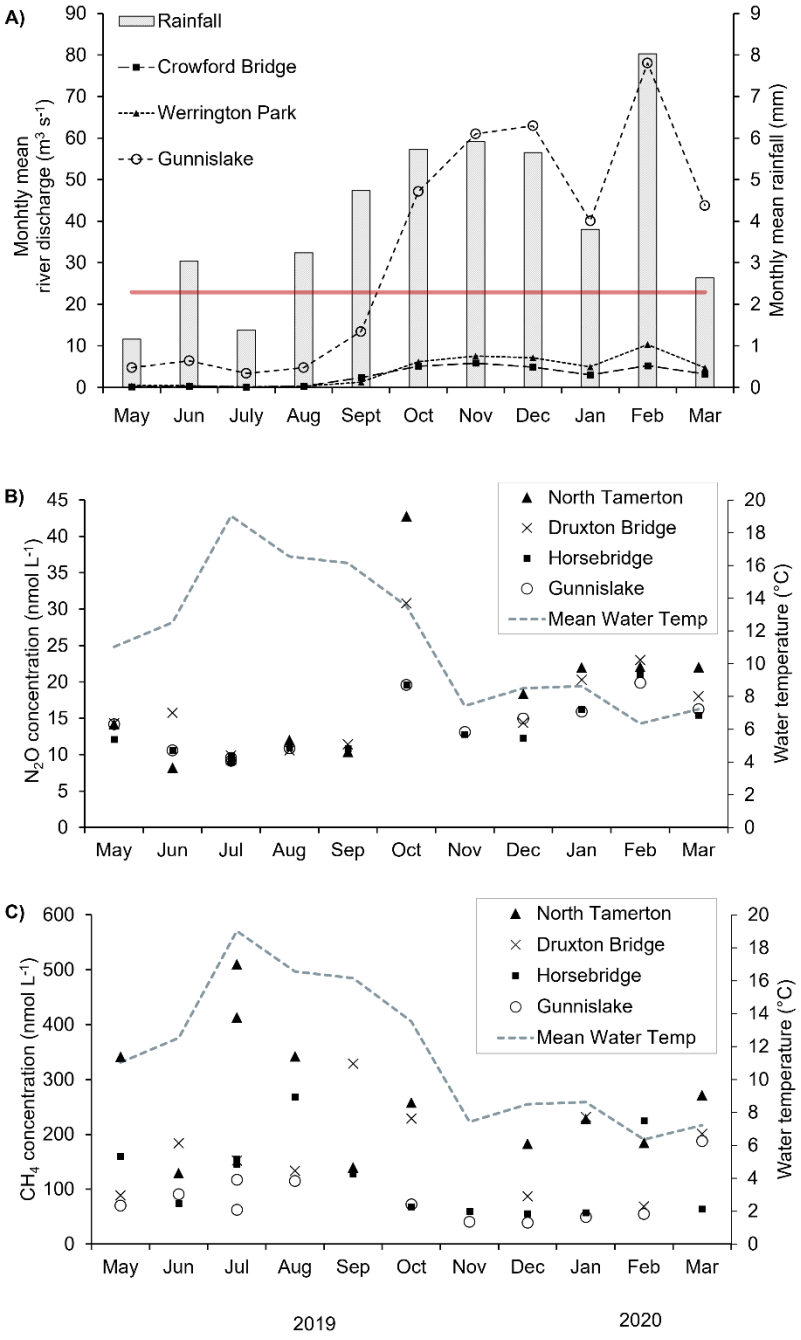

Figure 3.5. A) hydrological conditions during the sampling campaign. The red line shows the annual mean discharge for the Tamar catchment at 22.9 m^3 s^{-1}. B) dissolved N_2O concentrations and mean water temperature, and C) dissolved CH_4 concentrations and mean water temperature measured at the four freshwater sampling stations on the River Tamar. The stations are shown in the figure legend in order from upstream to downstream; North Tamerton, Druxton Bridge, Horsebridge and Gunnislake.

Estuary N_2O concentrations ranged between 8.8 and 21.6 nmol L^{-1} (Figure 3.6A) and CH_4 from 16.5 to 737 nmol L^{-1} (Figure 3.6B). Other than in March 2020, estuary observations of both N_2O and CH_4 show an overall non-conservative mixing behaviour, decreasing as the transect moved towards higher salinity values. A production of N_2O can be seen in the mid estuary (salinity 10 – 15) in September and November 2019 and a production of CH_4 in the mid estuary in February 2020. A Kruskal-Wallis test showed significant differences between N_2O concentrations along the salinity gradient (X^2 = 19.41, df = 5, p = < 0.05). Dunn's post-hoc test with Bonferroni correction confirmed N_2O concentrations were significantly higher in samples from within the salinity target 10 than salinity target 30 (Z = 3.02, p = 0.04). An ANOVA revealed a significant seasonal effect on estuary N_2O concentrations (F(3, 29) = 3.30, p = 0.03), further identified through a Turkey's HSD post-hoc test as significantly lower summer concentrations compared to autumn (mean difference = −4.05, p = 0.02). No significant differences in CH_4 concentrations were found among salinity targets (F(5, 27) = 0.51, p = 0.77), but concentrations were significantly lower in winter compared to autumn (Z = -3.19, p-value = <0.01) and spring (Z = -2.76, p = <0.05). These spikes in observed N_2O and CH_4 concentrations coincide with extremes in fluvial inputs to the estuary, with Q measuring 3.37 m^3 s^{-1} on the sampled day in September 2019, less than half the annual average river flow, and 67.3 m^3 s^{-1} in February 2020, almost four times above the average river flow.

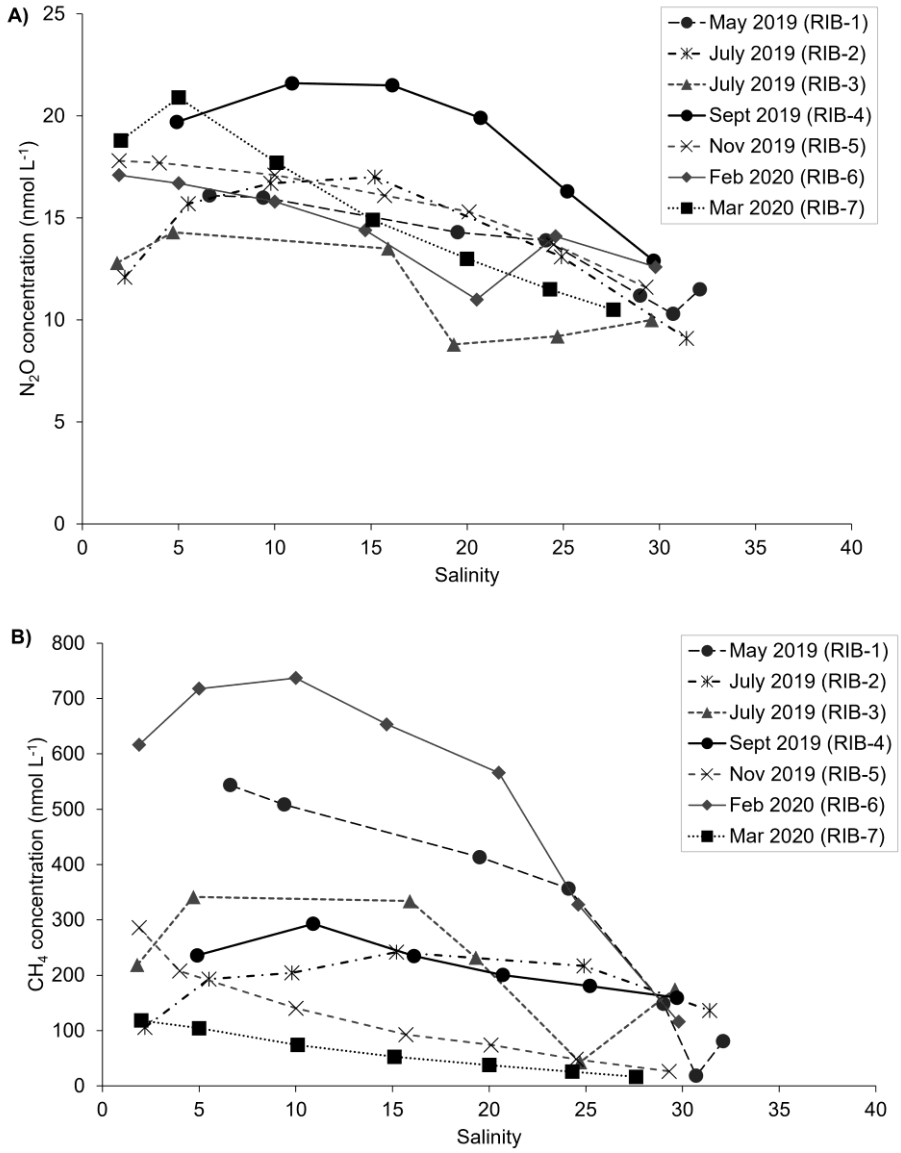

Figure 3.6. Dissolved concentrations of A) N_2O and B) CH_4 measured across 7 sampling campaigns in the Tamar Estuary between 2019 and 2020

3.3.3 Relationship of GHG concentrations to hydrological and hydrochemical water variables

River data were grouped by station to explore differences in correlations of river GHG concentrations with hydrological and hydrochemical variables at the four represented sections of the River Tamar (Figure 3.7). Relationships with N_2O are shown in Figure 3.7A and those with CH_4 are in Figure 3.7B.

At all river stations, mean N_2O concentrations were negatively correlated with water temperature (r = -0.65 to -0.76, p = < 0.05, n = > 10). N_2O concentrations were significantly negatively correlated with pH at North Tamerton (r = -0.66, p = 0.03, n = 11), Druxton Bridge (r = -0.72, p = 0.02, n = 10) and Horsebridge (r = -0.66, p = 0.02, n = 12) and conductivity at North Tamerton (r = -0.72, p = 0.02, n = 11). All stations displayed significant correlations between N_2O concentrations and river discharge (Q) (r = >0.65, p = < 0.05. n = > 10). N_2O concentrations were most positively significantly correlated with the 30-day average rainfall (r = >0.65, p = < 0.05, n = >10) compared to the daily or 3-day average at all sites. Horsebridge and Gunnislake, stations furthest downstream, showed a significantly positive correlation with CDOM (r = >0.66, p = < 0.05, n = >11) and NO_3^- (r = >0.64, p = < 0.05, n = >11).

River CH_4 presented fewer significant relationships compared to observations between N_2O and environmental variables. No significant correlations were found between CH_4 and water temperature or pH. CH_4 concentrations at Horsebridge show a significant strong positive relationship with conductivity (r = 0.68, p = 0.02, n = 12), and significant negative relationships with hydrological influences including Q (r = -0.62, p = 0.03, n = 12), V (r = -0.64, p = 0.03, n = 12) and 30-day average rainfall (r = -0.64, p = 0.03, n = 12). Significantly negative correlations were found between NO_3^- and CH_4 at North Tamerton (r = -0.69, p = 0.02, n = 11) and Horsebridge (r = -0.61, p = 0.04, n = 12).

A)

N_2O

Upstream to downstream

Station	North Tamerton	Druxton Bridge	Horsebridge	Gunnislake
Water Temp	-0.65 *	-0.70 *	-0.76 **	-0.74 *
pH	-0.66 *	-0.72 *	-0.66 *	-0.55
Conductivity	-0.72 *	-0.59	-0.55	-0.51
Q	0.65 *	0.76 *	0.80 **	0.75 *
30-Day Avg. Rainfall	0.71 *	0.73 *	0.72 *	0.65 *
CDOM	0.35	0.27	0.71 *	0.66 *
NO_3^-	0.45	0.59	0.71 **	0.64 *
PO_4^{3-}	0.57	-0.10	0.15	-0.21

ρ 1 0.5 0 -0.5 -1

B)

CH_4

Upstream to downstream

Station	North Tamerton	Druxton Bridge	Horsebridge	Gunnislake
Water Temp	0.52	0.25	0.39	0.34
pH	0.25	-0.07	0.49	0.42
Conductivity	0.26	-0.15	0.68 *	0.37
Q	-0.59	-0.13	-0.62 *	-0.34
30-Day Avg. Rainfall	-0.28	0.21	-0.64 *	-0.15
CDOM	-0.50	0.49	-0.30	-0.27
NO_3^-	-0.69 *	-0.03	-0.61 *	-0.41
PO_4^{3-}	-0.35	0.39	-0.04	0.33

ρ 1 0.5 0 -0.5 -1

Figure 3.7. Spearman's Rank Correlation matrix of river samples. Correlation coefficients of A) N_2O concentrations with hydrological and hydrochemical variables B) CH_4 concentrations with hydrological and hydrochemical variables

* Correlation significant at the 0.05 probability level

** Correlation significant at the 0.01 probability level

In the estuary, CH_4 concentrations were positively correlated with tidal amplitude (r = 0.85, p = < 0.001, n = 35) and nitrite (r = 0.38, p = 0.02, n = 35), and negatively correlated with rainfall (r = -0.43, p = 0.01, n = 35). N_2O concentrations in the estuary showed a positive relationship with CDOM (r

= 0.60, p = < 0.001, n = 35), ammonium (r = 0.40, p = 0.02, n = 35), nitrate (r = 0.51, p = < 0.001, n = 35) and silicate (r = 0.46, p = 0.01, n = 35), and were negatively correlated with salinity (r = -0.47, p = < 0.001, n = 35). Estuary samples were then binned into salinity 'targets' of 0, 5, 10, 15, 20, 30 and 35 to identify any spatially important correlations along the sampled salinity gradient. No further information was gained on correlations with CH_4, but this grouping did reveal that N_2O concentrations strongly correlated with the 10-day average river discharge at salinities in target 5 (r = 0.79, p < 0.05, n = 7), indicating freshwater inputs are important for concentrations in the lower salinity region of the upper estuary. Whilst not statistically significant, tidal amplitude showed an increasingly positive correlation with N_2O at higher salinity values. A strong positive relationship between N_2O and PO_4^{3-} for samples in salinity target 15 (r = 0.89, p = 0.03, n = 6) was also identified.

3.3.4 Principal Component Analysis

The PCA provided further understanding of spatial and temporal variance in relationships of GHG to hydrological and hydrochemical variables. After data cleaning, 44 river observations were used, representing the four stations on the main River Tamar (North Tamerton, n = 11; Druxton Bridge, n = 10; Horsebridge, n = 12; Gunnislake, n = 11). These were also grouped into spring (Mar – May, n = 8), summer (Jun – Aug, n = 15), autumn (Sept – Nov, n = 9), and winter (Dec – Feb, n = 12). A total of 65.9 % of the variance can be explained (Dim1 42.9%, Dim2 23%) (Figure 3.8). Two key insights can be taken from this figure. First, there is a contrast between conditions correlated to observations in winter and summer samples. Winter conditions can be characterised by higher river flows, rainfall and nitrate concentrations, which also aligns with higher N_2O concentrations, whereas summer conditions leading to warmer water temperatures show closer alignment with higher CH_4 concentrations, phosphate and CDOM. The loadings of spring and autumn are represented in all dimensions, likely caused by variability in the river flows and temperatures sampled during these months, rather than extreme differences in weather conditions as

expected between summer and winter. Secondly, there is a difference between the dominant mechanisms in the upper vs the lower catchment. North Tamerton and Druxton Bridge (upstream sites) in the upper PCA dimension aligned more closely with CDOM, phosphate and CH_4 concentrations, whereas most Horsebridge and Gunnislake (downstream sites) samples fall into the lower dimension and were more correlated to river flows, nitrate and rainfall.

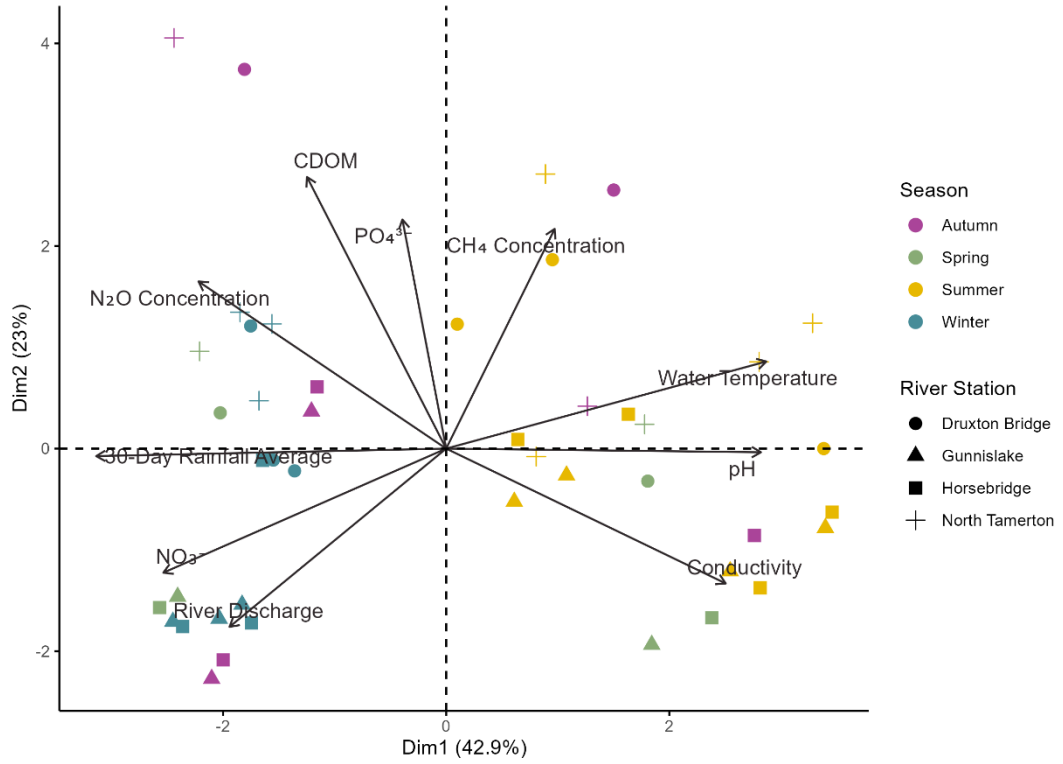

Figure 3.8. Principal Component Analysis (PCA) biplot representing freshwater samples. Seasons are indicated by green (spring; Mar - May), yellow (summer; Jun - Aug), pink (autumn; Sept - Nov), and blue (winter; Dec - Feb). River stations are differentiated by shape. The first two dimensions explained 65.9 % of the total variance (Dim 1 42.9 %, Dim 23%). The vectors (shown in black lines) direction and length indicate each variables contribution to the first two dimensions.

The estuary PCA was performed on 33 observations grouped by season (spring, *n* = 9; summer, *n* = 9; autumn, *n* = 10; winter, *n* = 5). A total of 62.9 % of the variance can be explained (Dim1 34.8%, Dim2 28.1%) (Figure 3.9). The most interesting findings that emerge are the close grouping of high ammonium, CDOM and N_2O concentrations. All nutrients, CDOM and GHG concentrations were higher in the lower salinity values in the upper section of the estuary, with nitrate and silicate also largely correlated to higher river inputs and rainfall. A seasonal impact of water temperature can be seen, with winter characterised by high river flows bringing cool, silicate- and nitrate-rich freshwater into the estuary, whereas the PCA loadings for summer samples indicate low freshwater inputs and warmer estuary temperatures with higher nitrite concentrations. Again, spring and autumn samples are more sporadically placed, indicating more variability in the weather conditions sampled during those months.

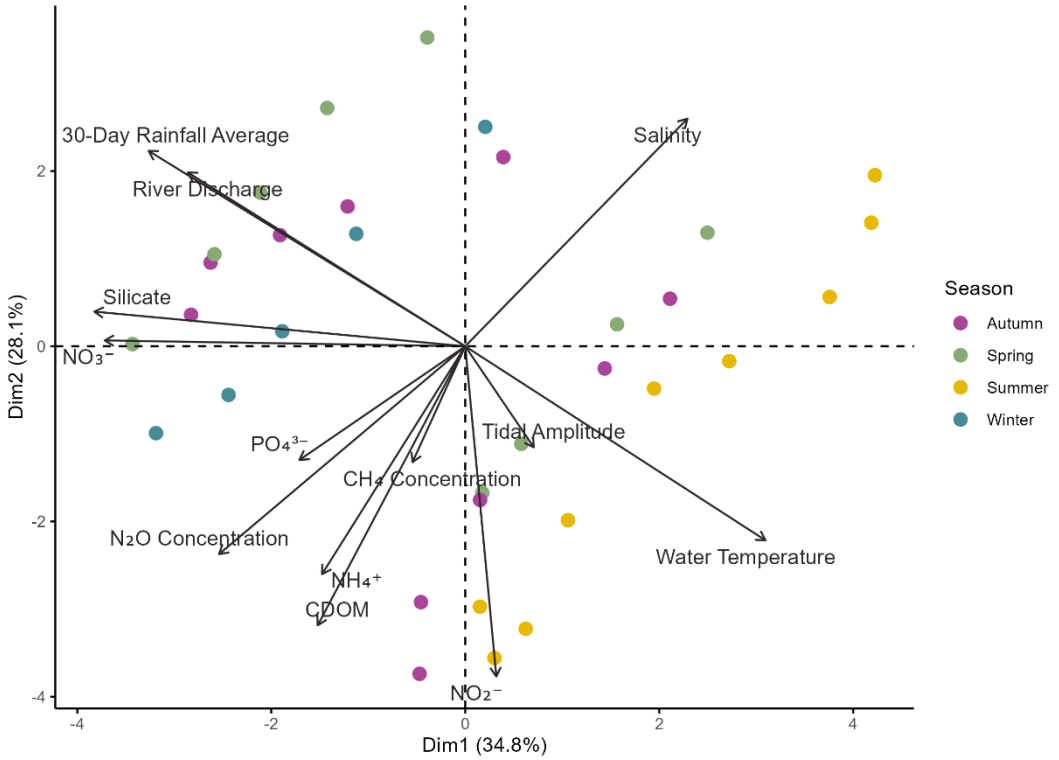

Figure 3.9. Principal Component Analysis (PCA) biplot representing estuary samples. Seasons are indicated by green (spring; Mar - May), yellow (summer; Jun - Aug), pink (autumn; Sept - Nov), and blue (winter; Dec - Feb). The first two dimensions explained 62.9% of the total variance (Dim 1 34.8%, Dim 2 28.1%).

3.3.5 Relative contributions to GHG fluxes

The emission fluxes for each sampling station are grouped by waterbody type and displayed as a whisker plot to show the relative contribution of river, estuary and coastal waters of the Tamar catchment to seasonal fluxes of N_2O (Figure 3.10A) and CH_4 (Figure 3.10B). A Signed-Log transformation was applied to enable visual comparison and retain negative flux values. In both cases, river and estuary surface waters more often acted as a source rather than sink in contrast to coastal waters. The untransformed values for each environment are summarised in text here and in Table 3.1.

The median values of all river stations show the largest N_2O emissions in the winter (11.1 μmol m^{-2} d^{-1} ± 32.6), with the river overall acting as a small sink during summer (-0.25 μmol m^{-2} d^{-1} ± 9.55). The estuary was a continuous source of N_2O across all seasons, with smallest emissions in the summer (median 0.87 μmol m^{-2} d^{-1} ± 0.48) and largest in the autumn (median 6.46 μmol m^{-2} d^{-1} ± 3.02). Coastal waters of L4 are generally very close to equilibrium with the atmosphere, overall acting as a small sink but with a low, positive flux to the atmosphere in the summer (median 0.48 μmol m^{-2} d^{-1} ± 0.9).

CH_4 emissions were substantially higher in river and estuary waters compared to the coast. Median river flux emissions were consistently positive with little variation between seasons (range 151 μmol m^{-2} d^{-1} ± 737 to 314 μmol m^{-2} d^{-1} ± 894). Estuary CH_4 emissions show greater seasonal variability compared to N_2O, smallest in summer (32.9 μmol m^{-2} d^{-1} ± 30.3) and largest during winter (1012 μmol m-2 d-1 ± 379). Flux emissions in coastal waters behaved similarly to N_2O in acting as a CH_4 sink majority of the time, reflecting the relatively low dissolved concentrations of CH_4, with a small flux to the atmosphere in summer (0.2 μmol m^{-2} d^{-1} ± 1.1).

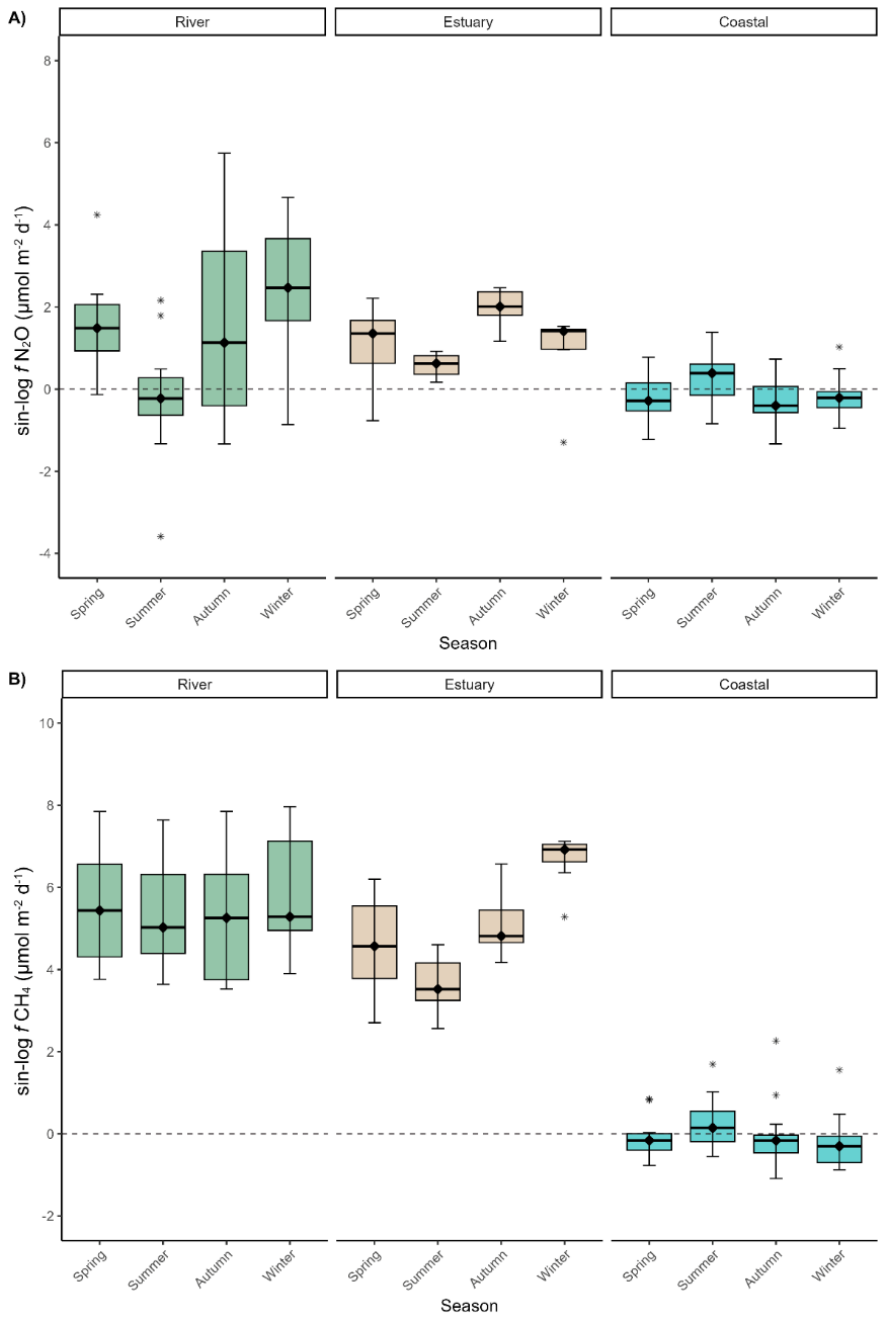

Figure 3.10. Whisker plots showing seasonal variability in estimated fluxes of A) N_2O and B) CH_4 in river (green), estuary (brown) and coastal (blue) waters. Boxes contain the 25th to 75th percentiles of the dataset with black horizontal lines denoting the median value (50th percentile). Black whiskers show the 5th to 95th percentile, with grey stars to symbolise outliers from these bounds.

Mapping the average fluxes (Figure 3.11) reveals the upper river catchment was an important hotspot of both N_2O and CH_4 emissions and relatively little emission contributions came from coastal waters. Average river fluxes were largest at the northernmost river site at North Tamerton (N_2O 50.4 µmol m^{-2} d^{-1} ± 87.3; CH_4 1906 µmol m^{-2} d^{-1} ± 698) and smallest at Horsebridge (N_2O 1.0 µmol m^{-2} d^{-1} ± 2.2; CH_4 61.3 µmol m^{-2} d^{-1} ± 43.5).

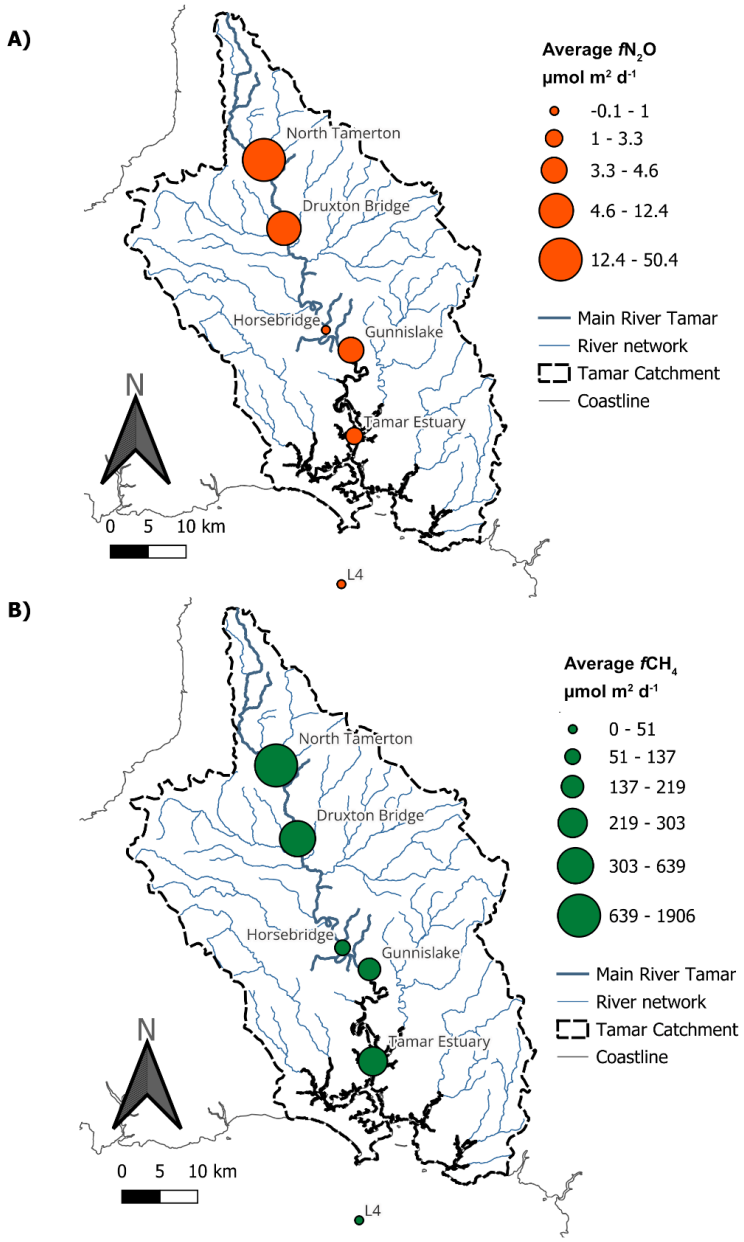

Figure 3.11. Spatial variability in average A) N_2O and B) CH_4 fluxes in the Tamar catchment from river-to-coast

Table 3.1. Range, average and standard deviation of environmental conditions, nitrous oxide (N_2O) and methane (CH_4) for each study location. (***Average*** *+/- SD)*. *Q* = river discharge.

Station	**Type**	**Water Temp (°C)**	**Salinity**	***Q*** **m^3 s^{-1}**	**N_2O nmol L^{-1}**	***f*N_2O µmol m^2 d^{-1}**	**CH_4 nmol L^{-1}**	***f*CH_4 µmol m^2 d^{-1}**
North Tamerton	River	6.3 - 19.0	0	0.1 - 5.91 *(**1.75** ± 1.90)*	8.2 - 42.8 *(**17.47** ± 9.61)*	-35.1 – 311.4 *(**50.4** ± 87.3)*	119.1 - 510.4 *(**273.03** ± 119.14)*	651.2 – 2877.5 *(**1906.4** ± 697.9)*
Druxton Bridge	River	6.1 – 20	0	0.13 -14.7 *(**3.29** ± 4.36)*	9.9 - 30.8 *(**16.84** ± 6.47)*	0.0 – 46.8 *(**12.4** ± 15.7)*	68.6 - 328.7 *(**170.48** ± 80.93)*	98.3 – 1205.2 (***385.6*** ± *316.6*)
Horsebridge	River	6.4 - 19.9	0	3.07 - 99.8 *(**27.36** ± 29.97)*	9.0 - 21.0 *(**13.40** ± 3.86)*	-1.4 – 5.1 (***1.0*** ± *2.2)*	55.6 - 267.9 *(**121.58** ± 71.35)*	33.0 – 195.7 (***61.3*** ± *43.5)*
Gunnislake	River	6.6 - 19.8	0	3.07 - 99.8 *(**27.36** ± 29.97)*	3.7 - 19.9 *(**14.03** ± 3.75)*	-2.8 – 21.9 (***4.6*** ± *7.2)*	38.8 - 187.7 *(**81.79** ± 44.26)*	72.8 – 530.5 (***175.6*** ± *120.2)*
Tamar Estuary	Estuary	6.4 - 22.9	1.8 - 34.1	3.07 - 67.3 *(**24.35** ± 26.44)*	8.8 - 21.6 *(**14.69** ± 3.34)*	-2.7 – 10.8 (***3.3*** ± *3.2)*	16.5 – 737 *(**235.96** ± 194.07)*	12.0 – 1236.9 (***261.4*** ± *336.9*)
L4	Coast	8.0 – 17.6	33.5-35.7	-	7.08 – 13.76 *(**9.69** ± 1.12)*	-2.8 – 3.0 (***-0.1*** ± *0.9)*	1.05 – 11.74 *(**2.92** ± 1.57)*	-2.0 – 8.6 (***0.2*** ± *1.5)*

3.4 Discussion

3.4.1 River-to-coast GHG variability

This study provides a valuable description of GHG variability along a river-to-coast continuum, demonstrating the complexity in disentangling distinct drivers of GHG production between river, estuary and coastal ecosystems. The results agree with a growing number of observations that headwaters are an important source of N_2O and CH_4, supporting the case for spatial targeting of site specific interventions to reduce river emissions (Borges *et al.,* 2019; Hu *et al.,* 2016; Marzadri *et al.,* 2021; Saunois *et al.,* 2024a; Tian *et al.,* 2024). Both GHG concentrations were on average highest in the upper freshwater reaches of the Tamar, which can be characterised by relatively exposed, narrow and shallow river channels, lower river flows and dominated by agricultural land use. Dissolved GHG produced by microbial processes in agricultural soils can enter streams and rivers during high precipitation and run off events (Lu *et al.,* 2021; L. Tian *et al.,* 2019). Tracer experiments have found that the Upper Tamar receives sediment from eroded river channels and pasture land (Smith and Blake, 2014) and bankside erosion, poor soil management and poor nutrient management continue to be Reasons for Not Achieving Good (RNAG) by the Water Framework Directive (WFD) classification system. These inputs could explain the higher average concentrations of both N_2O and CH_4 in these headwaters, or it could be a result of the shallow, exposed channels where there is greater vulnerability to nutrient loading and increased summer water temperatures driving microbial respiration.

Visual declines in GHG concentrations can be seen between the upstream and downstream freshwater study locations. Significant correlations with hydrological conditions suggest this is a result of dilution, gradual outgassing and/or consumption of GHG moving along the river transect.

N_2O and CH_4 concentrations at Horsebridge and Gunnislake showed greater correlation with NO_3^- availability (Figure 3.7). This could suggest the importance of riverine delivery of elevated nutrient inputs as we transition to river sections draining a larger catchment area, or increasing sources of urban wastewater which could lead to enhanced N_2O via greater ammonium availability for nitrifying bacteria, and increased substrate availability for CH_4 production via anaerobic methanogenesis (Evans *et al.,* 2019; Hanson and Hanson, 1996) in the lower sections of the Tamar estuary. These findings add to similar reports of N_2O and CH_4 across rural-urban interfaces, where diffusive agricultural pollution, urban wastewater and varying hydrological conditions have been found to drive variability in hotspots of GHG (Brown *et al.,* 2023; Que *et al.,* 2023).

Freshwater flushing times in the Tamar Estuary range between 6.5 to 13.5 days, and can be twice as long during neap tides compared to spring tides (Uncles and Torres, 2013). Our observations of estuarine GHG suggest freshwater flushing of the estuary system is important for dissolved N_2O and CH_4 variability. Elevated N_2O concentrations were observed, particularly in in the upper to mid estuary regions within salinity values of 5 – 15, during the September sampling event (Figure 3.6). This coincides with a small increase in river flows, though they remained below average (Figure 3.5). This observation is similar to previous observations in the Tamar (Law *et al.,* 1992; Upstill-Goddard and Barnes, 2016) and other mixed temperate estuaries (Brown *et al.,* 2022; Harley *et al.,* 2015), where interactions between variable freshwater inputs and the estuary Turbidity Maximum Zones (TMZ) have been recognised as important for GHG cycling. The Tamar TMZ retains suspended particulate matter (SPM) from fluvial sources within lower salinity regions of the estuary, with increasing tidal range leading to resuspension of bed sediments and enhanced levels of SPM (Uncles and Stephens, 1993). Most of the estuary observations in this study commenced at high tide and followed the tide out. Changes in hydrological dynamics may lead to increased CH_4 oxidation (CH_4 removal) by methanotrophs (Abril *et al.,* 2007) and enhanced nitrification (N_2O

production) (Barnes and Upstill-Goddard, 2011). Whilst freshwater input can be an important source of estuarine N_2O, low summer river flows can increase the flushing time of estuaries and reduce the dilution of nutrient concentrations in the upper estuary region (Huggett *et al.,* 2021b). Together with warmer water temperatures and depleted oxygen, this could have facilitated enhanced denitrification in estuary sediments and within the water column resulting in an accumulation of N_2O in the low salinity surface waters of the estuary (Abril *et al.,* 2000; Law *et al.,* 1992).

Bioturbation under warmer temperatures during this time may also have contributed to elevated N_2O concentrations, driven by increased sedimentation of organic material and increased microbial remineralization of ammonium leading to nitrification (Law *et al.,* 1991). Whilst exploring their impact is beyond of the scope of this paper, the Tamar is also impacted by the release of sewage and untreated wastewater during storm overflows which can enhance levels of ammonium and particulates available for nitrifying bacteria (Barnes and Upstill-Goddard, 2011; Law *et al.,* 1992). The strong positive relationship between N_2O and PO_4^{3-} could suggest an impact of wastewater entering the upper to mid-estuary, where storm overflow pipes are located and sewer flooding is known to occur (South West Water, 2023). Alternatively, this could be a result of rainfall and land runoff causing the flushing of nutrients and N_2O from terrestrial sources to surface waters.

Production of CH_4 in the mid estuary in February suggests a seasonal shift in microbial activity favouring methanogenesis, but with the observations available, causes of this increase are more challenging to resolve. These observations may be explained by an increased transport of river CH_4 during higher-than-average freshwater discharge to the estuary, leading to higher availability of substrates for enhanced CH_4 production within the water column. Additionally, a particularly high tidal amplitude was observed during the February sampling event. During the low tide, sedimentary production of CH_4 may have taken place followed by physical disturbance to the

estuarine bed causing a release of trapped CH_4 bubbles from estuarine sediments into surface waters (Abril and Iversen, 2002; Bussmann *et al.,* 2022; Rosentreter *et al.,* 2021b). All but one of the estuary surveys were completed on a falling tide, with the surveys commencing at high tide at the top of the estuary. Correlations with tidal amplitude suggest this survey timing and tidal mixing is important for observations of both CH_4 and N_2O dissolved concentrations.

3.4.2 Hotspots of GHG emissions

Mean river GHG flux densities were 632 ± 295 μmol CH_4 m^{-2} d^{-1} and 17.1 ± 28.1 μmol N_2O m^{-2} d^{-1} in the river, and 273 ± 311 CH_4 μmol m^{-2} d^{-1} and 3.5 ± 2.9 N_2O μmol m^{-2} d^{-1} in the estuary. When combining the GHG contributions of the river and estuary to give a catchment total, annual emissions are estimated to be 4.6 x 10^6 mol CH_4 yr^{-1} and 6.6 x 10^4 mol N_2O yr^{-1}. The river had a greater contribution to the Tamar's total emissions, largely driven by higher emissions from narrower river sites in the upper catchment, particularly during winter and early spring where higher river flows and elevated GHG concentrations led to enhanced air-water gas exchange.

The vulnerability of the shallow, narrow upper reaches of river catchments to human perturbations of biogeochemical cycling, oxygen availability and hydrological connectivity affect their contributions to GHG budgets as a source or sink (Aho *et al.,* 2023; Mwanake *et al.,* 2023b). In this study, the river acted as a weak sink of N_2O in the summer. This is driven by lower river flow values applied to the empirical models used to predict *k*, which may suggest decreased turbulence driving gas exchange with the atmosphere. This may also be explained by net microbial N_2O consumption via denitrification, and lower rainfall causing reduced land run-off inputs of dissolved gases from agricultural land to the river (Mwanake *et al.,* 2023b; Raymond *et al.,* 2012). However, without being able to identify the exact

source of the measured N_2O concentrations, it is challenging to further constrain this observation.

Nonetheless, it can be ascertained that the upper headwaters of the Tamar were a hotspot of GHG production and emissions. In total, global inland waters have been estimated to contribute 10.6 – 19.8 Gmol N yr^{-1} in the form of N_2O emissions via denitrification and nitrification (Maavara *et al.,* 2019) and 1.74 [1.04 – 2.48] Tmol yr^{-1} CH_4 (Rocher-Ros *et al.,* 2023). Small streams less than 10 m wide, such as those in the Tamar's headwaters, have been highlighted as major hotspots of global river N_2O emissions despite covering a relatively small surface area (Marzadri *et al.,* 2021). Under business-as-usual scenarios, these contributions could increase with growing demands for food production and urban sprawl into rural areas increasing pressures on wastewater treatment works (WWT), adding to already nutrient stressed inland waters (Brown *et al.,* 2022; Mwanake *et al.,* 2023b; Nedwell *et al.,* 2002; Que *et al.,* 2023).

Seasonal changes in GHG fluxes from the estuary were expected due to temperature variations affecting CH_4 and N_2O producing microbes, and variable windspeed which is the main driver of gas exchange in open waters (Upstill-Goddard and Barnes, 2016). Lower estimated estuary emissions compared to freshwater agree with eddy covariance flux measurements in the Tamar (Yang *et al.,* 2016). Emissions of both N_2O and CH_4 were lowest in the summer where wind conditions are relatively low compared to autumn and winter when the southwest coast is impacted by south-westerly trade winds and a high frequency of storms. Higher emissions in autumn and winter months could also indicate an influence of increased fluvial transport of GHG downstream, with export into the estuary increasing with higher river flow conditions (Yan *et al.,* 2012). Higher CH_4 emissions from the Tamar Estuary have also been linked to elevated CH_4 concentrations in estuary outflows driven by tidal mixing (Yang *et al.,* 2016), which may have been more turbulent during the winter surveys.

3.4.3 Implications for river-to-coast management of aquatic ecosystems

This study agrees with previous reports that headwaters can act as hotspots of N_2O and CH_4 production and emissions to the atmosphere, providing further evidence to support measures targeted at reducing GHG emissions from inland aquatic ecosystems (Saunois *et al.,* 2024b; Tian *et al.,* 2024). Despite the improved representation of natural and indirect sources of GHG in global budgets, there is a distinct lack of government policies or ecological guidance which specifically aims to reduce anthropogenic modifications to emissions of non-CO_2 gases such as N_2O and CH_4 from inland waters, estuaries and coastal seas. There is no detailed consideration of human exacerbations to aquatic GHG sources in the UK's 2035 Nationally Determined Contribution (NDC) which proposes the UK's strategies towards reducing all GHG emissions by at least 81 % of 1990 levels by 2035 (UK Government, 2025). Table 3.2 and 3.3. show the annual emissions of N_2O and CH_4 from UK sectors reported in the NDC (1990 – 2022 mean), the Tamar Estuary (0.002 kt N_2O yr^{-1} and 0.06 kt CH_4 yr^{-1}) and the total UK estuaries (0.22 kt N_2O yr^{-1} and 6.16 kt CH_4 yr^{-1}). The emissions from the total UK estuaries were calculated by extrapolating emissions from the Tamar Estuary to the 4225 km^2 combined area of UK inner and outer estuaries (Barnes and Upstill-Goddard, 2011). We find that UK estuaries emit 0.17 % CH_4 and 0.23 % N_2O of the mean total UK reported sector emissions currently informing the NDC. When we compare the UK estuary emissions to each individual sector, we see that N_2O emissions from UK estuaries are 1.5 times higher than emissions from 'Energy - fugitive emissions from fuels' (Table 3.2), whilst CH_4 UK estuary emissions are 7 times higher than emissions reported under 'Other (Production Processes/Agriculture)' (Table 3.3). This warrants further investigation and consideration of anthropogenic modifications to estuary and other inland water sources of GHG in UK reduction targets and management strategies.

Table 3.2 Annual emissions of N_2O (kt) categorized by UK Nationally Determined Contribution (NDC) sectors (1990 - 2022 mean), Tamar Estuary, and Total UK Estuaries.

Category	**Annual N_2O emissions (kt)**
Agriculture - manure management	10.4
Agriculture - soils	44.2
Energy - fugitive emissions from fuels	0.14
Energy - Mobile Combustion	4.71
Energy - stationary combustion	4.75
Industrial processes and product use	22.5
Land use, land use change and forestry	5.84
Waste	4.70
Tamar Estuary	0.002
Total UK Estuaries	0.22

Table 3.3 Annual emissions of CH_4 (kt) categorized by UK Nationally Determined Contribution (NDC) sectors (1990 - 2022 mean), Tamar Estuary, and Total UK Estuaries.

Category	**Annual CH_4 emissions (kt)**
Agriculture - enteric fermentation	906
Agriculture - manure management	159
Energy - fugitive emissions from fuels	576
Energy - Mobile Combustion	18.4
Energy - stationary combustion	49.9
Industrial processes and product use	6.25
Land use, land use change and forestry	200
Other (Production Processes/Agriculture)	0.85
Waste	1650
Tamar Estuary	0.06
Total UK Estuaries	6.16

The application of NbS and other measures towards ecosystem restoration and protection have been recommended in the latest guidelines for achieving NDCs (Nature4Climate Coalition, 2024; Seddon *et al.,* 2020). The '2013 Supplement to the 2006 IPCC Guidelines for National Greenhouse Gas Inventories: Wetlands' also encourages the inclusion of wetlands in national GHG inventories. This recognises the impacts of wetlands on surrounding inland waters, for example identifying the high percentage of peat-derived DOC which is remineralized in headwaters. These guidelines could be extended further to identify specific measures to reduce human modifications to N_2O and CH_4 emissions from river and estuary surface waters and facilitate progress towards Net-Zero and commitments of the NDCs.

A key message for managers of the Tamar system and others like it is that by managing water on a source-to-sea scale (Mathews *et al.,* 2019), preventing nutrient and C loading, and restoring natural hydrological regimes in the upper catchment, can have wide-ranging benefits for downstream ecosystems. This approach has been successfully implemented through partnerships under the Catchment Based Approach (CaBA) and others like it across UK catchments where nutrient management has been prioritised to meet water quality targets (Collins *et al.,* 2020) (Rees *et al.,* in prep). Recognising the potential of NbS, alongside direct action towards improving farm nutrient storage, livestock management and minimising applications of synthetic fertilisers, through specific guidance and 'payments for environmental goods and services' in programmes such as the Environmental Land Management (ELM) schemes in the UK would be a significant step towards halting the growth of atmospheric N_2O and CH_4.

3.4.4 Site selection for targeted nature-based solutions (NbS) to GHG emissions

This study shows that the River Tamar's upstream sites (North Tamerton and Druxton Bridge) emerged as hotspots of both N_2O and CH_4 production and emissions, whereas the downstream sites (Horsebridge and Gunnislake) appear more important for transporting GHG downstream into the estuary. This would suggest most GHG cycling is happening in the upper reaches of the catchment which is also mostly dominated by agricultural land uses. NbS which restore habitats recognised for their role in key ecosystem services (ES), such as flood prevention and nutrient retention, also have significance for GHG cycling and the spatial variability of N_2O and CH_4 fluxes. This includes rewetting peatlands (Evans *et al.,* 2021; Mander *et al.,* 2023), the return of European beaver (*Castor fiber*) engineered wetlands (Nummi *et al.,* 2018; Puttock *et al.,* 2021, 2018), and intertidal wetland restoration (Adams *et al.,* 2012; Zou *et al.,* 2022). Restoring these ecosystems may improve the hydrological connectivity along the LOAC,

preventing rapid changes in water table height, river flows, and frequency of wetted areas which can control the delivery of nutrients and transport of dissolved concentrations of N_2O and CH_4 downstream (Evans *et al.,* 2021).

Simple interventions could also have drastic impacts. Preventing river channel erosion through bank stabilisation or fencing are an effective measure for reducing GHG in agriculturally impacted waters such as drainage ditches and riparian zones, preventing nutrients entering rivers through land runoff or livestock disturbance to sediments (Odebiri *et al.,* 2024; Paranaíba and Kosten, 2024; Wang *et al.,* 2024). Targeting measures which reduce nutrient and sediment loading in headwaters could limit resources available for nitrification and methanogenesis, reducing microbial production of N_2O and CH_4 and eventually limiting the export of GHG into the estuary (Borges *et al.,* 2018; Marzadri *et al.,* 2021).

Rebalancing nutrient ratios by reconnecting rivers with their floodplains has proved effective in preventing eutrophication and poor water quality (Stutter *et al.,* 2018) which would otherwise exacerbate N_2O and CH_4 emissions in inland waters (Brown *et al.,* 2023; Wang *et al.,* 2022). However, unless complete denitrification is achieved under anoxic conditions, there is potential for enhanced N_2O due to increased availability of organic matter exported from floodplains and opportunities for incomplete denitrification under variable low oxygen conditions created by water inundation. Further work is needed to understand the specific N_2O or CH_4 pathways to facilitate the spatial targeting of NbS.

3.5 Conclusion

By constraining the spatial variability of N_2O and CH_4, this study enables the identification of key areas in the Tamar Catchment which could benefit from interventions focused on reducing hotspots of GHG emissions from natural sources. The upper reaches of the Tamar catchment should be prioritised, where shallower, narrower stretches of the river may be more vulnerable to nutrient loading and temperature shifts that promote respiration of N_2O and CH_4 producing microbes. Furthermore, the transport of river GHG concentrations into the estuary should also be considered when designing river-to-coast catchment management plans. Existing designations of sensitive areas, such as Nitrate Vulnerable Zones (NVZ), could be built upon to identify risks of exacerbating GHG from inland waters. Another important take away from this work is that anthropogenic modification to natural sources of GHG emissions should be included in national emission reduction targets such as the NDCs. This will help drive efforts to better understand key biological pathways driving GHG emissions from natural sources. Further research into the specific GHG cycling pathways using stable isotopic signatures of N and C would enable a better understanding of how NbS and management interventions could minimise GHG production under changing land use practices and climate conditions. Overall, this continued effort towards understanding the impact of GHG from natural sources will improve the effectiveness of environmental policy and international efforts towards climate change mitigation.

Chapter 4: Monitoring the effectiveness of intertidal wetland restoration for climate change mitigation

Abstract

Wetlands are an internationally important carbon (C) store, but their global extent has suffered a net loss of 21 % due to land conversion since the 18th century. Wetland restoration has become a large focus towards restoring biodiversity richness and enhancing C sequestration to offset anthropogenic greenhouse gas (GHG) emissions. However, wetlands are also a substantial source of methane (CH_4) and nitrous oxide (N_2O), the second and third most potent GHGs after carbon dioxide (CO_2), which have the potential to offset the C sequestration benefits of wetland restoration. This study presents relatively high-resolution biogeochemical monitoring during the initial 12 months following the restoration of an intertidal wetland in the Tamar Estuary, southwest England. Dissolved concentrations in water draining out of the wetland ranged between 17 – 57 nmol N_2O L^{-1} and 91 – 932 nmol CH_4 L^{-1}. Calculated daily changes in concentrations reveal that the restored wetland overall acted as a source of both N_2O and CH_4. Crude estimates show that the GHG concentrations exported from the wetland into the estuary were 4 x more N_2O and 20 x more CH_4 per km^2 compared to concentrations transported from the river into the estuary. This study strongly emphasises the need for early high-resolution GHG monitoring to be included in ecological restoration management plans to accurately forecast the climate change mitigation benefits of restored wetlands, and to set realistic targets for environmental managers through evidence-based environmental frameworks. More fine scale measurements of N_2O and CH_4 fluxes from restored wetlands will continue to constrain the variability in the effectiveness of wetland restoration to climate change mitigation and has potential to inform interventions integrated into restoration plans which prevent exacerbating natural sources of GHG.

4.1 Introduction

Nature-based solutions (NbS) and natural climate solutions (NCS) refer to environmental management options which encourage the protection and restoration of ecosystems to simultaneously tackle the biodiversity and climate crises (Anderson *et al.,* 2019; Griscom *et al.,* 2017; Seddon *et al.,* 2020). Wetland ecosystems are a globally important carbon (C) store with the potential to provide 2.7 $GtCO_{2e}$ yr^{-1} in additional climate mitigation services (Smith *et al.,* 2019). Despite covering just 6% of the Earth's surface, they support 40 % of the world's biodiversity (Kopf *et al.,* 2015; Ramsar Convention on Wetlands, 2018). Yet wetlands remain one of the most globally threatened ecosystems. Recent estimates suggest a global net loss of 21 % of wetlands to land conversion since the 18th century, equating to 3.4 million km^2 (Fluet-Chouinard *et al.,* 2023). A focused analysis of tidal wetlands found a loss of 13,700 km^2 in the last two decades, though there has also been the creation of 9700 km^2 in this time (Murray *et al.,* 2022). Other drivers of wetland loss include reduced hydrological connectivity between rivers and floodplains (Belletti *et al.,* 2020; Pal and Singha, 2023), and the increasing threat of flooding, drought and sea level rise (Leonardi *et al.,* 2018; Wu *et al.,* 2023). The loss or degradation of wetlands also leads to the loss of essential ecosystem services (ES) including C sequestration (Tan *et al.,* 2022), flood and storm protection (Costanza *et al.,* 2021), nutrient retention and water quality regulation (Jickells *et al.,* 2016), and economic values through fisheries, tourism and recreation (Wood *et al.,* 2024). The loss of natural wetlands to land-use and land-cover change (LULUC) also impacts the cycling of the three most important greenhouse gases (GHG); carbon dioxide (CO_2), nitrous oxide (N_2O) and methane (CH_4) (Tan *et al.,* 2020).

The net climate benefits of restoring freshwater wetlands (0.82 $GtCO_{2e}$ yr^{-1}) and coastal wetlands (0.84 $GtCO_{2e}$ yr^{-1}) together account for over 50% (1.7 $GtCO_{2e}$ yr^{-1}) of the estimated total climate mitigation potential of wetland restoration (Smith *et al.,* 2019). Protecting and restoring wetlands is

therefore a global conservation priority and has been implemented as a strategy towards offsetting anthropogenic GHG emissions in international climate mitigation strategies (Adams *et al.,* 2012; Needelman *et al.,* 2018; Yi *et al.,* 2024). However, there is often a competing agenda between biodiversity restoration, water quality improvement and GHG mitigation. For example, reconnecting riparian wetlands can increase the mobilisation of dissolved organic matter (DOM) and dissolved organic carbon (DOC) in inland and coastal waters which could lead to an increased source of atmospheric C (Kurek *et al.,* 2024). Utilising the water filtration and nutrient retention services of restored or constructed wetlands has emerged as a viable solution for wastewater treatment (Vymazal, 2010; Wu *et al.,* 2015), but the increased nutrient loading also drives increased competition between plant species and an overall decline in species diversity (Keenan and Lowe, 2001). Furthermore, increased nutrient loading and uptake in wetlands also has substantial implications for the cycling of CH_4 and N_2O which have a global warming potential (GWP) of 27 and 273 times higher than CO_2, respectively, over a 100-year time horizon (Calvin *et al.,* 2023). The cost-effectiveness and GHG mitigation potential of restoring versus protecting existing wetlands from degradation is varied depending on the considered time horizon, spatial scale and site specific factors which affect GHG cycling (Cook-Patton *et al.,* 2021). But even minor increases of N_2O and CH_4 production have a high potential to offset the C sequestration benefits of wetland restoration.

4.1.1 N_2O and CH_4 cycling in wetlands

Wetlands provide what is typically considered the optimal conditions for N_2O and CH_4 production by anaerobic bacteria in the way of low oxygen soils with high organic matter (OM) content, particularly in agriculturally dominated catchments (Adams *et al.,* 2012). Incomplete denitrification, nitrification, and nitrifier-denitrification are the major pathways commonly associated with indirect N_2O production in low oxygen (O_2), high OM and dissolved inorganic nitrogen (DIN; NO_2^-, NO_3^-, NH_4^+) rich soils (Hu *et al.,*

2015). Complete anaerobic denitrification, the transformation of nitrate to nitrogen gas (N_2), was traditionally seen as the main pathway for N_2O reduction under anoxic conditions. However recent discoveries of hybrid archaeal N_2O formation under suboxic conditions (Trimmer *et al.,* 2016) and the unexpected presence of the N_2O reductase enzyme (N_2OR) in oxic marine environments controlled by the *nosZ* gene (Bertagnolli *et al.,* 2020; Rees *et al.,* 2021) highlight the importance of site-specific conditions on N_2O cycling. Ammonia oxidation is both an indirect and direct source of N_2O, with nutrient management practices an important moderator of emissions from wetland soils due to differences in cycling between ammonia-oxidising bacteria (AOB) and ammonia-oxidising archaea (AOA) (Hink *et al.,* 2018; Prosser *et al.,* 2020). Biogeochemical pathways leading to CH_4 emissions are equally complex. As previously detailed in Chapter 1, salinity gradients and OM substrate availability are key drivers of CH_4 emissions from methanogenic bacteria, particularly in intertidal wetlands (Adams *et al.,* 2012; Poffenbarger *et al.,* 2011). CH_4 oxidation by anaerobic methanotrophs is reliant on the presence of electron acceptors such as O_2, NO_2^-,NO_3^-, sulfate (SO_4^{2-}), iron (Fe_3^+) and DOM (Stanley *et al.,* 2016). Salinity can suppress CH_4 concentrations by changing to availability of these ions and limiting methanogenesis (Soued *et al.,* 2024). This is particularly important to consider in the development of intertidal wetlands.

4.1.2 Effects of wetland restoration on N_2O and CH_4 emissions

A recent analysis of 253 studies on the effects of ecological restoration on GHG emissions found wetland restoration to increase CH_4 emissions by 544.4 %, whereas N_2O emissions decreased by 68.8 % (He *et al.,* 2024). Other studies have found that CH_4 and N_2O emissions can be reduced in newly restored wetlands through hydrological engineering measures designed to manage wetland rewetting and water table height fluctuation (Wang *et al.,* 2022; Yang *et al.,* 2020). For example, a 50 % reduction in the effective water table depth in agricultural peatlands could lead to a 65 % reduction in current CO_2 and CH_4 emissions (Evans *et al.,* 2021). In coastal

wetlands, variable water inundation due to tidal range is also an important factor for GHG cycling in restored wetlands. Arias-Ortiz *et al.,* (2021) found a restored intertidal wetland in California's San Francisco Bay-Delta acted as an immediate CH_4 sink compared to nontidal freshwater and brackish wetlands which took between 2 – 8 years before a net cooling effect (organic-C stored > CH_4 emitted) was observed. Cadier *et al.,* (2023) and Holmquist *et al.,* (2023) also argue that the tidal restoration of freshwater impounded wetlands leads to lower CO_2 equivalent emissions of N_2O and CH_4 due to saline inhibition of GHG production.

As increasingly more fine scale measurements of N_2O and CH_4 fluxes from restored wetlands are reported, the variability in the success of GHG mitigation through wetland restoration and the importance of site selection becomes more evident (Rosentreter *et al.,* 2021a). The disparity between findings creates significant challenges in accurately forecasting the climate mitigation benefits of restoring wetlands, limiting the decision makers ability to effectively reduce natural sources of GHG.

4.1.3 The role of carbon credits in wetland restoration

The latest International Panel on Climate Change (IPCC) reports have warned that simply reducing further greenhouse gas (GHG) emissions is no longer sufficient to prevent global warming beyond 1.5 degrees. Active CO_2 removal (CDR) is now a necessary addition to GHG reduction measures to limit increasing global surface temperatures (Calvin *et al.,* 2023). However, the nuances of this are difficult to translate into environmental monitoring and management plans. Whilst the IPCC emphasises CDR is not a substitute for reducing GHG emissions, there is risk of an emerging dangerous narrative giving the impression that CDR could allow industry to

continue along a path close to ‘business-as-usual’ with minimal climatic consequences.

The carbon market has become an integral part of government and private climate strategies, where GHG emission offsetting is effectively bought in exchange for financial contributions to mitigation practices such as the ecological restoration of habitats with high C-storage potential (Smith *et al.,* 2024). Among other green financing frameworks, carbon credits have therefore become an appealing source of funding for ecosystem restoration and conservation initiatives through increased interest from government and private sector partners (Dunklin *et al.,* 2024; Zu Ermgassen *et al.,* 2025). This is leading to government-led carbon-specific policy and legislative development. At the time of writing, new UK government-backed green finance standards are entering consultation to steer the future of private investment in nature recovery and climate mitigation strategies, including the Natural Carbon Standard which seeks to set requirements for high impact CDR and non-CO_2 GHG reductions delivered by NbS and NCS in the UK (UKGOV, 2025).

However, the provision and implementation of scientific evidence to accurately assess the effectiveness of carbon crediting schemes has not kept up with their rapid uptake. Substantial challenges arise when assessing the additional GHG mitigation benefits (more than what would have happened without human intervention) and the permanency of such benefits (the longevity of the habitat created and subsequent century scale C storage). This inevitably leads to a reliance on scaled-up benefits modelled over decades to centuries. A recent analysis of one fifth of carbon credits issued to date found that less than 16 % of the credited projects reviewed actually achieved GHG emission reductions (Probst *et al.,* 2024). There is growing concern over the legitimacy of environmental benefits claimed by such schemes, which could therefore be undermining the advice of IPCC

reports and ultimately misleading global progress towards effective climate change mitigation (Hale *et al.,* 2022). Whilst restoring wetlands has undeniable far-reaching benefits beyond CO_2 sequestration, to achieve Net-Zero emissions also requires significant efforts to abate non-CO_2 GHG, including N_2O and CH_4. Accounting for this balance is often misrepresented in benefits claimed by restoration projects, further adding to uncertainty in the effectiveness of NbS for climate change mitigation and the scientific evidence underpinning the adoption of carbon credits (Rosentreter *et al.,* 2021a).

The uncertainties within the scientific research community and the rapid adoption of carbon-specific policies on a global level urgently require site specific monitoring of GHG fluxes to fill gaps in understanding and set appropriate expectations for restoration projects which identify climate mitigation as a benefit. This study aims to do exactly that by presenting observations from within the first year of monitoring a restored intertidal wetland in the Tamar Estuary. The questions guiding this inquiry are designed to support an initial assessment of the restored wetlands provision of ES, here focusing on climate change mitigation. Is the restored wetland acting as a source or sink of N_2O and CH_4? If so, how could restoration and management practices reduce the risk of increasing N_2O and CH_4 emissions? The results are explored in the context of the freshwater export of GHG entering the Tamar Estuary from the River Tamar to compare the relative contribution from the restored wetland. This chapter aims to inform future assessments of ES provided by restored wetlands and the appropriate application of carbon credits.

4.2 Methods

4.2.1 Study location

The Calstock intertidal wetland was created in 2021 in the Tamar Estuary, ~8 km downstream of the tidal limit at Gunnislake weir, during an Environment Agency Flood Defence Improvement Scheme (Figure 4.1). An area of 11 hectares was restored by creating scrapes and channels in a formerly sheep-grazed field, with the recovered sediment used to build an improved flood defence bank to protect the village of Calstock (Figure 4.2). In November 2021, the old flood bank was breached to allow the River Tamar and the upper Tamar estuary to cyclically flood the area and allow it to naturally develop into an intertidal wetland. The wetland has since been managed and monitored by a collaborative local partnership between the Environment Agency, Tamar Valley National Landscape, Tamar Community Trust, Calstock Parish Council, Calstock Footpath Society, Cornwall County Council, the University of Plymouth and Plymouth Marine Laboratory.

The wetland receives water draining from the predominantly agricultural landscape of the River Tamar into the transitional waters of the Tamar Estuary, mostly consisting of improved grassland (81 %) (Morton *et al.,* 2024) (Figure 4.1A). In 2022 the Lower River Tamar and the Tamar Estuary both received ‘moderate ecological status’ under the Water Framework Directive (WFD) classification. Reasons for not achieving good (RNAG) for the Lower Tamar include bankside erosion, poor nutrient and soil management associated with agriculture and rural land management, and sewage discharge associated with the water industry. Five protected areas are included within the ~30 km2 area of the estuary; Plymouth Sound & Estuaries Special Area of Conservation (SAC), Tamar Estuaries Complex Special Protection Area (SPA), and three Bathing Water Directives; Plymouth Firestone Bay, Plymouth Hoe West and Plymouth Hoe East (Figure S1, Appendix B). The desired benefits of restoring the Calstock wetland, in addition to improving flood resilience of Calstock village,

included increased C sequestration and nutrient retention to improve water quality downstream, thereby reducing pressures on protected habitats and the communities reliant on them, whilst enhancing biodiversity.

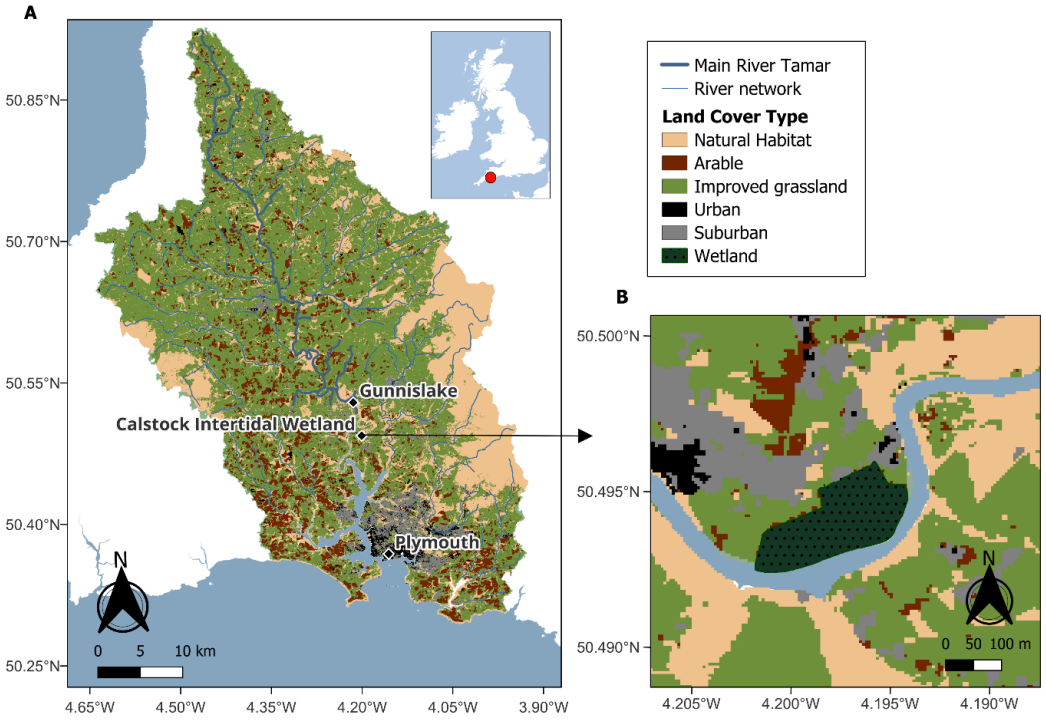

Figure 4.1. A) Map of Tamar Catchment in southwest England showing Land Cover Type and position of Gunnislake (upper tidal limit of Tamar Estuary), Calstock Intertidal Wetland and Plymouth City. B) Extent of Calstock Intertidal Wetland and surrounding land cover type

Figure 4.2. Timeline of wetland development between 2020 and 2023. White stars show where samples were collected from in the channel entering the wetland. Images source: Google Earth Pro

4.2.2 Water sample collection

The sampling protocol was designed to capture the tidal inflow and outflow of water at the breach, or channel, created to connect the restored wetland to the estuary (identified as a star in Figure 4.2). Water samples were collected every 30 minutes over a 6-hour period, 3 hours either side of high tide during neap tides (Figure 4.3). Samples were collected using a thrice rinsed bucket which was subsampled for further analysis. Samples were analysed for dissolved concentrations of N_2O (nmol L^{-1}) and CH_4 (nmol L^{-1}) using methods described in Chapter 2. CDOM and nutrient concentrations (µmol L^{-1}) were determined using methods described in Chapter 3. Measurements of water temperature and salinity were taken from the sample bucket immediately on collection using a YSI probe (Model PRO30).

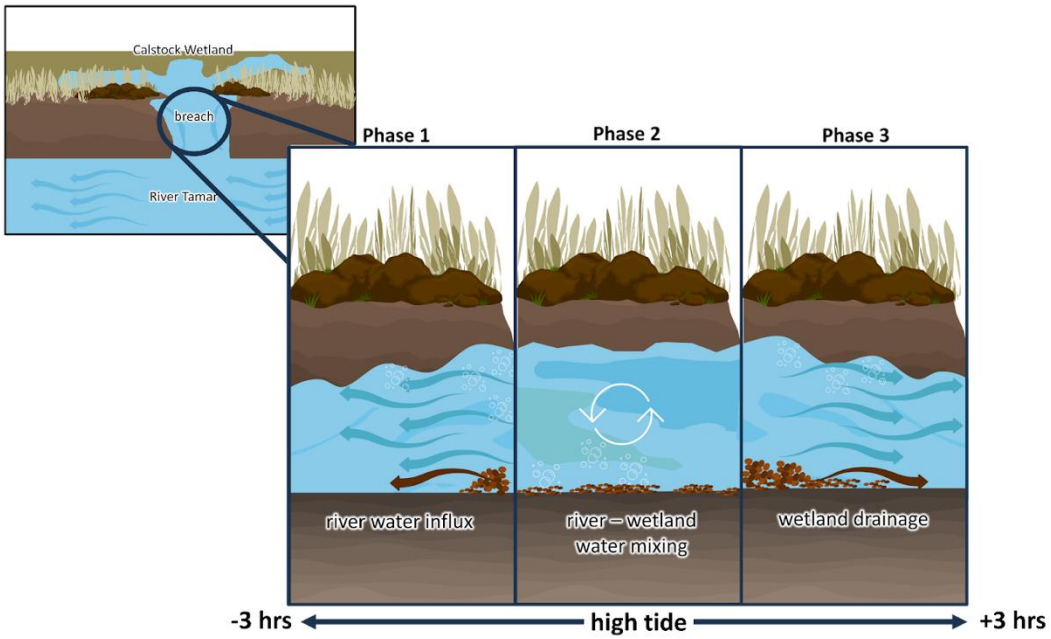

Figure 4.3. Diagram showing the phases of water exchange between Calstock wetland and the Tamar Estuary through the breach (channel created in the old flood bank) during 3 hours before (-3 hrs) and 3 hours after (+3 hrs) high tide when samples were collected.

4.2.3 Environmental data

Records of daily average river flow were accessed for Gunnislake (immediately above the tidal limit of the Tamar Estuary) from the National River Flow Archive via the Environment Agency Hydrology Explorer. Tidal heights were accessed from the UK Hydrographic Office via the ADMIRALTY EasyTide service (www.easytide.admiralty.co.uk).

4.3 Results

4.3.1 Environmental conditions

Daily average river flow conditions on the sampled days were lowest at 2.8 m^3 s^{-1} in August 2022 and highest at 96.0 m^3 s^{-1} in December 2022 (Figure 4.4). Tidal height ranged between 1.0 – 3.9 m with an average tidal amplitude of 0.4 m during the 6 hours of sampling (Figure 4.5).

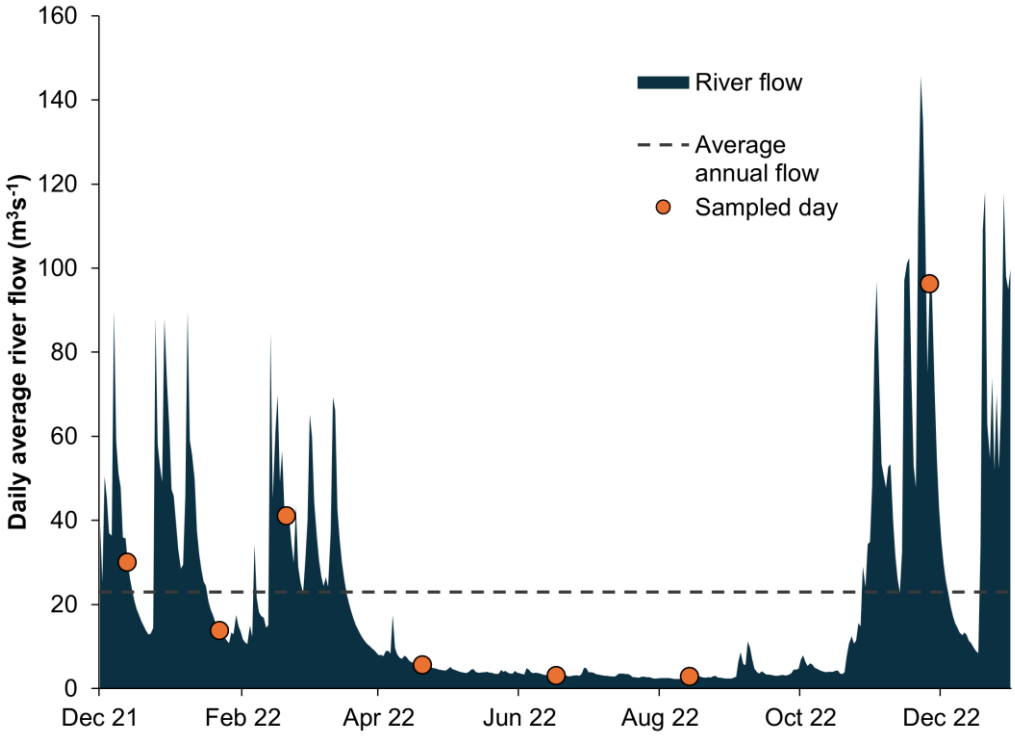

Figure 4.4. Daily average river flow measured at Gunnislake. Sampled days are displayed as orange circles. Annual average river flow (22.9 m^3 s^{-1}) marked by dashed horizontal line.

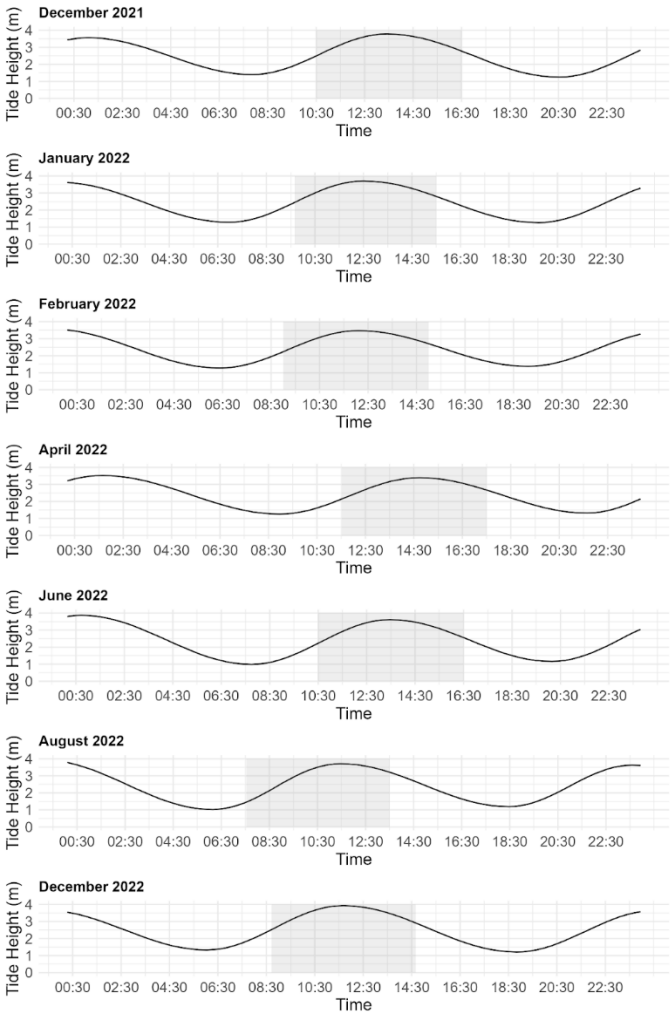

Figure 4.5. Tidal height on each day of sampling. Sampled timeframes (6 hours) are shown in grey.

4.3.2 Water properties

Table 4.1. summarises the sampled water properties throughout the 7 sampling events within the first year of the wetland being created. Water temperatures ranged between 5.8 °C in February 2022 to 24.3 °C in June 2022. Salinity ranged between 0 and 7.3. In 4 out of the 7 sampling events, salinity rarely measured beyond 0.1, showing a weak mixing of seawater entering the wetland from the upper estuary and indicating a more dominant freshwater influence of the River Tamar (Figure 4.6). In April, June and August 2022, a higher saline input to the wetland was recorded, which

coincides with lower river flows (Figure 4.4) and suggests greater influence of estuary waters entering the wetland during these sampling events.

Table 4.1. Average (± SD) and range of water temperature and salinity

	Water Temperature (°C)		Salinity	
Date Sampled	**Average ± SD**	**Range**	**Average ± SD**	**Range**
December 13, 2021	10.8 ± 0.1	10.5 – 10.9	0.1 ± 0.0	0.1 – 0.2
January 27, 2022	7.6 ± 0.4	7.1 – 8.5	0.1 ± 0.0	0.1 – 0.1
February 25, 2022	8.0 ± 1.2	5.8 – 10.2	0.1 ± 0.0	0.1 – 0.1
April 25, 2022	14.8 ± 1.5	13.5 – 18.8	2.8 ± 1.0	0.0 – 4.3
June 22, 2022	21.5 ± 1.6	19.7 – 24.3	3.9 ± 1.8	0.0 – 5.5
August 19, 2022	21.5 ± 1.1	19.7 – 23.5	6.5 ± 0.8	4.2 – 7.3
December 1, 2022	9.4 ± 0.3	8.8 – 10.1	0.1 ± 0.0	0.1 – 0.1

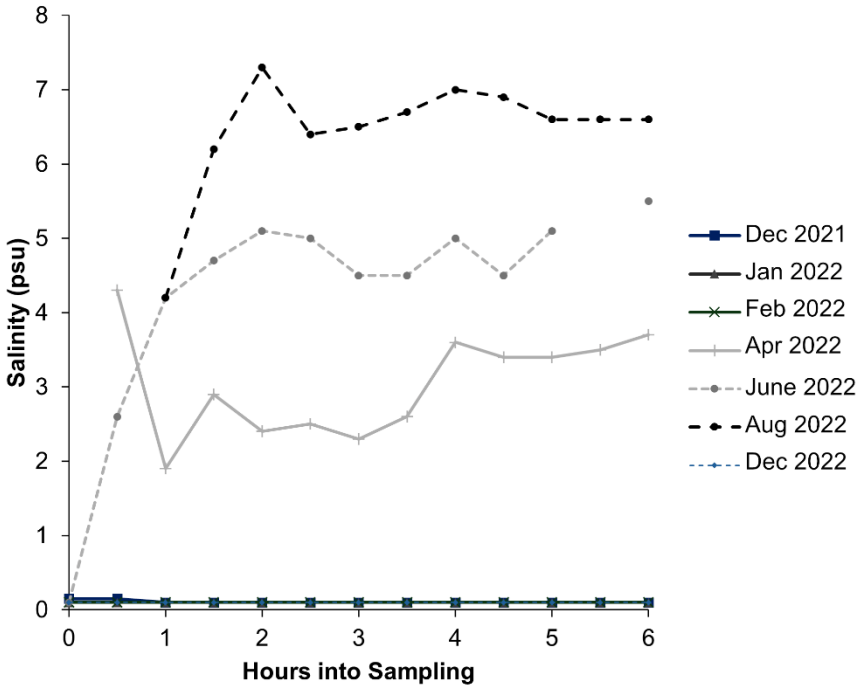

Figure 4.6. Observed changes in salinity during sampling events

4.3.3 Dissolved GHG concentrations

Dissolved GHG concentrations ranged between 16 – 107 nmol L^{-1} N_2O (Figure 4.7) and 91 - 932 nmol L^{-1} CH_4 (Figure 4.8). Concentrations of both gases were often initially high in the first hour of sampling. This is thought to be the traces of enhanced GHG concentrations in water that had been sat in the wetland channel prior to being diluted with inflowing water, which was predominantly fresh rather than saline, during the incoming tide. The highest N_2O concentrations were observed in the first hour of sampling in January 2022, but this rapidly decreased and maintained a relatively stable average concentration of 24 nmol L^{-1} during the remainder of the sampling event. The highest CH_4 concentrations were recorded in August 2022, where concentrations increased by 529 nmol L^{-1} between the first and last sample. Across all sampling events, concentrations of both gases followed an increasing trend during the outflow of water from the wetland, most notable in the last 3 hours of sampling when the tide transitioned from high tide to a falling tide causing the wetland to drain. On average, N_2O increased by 8 ± 18 nmol L^{-1} and CH_4 increased by 124 ± 292 nmol L^{-1} between high tide and the final sample.

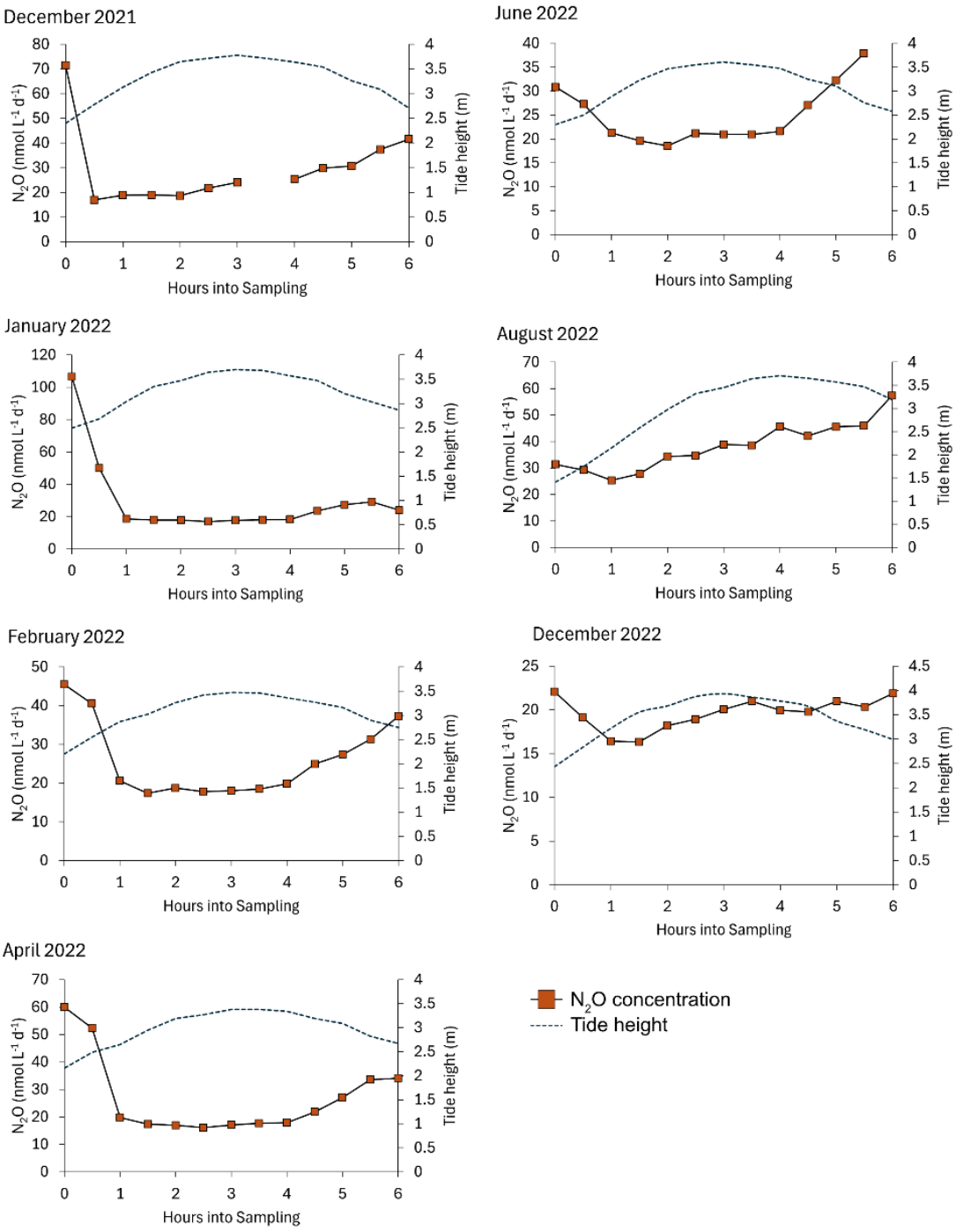

Figure 4.7. Dissolved concentrations of N_2O profiles measured over 6 hours in the channel connecting Calstock wetland and the Tamar Estuary. Note changes in scale. Dashed blue lines show the tide height during sampling.

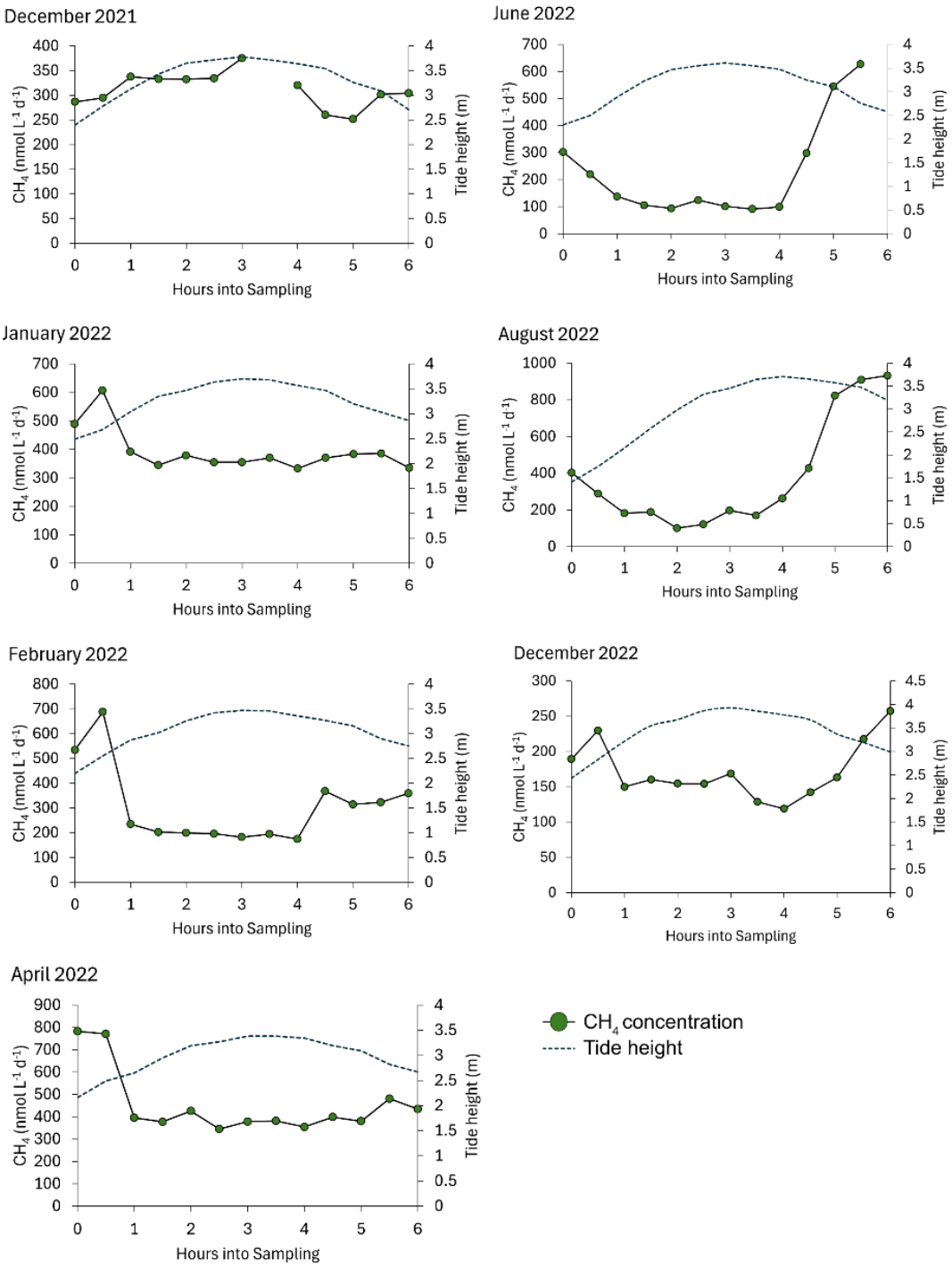

Figure 4.8. Dissolved concentrations of CH_4 profiles measured over 6 hours in the channel connecting Calstock wetland and the Tamar Estuary. Note changes in scale. Dashed blue lines show the tide height during sampling.

4.3.4 GHG wetland export to the Tamar Estuary

The daily rate of change in GHG concentration (ΔGHG) (Figure 4.9) quantifies the amount of N_2O and CH_4 exported from the wetland into the Tamar Estuary in the outflow of water after HT (last 3 hours of each sampling event). This was calculated by extrapolating the hourly change in concentration to a 12-hour tidal cycle and assumes concentrations increased or decreased at the same rate on each outgoing tide of a full tidal cycle. Across all sampling events, the wetland acted as a source of N_2O, with the highest export to the estuary in June 2022 (85 ± 15 nmol L^{-1} d^{-1}) and lowest in December 2022 (5 ± 3 nmol L^{-1} d^{-1}). CH_4 export shows a seasonal effect, initially acting as a small sink (more CH_4 removed than exported) in December 2021 (-290 ± 201 nmol L^{-1} d^{-1}), and highest exports in August 2022 (3640 ± 538 nmol L^{-1} d^{-1}).

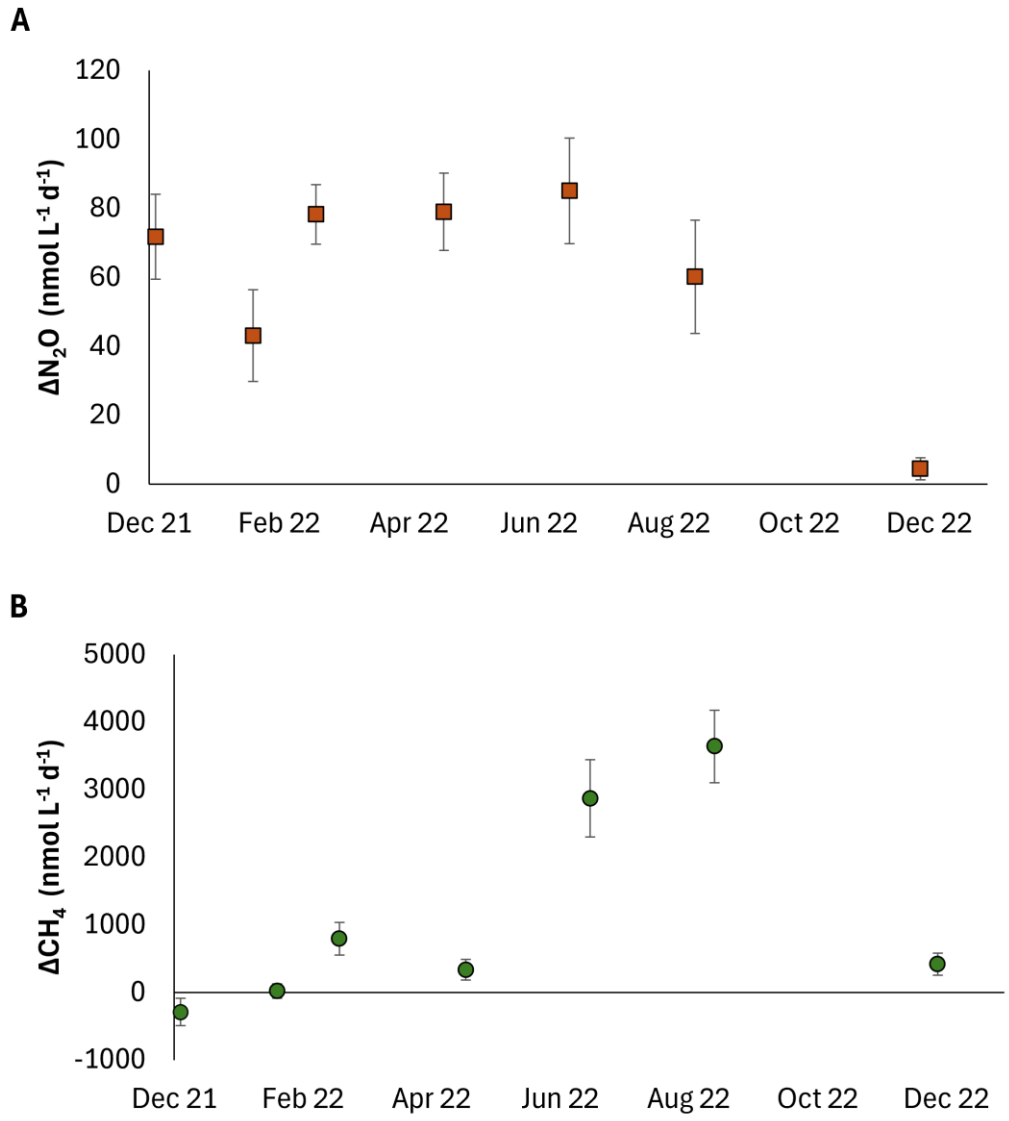

Figure 4.9. Daily rate of change (Δ) in A) N_2O and B) CH_4 concentrations. Values extrapolated from hourly rate of change in measured concentrations in wetland outflow (+3 hours after high tide). Negative values mean removal/sink and positive values mean export/source.

4.3.5 Nutrient uptake

Further to GHG export, the daily changes in DIN ($NH4^+$ + NO_2^- + NO_3^-) concentrations in the outflow of water draining from the wetland were investigated to understand the nutrient uptake benefits provided (Figure 4.10). This revealed an interesting trade-off between ammonium and nitrate. Ammonium uptake was often offset by nitrate export, and vice versa.

Ammonium export gradually increased from 4.3 ± 1.0 μmol L^{-1} d^{-1} in April to 37.4 ± 4.6 μmol L^{-1} d^{-1} in August, with less nitrate uptake also during that time. Ammonium retention was highest at -34.4 ± 19.4 μmol L^{-1} d^{-1} in December 2022 with nitrate increasing by 14.4 ± 63.1 μmol L^{-1} d^{-1}. Nitrite concentrations remained relatively stable throughout all sampling events, other than a small increase of 5.2 ± 0.2 μmol L^{-1} d^{-1} in August.

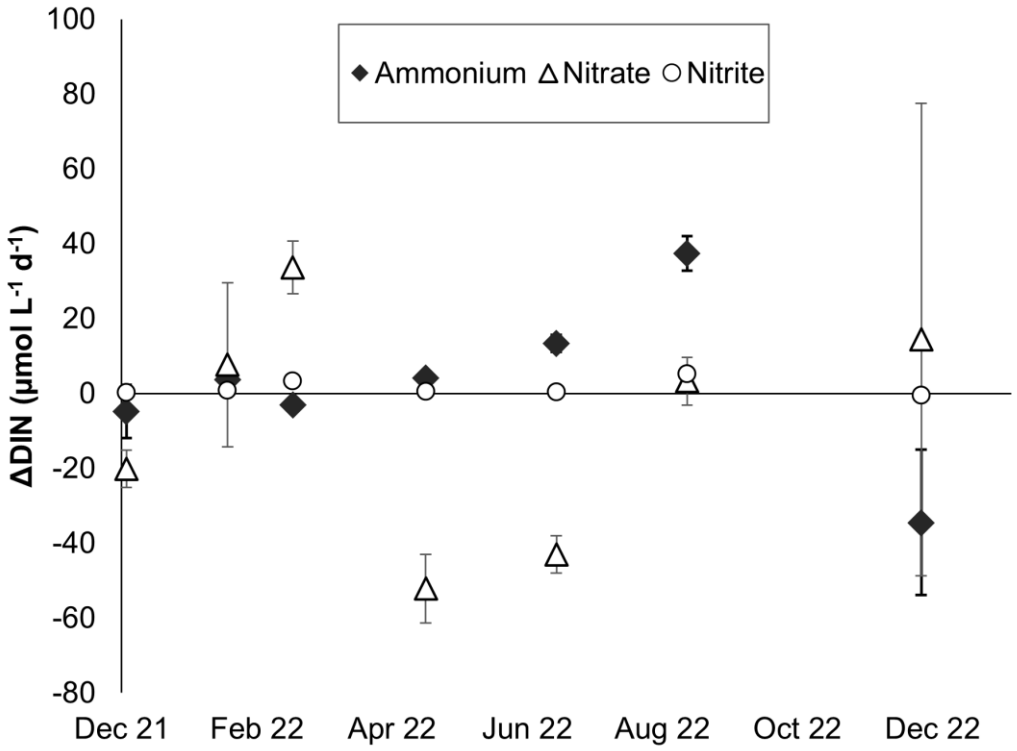

Figure 4.10. Daily rate of change (∆) in DIN (NH_4^+ + NO_2^- + NO_3^-) concentrations. Values extrapolated from hourly rate of change in measured concentrations in wetland outflow (+3 hours after high tide).

4.3.6 Drivers of GHG concentrations

A linear regression analysis was performed to assess the relationship of N_2O and CH_4 to key environmental predictors during each day sampled. Table 4.2 and Table 4.3 present only significant relationships (*p value* < 0.05) with an explanatory strength of $R^2 \geq 0.50$ to identify the most important correlations to GHG concentrations.

Table 4.2. Linear regression results identifying key variables correlated to N_2O concentrations

Date	Variable	Coefficient	SE	R^2	*p value*	Direction
December 13, 2021	Ammonium	9.48	2.55	0.58	0.004	Positive
	CDOM	7.41	0.56	0.95	<0.001	Positive
	Nitrate	-3.25	0.14	0.98	<0.001	Negative
	Nitrite	59.35	6.85	0.88	<0.001	Positive
	DOC	2.05	0.33	0.80	<0.001	Positive
	DON	30.72	5.42	0.76	<0.001	Positive
	Water temp	-133.77	20.49	0.81	<0.001	Negative
January 27, 2022	Ammonium	20.92	4.51	0.66	<0.001	Positive
	CDOM	5.78	1.16	0.69	<0.001	Positive
	Nitrate	-3.22	0.76	0.62	0.001	Negative
February 25, 2022	Nitrate	1.39	0.23	0.77	<0.001	Positive
April 25, 2022	Ammonium	8.87	0.76	0.93	<0.001	Positive
	CDOM	3.39	0.21	0.96	<0.001	Positive
	Nitrate	-1.65	0.15	0.92	<0.001	Negative
	Nitrite	44.85	5.51	0.86	<0.001	Positive
	Phosphate	-57.78	4.67	0.93	<0.001	Negative
	Silicate	3.96	0.36	0.92	<0.001	Positive
	Water temp	8.66	1.13	0.84	<0.001	Positive
June 22, 2022	Phosphate	-20.90	5.74	0.57	0.005	Negative
	Water temp	3.19	0.84	0.59	0.003	Positive
August 19, 2022	Ammonium	2.24	0.47	0.67	<0.001	Positive
	Nitrite	11.74	3.11	0.57	0.003	Positive
	Phosphate	-21.46	5.21	0.61	0.002	Negative
	Water temp	6.99	1.11	0.78	<0.001	Positive

Most strong relationships with N_2O were found in December 2021 and April 2022 (Table 4.2). Ammonium, nitrite, nitrate, phosphate, CDOM and water temperature were consistently correlated to N_2O concentrations across multiple dates. December 2021, which was sampled just a few weeks after the wetland was flooded, was the only month where N_2O was significantly positively correlated to DOC and DON. Nitrite stands out as having a strong positive relationship with N_2O in December 2022 and April 2022. Ammonium showed a consistent positive relationship with N_2O concentrations, with R^2 values up to 0.93, though the size of the effects of these predictors varies

between dates. Phosphate was an important predictor in June and August, showing a positive relationship of a similar effect on both sampling occasions. The positive effect of CDOM on N_2O concentrations decreased gradually from 7.4 in December 2021 to 3.4 in April 2022. Water temperature displays a mixed relationship with N_2O, showing a strong negative effect in December 2021 which switches to a positive effect in warmer months of April, June and August.

Table 4.3. Linear regression results identifying key variables correlated to CH_4 concentrations

Date	Variable	Coefficient	SE	R^2	*p value*	Direction
January 27, 2022	Ammonium	68.0	11.8	0.75	<0.001	Positive
	CDOM	18.6	3.0	0.77	<0.001	Positive
February 25, 2022	Nitrate	24.1	2.5	0.90	<0.001	Positive
April 25, 2022	Ammonium	91.6	7.0	0.94	<0.001	Positive
	CDOM	33.9	3.1	0.92	<0.001	Positive
	Nitrate	-15.9	2.4	0.81	<0.001	Negative
	Nitrite	444.9	66.3	0.80	<0.001	Positive
	Phosphate	-561.5	74.1	0.84	<0.001	Negative
	Silicate	40.6	3.6	0.92	<0.001	Positive
	Water temp	89.4	11.1	0.86	<0.001	Positive
June 22, 2022	Water temp	106.9	20.8	0.73	<0.001	Positive
August 19, 2022	Ammonium	79.7	13.7	0.75	<0.001	Positive
	CDOM	44.5	8.7	0.73	<0.001	Positive
	Phosphate	-879.0	87.1	0.90	<0.001	Negative
	Water temp	205.4	50.6	0.60	0.002	Positive

For CH_4, April 2022 stands out again as an important month for biogeochemical processes (Table 4.3). Ammonium and CDOM had consistently strong positive relationships with CH_4 concentrations in January, April and August. Water temperature shows a positive correlation to increasing CH_4 concentrations in warmer months of April, June and August. The direction of relationships between CH_4 and nutrients show contrasting results for April 2022; ammonium, nitrite and silicate show positive relationships whereas nitrate and phosphate have strong negative

relationships with CH_4. In this instance, nitrite and phosphate had the largest effect on observations of CH_4 concentrations. Interestingly and unexpectedly, no strong or significant relationships emerged with CH_4 and DOC on any of the days sampled.

4.4 Discussion

4.4.1 Is the wetland an important GHG source?

The results show that Calstock wetland overall acted as a source of both dissolved N_2O and CH_4 to the estuary during the first year following its creation. In addition to biogeochemical monitoring, 3 high resolution drone surveys of the wetland have been completed to date since it was flooded in November 2021. This has allowed an initial assessment of the sediment accumulation and erosion at a scale of 1 cm resolution within the wetland ponds, enabling a rough estimation of the water storage capacity of the wetland. Based on the depth of the wetland ponds, it has been approximated that 180,000 m^3 d^{-1} of water drains from the 11-ha wetland. If I apply this to my calculations of GHG export, it is possible to explore the relative contribution of the Calstock wetland to GHG concentrations in the Tamar Estuary compared with the average daily export into the estuary from the River Tamar.

Based on 7 sampling events that took place between December 2021 to September 2022 and the respective average daily river discharge, dissolved GHG concentrations transported from the River Tamar at Gunnislake (the tidal limit) into the upper Tamar estuary averaged 21 mol d^{-1} N_2O and 91 mol d^{-1} CH_4 during the first year following the flooding of Calstock wetland. Over the 7 surveys presented, Calstock wetland exported an average of 0.01 mol d^{-1} N_2O and 0.2 mol d^{-1} CH_4 into the Tamar estuary. If we only compare those values, Calstock wetland is exporting less than 1 % of what is transported from the River Tamar into the Tamar Estuary. However, a

more meaningful exploration could be to compare the respective areas being drained. Gunnislake receives water draining a catchment area of 917 km^2, just over 50 % of the total Tamar Catchment area. Calstock is draining a much smaller total area of 0.11 km^2. If we report the GHG export by area, Gunnislake delivers 0.02 mol km^{-2} d^{-1} N_2O and 0.1 mol km^{-2} d^{-1} CH_4 into the estuary, whereas Calstock delivers 0.1 mol km^{-2} d^{-1} N_2O and 1.8 mol km^{-2} d^{-1} CH_4. By considering it from this perspective, the wetland is producing 4 x more N_2O and almost 20 x more CH_4 than what is transported by the river from the lower Tamar Catchment.

This leads us to the next important consideration, which is the accumulated effects of multiple wetland restoration projects. The Tamar Estuary, like many others across the UK, offers multiple promising opportunities for wetland restoration. By reconnecting the Tamar with its floodplains after centuries of being disconnected by agricultural land reclamation, vital species-rich habitat will be created for wetland birds, amphibians, fish and mammals. Within 10 km downstream of Calstock wetland are two other wetland restoration, or managed realignment, projects; Cotehele which has restored 1.4 ha of intertidal wetland and South Hooe which has restored 19 ha. A feasibility study has also taken place for a project at Haye Marsh, approximately 3 km downstream of Calstock wetland, to create an additional 7.5 ha of intertidal wetland, bringing the total area of the site to 17 ha (Jacobs, 2024). This study estimates the intertidal area will sequester 48.8 tonnes C yr^{-1} but also recognises the potential offsets due to capital costs of wetland construction and the potential for enhanced CH_4 emissions.

The high GWP of CH_4 and N_2O means that even small additions to the total GHG export to the estuary could have substantial impacts on the relative contribution of the estuary to GHG budgets and the resulting climate warming. This analysis should not be misconstrued as an argument against restoring wetlands but does demonstrate how essential it is to account for the potential offsetting of C sequestration benefits to ensure a

comprehensive understanding of the overall climate change mitigation benefits of wetland restoration. A more extensive timeseries analysis of all existing N_2O and CH_4 measurements in the Tamar Estuary (Barnes and Upstill-Goddard, 2011; Law *et al.,* 1991; Upstill-Goddard and Barnes, 2016), along with records of nutrient loading from the River Tamar (Rees *et al.,* in prep), is needed to fully understand how the creation of wetlands throughout the catchment has impacted estuary GHG emissions.

4.4.2 Insights for ecosystem restoration practices

The Tamar Valley Nature Recovery Plan identifies urgent action is needed to restore aquatic ecosystem health, including wetland restoration (Tamar Valley National Landscape, 2024). The results of this study provide insights for the management of wetlands before, during and after their restoration. Many proposed habitat restoration projects, including Calstock intertidal wetland, are taking place on land previously claimed for agricultural purposes with a desired benefit being improved water quality through increased nutrient uptake, particularly nitrate removal. In most cases, this land has received artificial improvements using synthetic fertilisers or has been subject to trampling and nutrient loading from grazing livestock for generations. It is likely, therefore, that excess nutrients exist in the sediments prior to any restoration works. Calstock wetland was grazed by livestock prior to the creation of scrapes and ponds. The disturbance of this sediment, followed by flooding and the promotion of anaerobic conditions, likely reduced the redox potential and contributed to the release of nutrients such as ammonium and nitrite from sediments into the sampled waters. This could have created conditions for the microbial nitrification of ammonium and denitrification of nitrate, contributing to N_2O production, as well as methanogenesis driving increased CH_4 emissions. Furthermore, the results here show that nitrate uptake benefits were often offset by N_2O production, or ammonium export to the estuary, further highlighting the challenge of balancing water quality and climate goals.

Unnaturally high nutrient availability has been shown as detrimental to the success of restored wetlands, preventing species richness or the establishment of high quality habitat indicator vegetation species (Moeslund *et al.,* 2023). Depending on the length of time the land has been in agricultural production prior to wetland restoration, residual excess nutrients can be present in soil depths of up to 1 m (Ewing *et al.,* 2012). This is an important consideration for GHG management in restored wetlands. Identification of key correlated variables in this study show that nutrient concentrations were an important factor for high N_2O and CH_4 concentrations draining out of Calstock wetland. A consistently positive relationship between N_2O and ammonium and nitrite could suggest nitrification was an important contributor to N_2O production. However, the negative relationship between N_2O and nitrate could also point to denitrification, which can lead to both the production and consumption of N_2O during the reduction of nitrate to nitrogen gas (N_2). Positive relationships between CH_4 and CDOM and ammonium could suggest the presence of decomposing and fermenting vegetation, and an increase of labile carbon substrates, was an important driver of high CH_4 concentrations. Without having measured the biological processes it is difficult to constrain these relationships to identify the dominant microbial transformations responsible for observed GHG concentrations.

The removal of topsoil prior to restoring wetlands on previously agricultural land is suggested to create near-natural conditions which support diverse wetland plant communities (Smith *et al.,* 2011). This could also be applied as a preventative measure to reduce nutrient or substrate availability and limit N_2O and CH_4 production during the flooding of restored or created wetlands. This could be particularly important during the initial flooding of the wetland where sediment erosion, vegetation decomposition and the mobilisation and export of nutrients from the wetland is likely to be high. However, removing topsoil could also lead to large losses of soil organic

carbon in the form of CO_2 (Kopittke *et al.,* 2024), further complicating the challenge of maximising the climate mitigation potential of restoration methods.

Another method of preparing sites prior to wetland restoration could be to plant and harvest cover crops which may remove excess nutrients in the soil (Ewing *et al.,* 2012). Cover crops are often adopted as an intervention to improve soil and water quality by reducing sediment losses from erosion and limiting N leaching from agricultural soils into waterbodies (De Notaris *et al.,* 2021). Rye (*Secale cereale*) is a popular cover crop due to its ability to 'scavenge' and remove excess nutrients from improved agricultural soils, preventing nutrient leaching into drainage water in agricultural river catchments (De Notaris *et al.,* 2021; Ewing *et al.,* 2012; Gupta *et al.,* 2023). Reductions in soil N_2O emissions of more than 50 % have also been reported following the use of rye as a cover crop under specific management practices (Fiorini *et al.,* 2020). Of course, this may not be an appropriate option for all sites suitable for wetland restoration, particularly those previously used for livestock grazing rather than arable production, but further research in this area could reveal interesting solutions to mitigate restored wetland GHG emissions. Early identification of land suitable for wetland restoration, and therefore early communication with landowners, could ensure the cessation of fertiliser applications and the removal of grazing of livestock long before the land was flooded. This could prevent an excess of nutrients available for nitrifying or denitrifying microbes, for example.

Other methods of altering soil biogeochemistry could be considered to change the availability of terminal electron acceptors to reduce favouring methanogenesis and nitrification. Higher concentrations of alternative electron acceptors such as sulfate has been shown to suppress CH_4 emissions by supporting a greater abundance of sulfate-reducing microbes which outcompete methanogenic microbes (Sela-Adler *et al.,* 2017). The

addition of biochar in peatlands has also been shown to immobilise nutrients and suppress microbial activity, leading to an overall reduction in GHG emissions (Jeewani *et al.,* 2025). This way of thinking could encourage more emphasis on microbial diversity restoration, adopting practices that support methanotrophic microbes, for example.

Wetland design and management of flooding time could also be important for limiting GHG production. Water level is recognised as important for controlling GHG emissions in river-connected wetlands (Treby and Carnell, 2023), as well as other wetlands such as peatlands (Evans *et al.,* 2021), due to the development of anaerobic conditions preferred by methanogens or denitrifying bacteria (Jin *et al.,* 2023). Managing the timing, frequency and extent of wetland flooding, and therefore the establishment of wetland vegetation, quantities of labile C, nutrients, oxygen, and fluctuations in water temperature, has been suggested as a way of controlling GHG emissions through limiting microbial productivity (Treby and Carnell, 2023). However, particularly in the case of ephemeral wetlands such as intertidal wetlands, it is difficult to predict or manage water levels or timing of flood inundation. Changes in hydrological dynamics due to sea-level rise, or 'coastal squeeze', and unseasonable variations in river flows present a challenge for limiting GHG emissions from coastal wetlands (Cadier *et al.,* 2023; Zhao *et al.,* 2020). There may be scope to consider this in the design of tidal ponds and channels in intertidal wetlands, such as management of wave energy, flooding extent and sedimentation which govern complex interactions between water temperatures, salinity, and C and N export (Reed *et al.,* 2018), but these interventions would need to be balanced against potential loss of biodiversity, coastal defence and flood water storage benefits.

4.4.3 Restoration vs. natural regeneration

There is an argument for focusing efforts on protecting existing inland and coastal wetlands from becoming degraded, and therefore larger sources of

GHG, by limiting erosion, sediment and nutrient loading, and restoring hydrological connectivity (Taillardat *et al.,* 2020; Zou *et al.,* 2022). The longevity of coastal wetland restoration has previously been called into question due to persisting environmental stressors in the surrounding landscape and large variability in the recovery times or success rates of wetlands returning to favourable ecological functioning (Simenstad *et al.,* 2006; Zedler and Callaway, 1999). Site specific factors create difficulty in applying a one-size-fits-all approach to balancing the cost-effectiveness of restoration vs. conservation (Rosentreter *et al.,* 2021a; Taillardat *et al.,* 2020). In terms of GHG mitigation, the large variability in the time it takes for the C sequestration rates to outweigh the initial N_2O and CH_4 emissions makes it very difficult to assess the benefits and drawbacks of restoration vs natural regeneration (He *et al.,* 2024). The likelihood of natural wetland regeneration is also largely dependent on the local climate, surrounding topography, hydrological regimes, and neighbouring land cover (Branton and Robinson, 2020). There are fewer studies that have reported positive or negative changes in GHG emissions during the natural regeneration of coastal wetlands without human interventions. Where wetland restoration is identified as part of flood defence improvement schemes or coastal realignment, timelines are governed by the need to ensure the safety of communities and pressured by the availability of funding, therefore often require active restoration. Whilst there is so much uncertainty, increasing efforts in mapping of wetlands at risk of becoming degraded could be an arguably more effective use of resources and a more long-term solution to protecting C storage benefits and avoiding enhanced N_2O and CH_4 emissions from deteriorated sites.

4.4.4 Key messages for decision-makers and policymakers

Whilst it is widely acknowledged that wetland restoration has high potential for meeting long-term GHG mitigation targets (Holmquist *et al.,* 2023; Iram *et al.,* 2021; Zou *et al.,* 2022), there is substantial uncertainty in the immediate or short-term impacts on GHG emissions that must be carefully

considered when translating scientific evidence into environmental policy (Rosentreter *et al.,* 2021a). The results of this study provide further evidence that newly restored wetlands can act as considerable sources of N_2O and CH_4, at least in the initial years following their creation. The key message for policy makers is to exercise caution in the development of carbon or natural capital policies, particularly regarding carbon crediting schemes. The development of frameworks such as the Natural Capital Standard will need to carefully consider the uncertainty of climate regulation ES provided by existing wetlands in the UK and ensure the appropriate management interventions are encouraged to avoid misrepresenting the potential of wetland restoration to offset UK GHG emissions. The application of these schemes in practice is still largely in its infancy, especially relative to the advances in high spatial and temporal resolution of in situ measurements of GHG concentrations and fluxes. The restoration of wetlands and other habitats identified as offering high GHG mitigation benefits must be continued to be seen as a complementary tool to tackle climate change, alongside active reductions in GHG emissions from other sectors such as industrial reliance on fossil fuels. Furthermore, creating new wetlands should not overshadow opportunities for the protection of existing wetlands from becoming further degraded by unresolved environmental stressors on aquatic ecosystems.

For decision-makers in ecological restoration, the findings of this study highlight the difficulty in accurately predicting and reporting on the GHG mitigation benefits of wetland restoration. However, this is not to say that the value of wetland restoration is diminished. The importance here is how we choose to define the values of ecological restoration. Wetland restoration has undeniably important benefits for biodiversity, human well-being and water quality improvement. Due to the large variability in site specific factors controlling biogeochemical processing, care needs to be taken when claiming large climate mitigation benefits without sufficient site-specific evidence. Despite the monumental challenge of meeting biodiversity restoration goals by 2030 and 2050, rushing restoration efforts

of high N_2O and CH_4 emitting habitats could lead to opposite desired results if it causes the acceleration of climate change. This also highlights the need for a greater collaboration between ecosystem managers and goal-setting committees, to ensure realistic, meaningful and achievable targets are being solidified in policy.

4.5 Conclusion

The significance of this study lies in its contribution to informing the application of NbS and the adoption of carbon credit schemes to financially support them. The evidence presented demonstrates the importance of monitoring non-CO_2 GHG and not only C sequestration rates to evaluate the effectiveness of intertidal restoration in providing climate change mitigation services. In the first year since its creation, the Calstock wetland acted as a considerable source of both N_2O and CH_4 relative to river contributions to the Tamar Estuary, therefore any carbon sequestered during this time may be offset by these contributions. It is also important to consider the trade-offs between the desired ES benefits, as demonstrated by the variability in nitrate and ammonium retention or export to the estuary which complicate the water quality improvement services provided by the wetland. Whilst this case study may not be an appropriate opportunity for the effective application of carbon credits towards achieving Net-Zero, this should not pull focus from the benefits of restoring aquatic ecosystems. More resilient ecosystems will be vital for adapting to the rapidly changing climate and subsequent changes to seasonality. It could also be that the discussed trade-offs will lessen over time as the wetland develops and stabilises, which will require continuous monitoring. However, this study should serve as a cautionary tale to avoid misleading expectations that may come with the adoption of carbon crediting schemes and the use of wetland restoration as a NbS to climate change mitigation. By including GHG monitoring within environmental monitoring and management plans, more effective evidence-based climate strategies can be developed, from local partnerships to international agreements.

Chapter 5: Final discussion and conclusions

5.1 Overview

This thesis broadly aimed to understand the variability of N_2O and CH_4 within the natural environment to better inform ecological restoration practices. Specifically, the focus of this research has been on the transport of GHG between river and estuary ecosystems which are internationally prioritised in restoration targets and are heavily relied upon to provide societally important ecosystem services. It was my objective to gain an understanding of how the increasing adoption of nature-based solutions (NbS), such as wetland habitat restoration, will influence the relative contributions of aquatic ecosystems to GHG emissions. To achieve this objective, I have reviewed the latest literature to understand GHG cycling pathways and emissions from natural sources; and interrogated data collected during the LOCATE and AgZero+ projects which provide high resolution monitoring of river catchments across the UK to understand the impact of changing land use and sustainable farming practices on carbon and GHG cycling. In Chapter 2, I investigated the application of empirical models to aid the understanding of N_2O and CH_4 emissions from freshwater and estuary surface waters, and in Chapter 3 I applied this when identifying hotspots of N_2O and CH_4 production and emissions in the Tamar from river-to-coast. In Chapter 4, I brought focus to a real example of a NbS through a case study of intertidal wetland restoration, exploring the role of ecosystem restoration in climate change mitigation and the impact on GHG emissions in hydrologically connected habitats.

It is evident that aquatic ecosystems are important sources of both N_2O and CH_4 (Saunois *et al.,* 2024b; Tian *et al.,* 2024). However, the challenge now is translating that knowledge into accessible and impactful messages that

can be incorporated into climate mitigation strategies whilst simultaneously working towards biodiversity recovery and GHG reduction targets. The introduction (Chapter 1) of this thesis refers to two highly relevant reports. The first is 'Quantifying the Potential Impact of Nature Based Solutions on Greenhouse Gas Emissions from UK Habitats' (Thom and Doar, 2021) and the second is 'Nature-based Solutions for Climate Change in the UK: A Report by the British Ecological Society' (Stafford *et al.,* 2021). These reports represent an important step towards bridging gaps between ecological restoration practices and GHG mitigation targets, and both highlight a need for more in situ measurements to support detailed investigations into the effects of restoration practices on GHG cycling. In the remainder of this final chapter, I will consolidate the key learnings from the research presented in this thesis and summarise its contribution to knowledge gaps highlighted by these reports. Finally, I will summarise remaining knowledge gaps whilst evaluating the limitations of methods applied in this thesis and recommend solutions to overcome these in future studies.

5.2 Research Significance

It is first important to recognise the difference between the significance, impact, and outcomes of the research presented in this thesis. Here I define the significance of this research as the knowledge gained; the impact as the change which that knowledge has the potential to bring about; and the outcome as the result of that change. These are summarised for each research chapter in Figures 5.1 – 5.3.

Chapter 2 (Figure 5.1) demonstrated the effect of including river-based empirical models in the estimation of GHG fluxes along a freshwater-estuary transect on the overall reported emissions from estuaries. The estuary emissions reported in this chapter were higher compared to previously reported for the Dart and Tamar estuaries (Barnes and Upstill-Goddard,

2011; Brown *et al.,* 2024; Upstill-Goddard and Barnes, 2016). This is an important finding in the understanding of how ecosystem management interventions may be spatially targeted based on the methods used to report the relative emissions from habitats along the LOAC. By comparing the different models used to predict gas exchange velocity (*k*) it was clear that considerable variability occurs between results driven by river hydrological variables. This analysis highlighted that river exports of GHG are an important contributing factor to estuary emissions and should be accurately accounted for and appropriately managed as such.

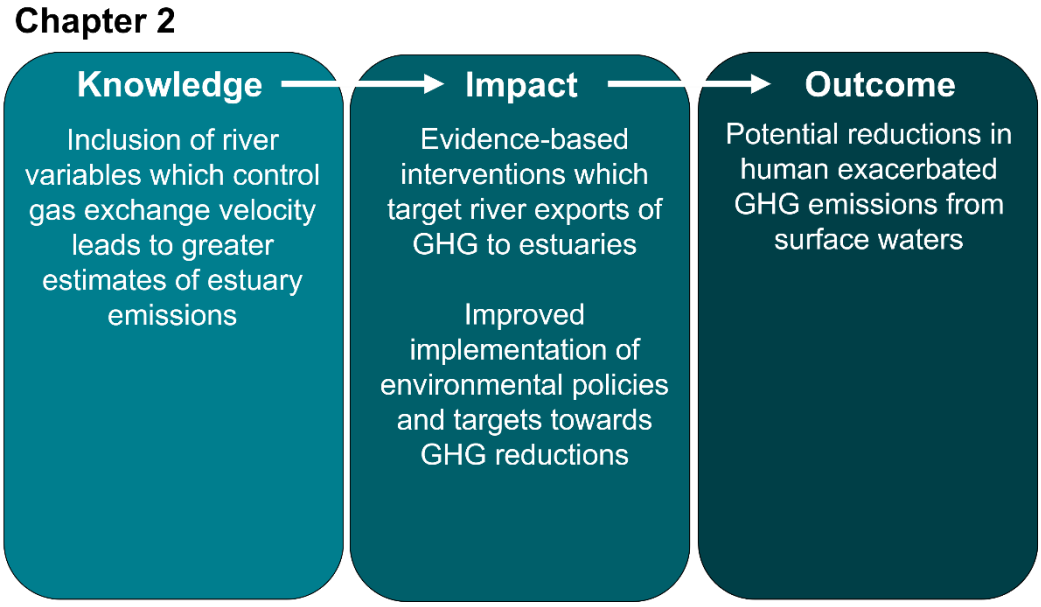

Figure 5.1. Research significance of Chapter 2: A comparison of empirical models of gas transfer velocity for estimating N_2O and CH_4 air-water fluxes

Chapter 3 (Figure 5.2) provides a river-to-coast overview of GHG concentrations in the Tamar catchment and identifies important correlations between GHG with nutrients and hydrological factors driving spatial variability in N_2O and CH_4 production. The key significance of this chapter is the identification of hotspots of N_2O and CH_4 emissions in the upper reaches of the Tamar Catchment. Providing a spatial assessment of GHG variability within the catchment allows the cost-effective targeting of NbS to

have the most positive impacts on GHG emissions. This study serves as evidence to support riparian habitat management and nutrient loading reductions in narrower, shallower upstream waters which may be more vulnerable to conditions which could support higher productivity of GHG producing microbes or an accumulation of GHG due to less flushing from large volumes of hydrological inputs. Whilst it is not clear which biological processes are dominating observations in this chapter, evidence of dilution or degassing of GHG at sampled locations moving downstream suggest hydrological residence times are important to the spatial variability of hotspots of dissolved GHG concentrations. The high spatial and temporal resolution of these measurements also enabled a comparison of the estuary contributions to GHG emissions to those from other UK sectors. To my knowledge, emissions from UK rivers or estuaries are not currently directly included within Nationally Determined Contributions (NDC) nor are they adequately, if at all, recognised in the Government guidance towards reducing overall human exacerbations to GHG emissions from natural sources. Whilst indirect N_2O emissions from agriculture and CH_4 emissions from urban wastewater are theoretically included within NDCs, a growing body of GHG data in surface waters will support the continued development of guidance on adopting nature-based solutions to tackle human changes to GHG emissions from natural sources.

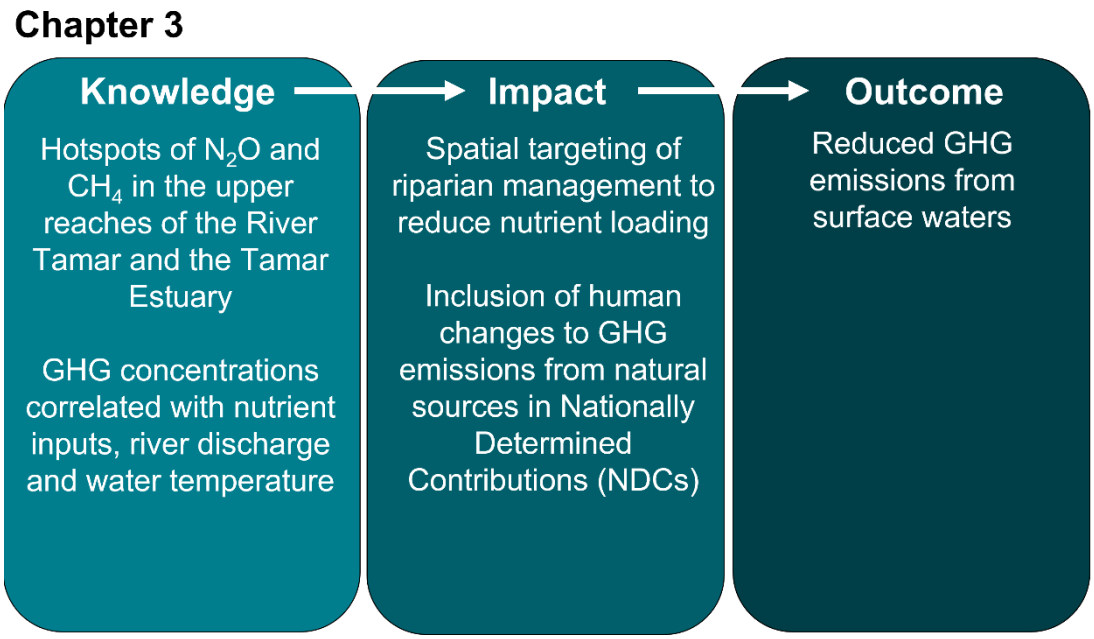

Figure 5.2. Research significance of Chapter 3: Emissions of N_2O and CH_4 along a river-to-coast aquatic continuum and opportunities for nature-based solutions

Chapter 4 (Figure 5.3) provides an assessment of GHG production from an intertidal wetland during the first year since its creation. The findings of this study agreed with previous reports that restored wetlands have the potential to increase sources of N_2O and CH_4 and further demonstrates the difficulty in balancing biodiversity objectives with GHG mitigation targets (Rosentreter *et al.,* 2021a). This research enabled consideration of interventions which could mitigate the export of GHG during wetland restoration. These findings should not be seen as a barrier to progress in habitat restoration efforts, but instead an opportunity to improve restoration practices and apply interventions to increase the climate change mitigation potential of ecosystem restoration. The main takeaway from this chapter is the need to build realistic expectations of the effectiveness of NbS to climate change mitigation. The widespread adoption of carbon crediting and natural capital schemes need to be supported by a robust foundation of scientific evidence. The C sequestration benefits claimed by a restoration project must accurately account for increased exports of N_2O and CH_4 which could offset climate mitigation services. This will enable the prioritisation of

ecological restoration efforts which offer the most long-term benefits towards slowing climate change. Overall, increased efforts towards understanding these trade-offs will ensure a holistic approach to tackling the climate and biodiversity crises.

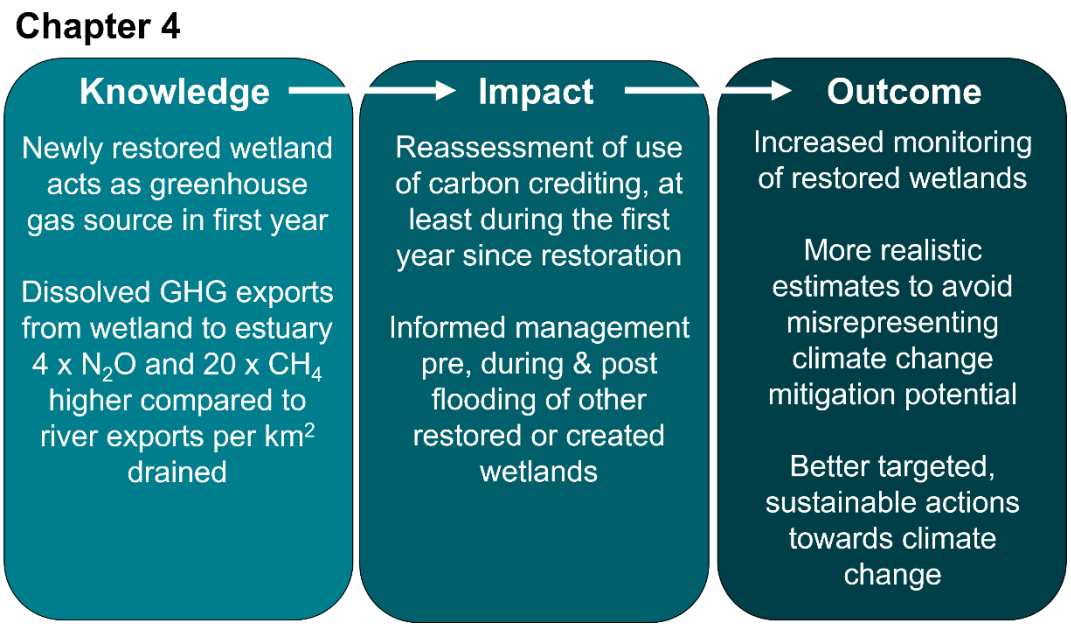

Figure 5.3. Research significance of Chapter 4: Monitoring the effectiveness of intertidal wetland restoration for climate change mitigation

5.3 Key lessons

5.3.1 Spatial planning of NbS is important for effective climate change mitigation

Ecosystem managers, researchers and decision-makers face the task of protecting 30 % of terrestrial, inland waters, coastal and marine areas by 2030 set by the Kunming-Montreal Global Biodiversity Framework (Target 3). The UK is also committed to reducing all GHG emissions by at least 81 % by 2035 compared to levels in 1990 (UK Government, 2025). Achieving these ambitious targets requires the spatial prioritisation of conservation

objectives whilst actively targeting potential hotspots of N_2O and CH_4. One of the key lessons of the research presented in this thesis is that the placement of NbS across a river catchment to coastal sea can not only restore habitat connectivity and biodiversity but could also influence the relative GHG contributions from rivers, estuaries and coastal waters. I have contextualised this in Figure 5.4 which identifies specific management interventions known to prevent nutrient loading to surface waters.

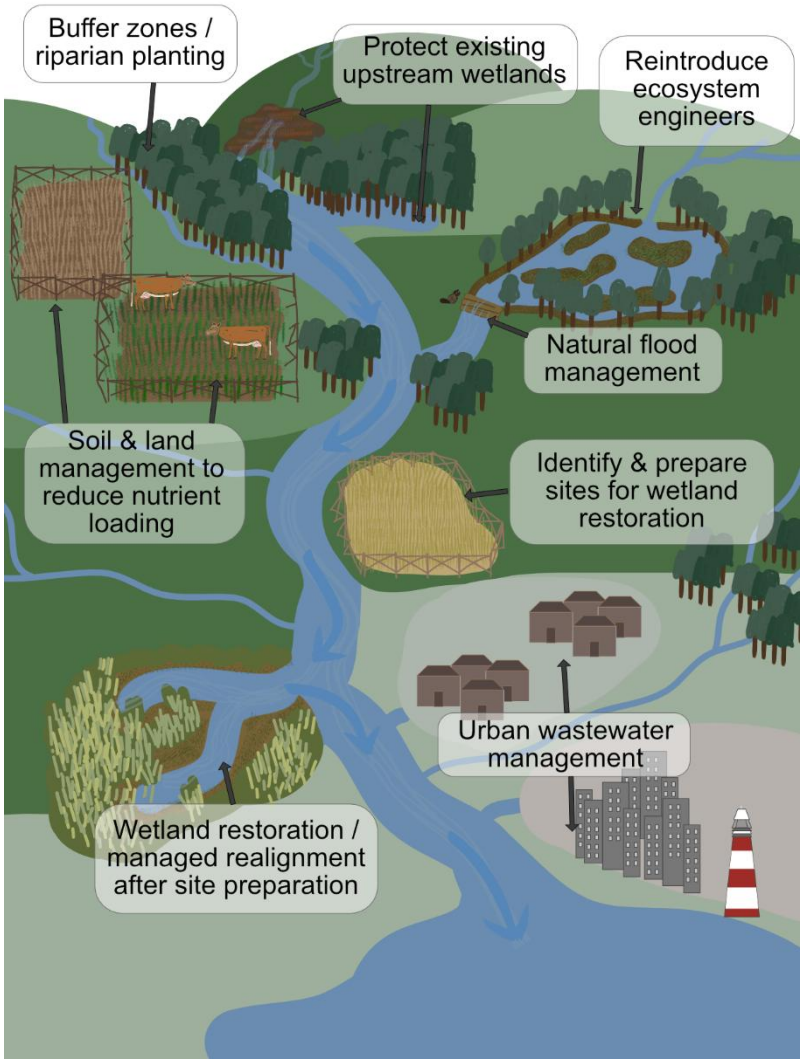

Figure 5.4 Schematic demonstrating the spatial planning of nature-based solutions to prevent nutrient loading into water catchments

Planting riparian woodlands, protecting existing wetlands from degradation, and the reintroduction of ecosystem engineer species such as the European beaver (*Castor fiber*) have a rich body of evidence to support their effectiveness in slowing the flow of rivers as natural flood management, retaining nutrients and carbon in soils, and preventing sedimentation of inland waters (Line *et al.,* 2016; Mander *et al.,* 2005; Puttock *et al.,* 2021, 2018). Based on the research presented in this thesis, I support the notion of prioritising 'upstream thinking' to reduce hotspots of GHG, restoring natural hydrological functioning and reducing nutrient loading up in the headwaters of river catchments which are often exposed to high agricultural inputs. This concept of a catchment-based approach to ecosystem management has been widely adopted in recent decades, leading to many resources for specific conservation and water quality objectives (Collins *et al.,* 2020). However, there are few resources which provide guidance on how these interventions may increase or decrease GHG emissions from natural sources. For example, the resource platform Conservation Evidence (conservationevidence.com) is a large collaborative project which aims to remove barriers between science and practice. It provides a summary of the available evidence and an assessment of the effectiveness for each conservation action. These platforms could be expanded to provide guidance for restoration and conservation managers specifically on maximising the climate change mitigation potential of restoration practices. Further work is needed to better integrate biodiversity and climate change mitigation priorities to inform the spatial planning of NbS. This would serve as a valuable exercise in applying lateral thinking across the fields of ecological restoration and biogeochemistry and demonstrates the value of the data collected during this research to making informed management decisions.

5.3.2 More evidence on NbS for climate change mitigation is needed

Securing a robust evidence base which can be easily implemented into landscape-scale NbS strategies is vital. In Chapter 4, the provision of in-situ measurements within the first month since Calstock intertidal wetland was created was of paramount importance for accurately representing the climate change mitigation potential of the project. This serves as an essential reminder for future restoration projects to include GHG monitoring within the early stages of environmental monitoring and management plans. At present, the evidence base for NbS is largely focused on biodiversity and carbon sequestration, but less evidence exists for targeting emissions of non-CO_2 gases. As this body of evidence grows, the effectiveness of future policies and frameworks on maximising C sequestration and minimising the production of N_2O and CH_4 will improve.

5.3.3 Policy and conservation framework development must be transdisciplinary

A transdisciplinary approach is needed to effectively tackle the climate and biodiversity crises. Environmental conservation frameworks, policies and legislation are continuously evolving and face the challenges of political disruption. To provide impactful stewardship of the most vulnerable ecosystems, scientific knowledge must also continuously evolve alongside decision-making infrastructure. The rapid advancement of data sharing across the world enables ecological, biogeochemical, hydrological and physical expertise to be incorporated into management frameworks. This further allows for improved spatial targeting of NbS to reduce human exacerbations to natural GHG sources.

It could also be argued that a shift in perspective is needed. Whilst there is justified urgency to meet habitat restoration targets, the rapid creation of ecosystems which would otherwise take decades or centuries to stabilise

presents both scientific and practical challenges. Data collected in Chapter 4 of this thesis shows that restored intertidal wetlands may initially act as sources of dissolved N_2O and CH_4 to connected surface waters, complicating their climate mitigation potential. Existing management frameworks and environmental funding structures often prioritise short-term restoration outcomes and often do not account for long-term changes in services such as carbon sequestration, making it challenging to evaluate the climate change mitigation benefits of habitat restoration. Transdisciplinary collaboration can lead to better aligned restoration goals with broader objectives to ensure realistic, evidence-based targets are driving management plans.

5.4 Remaining knowledge gaps and recommendations for further research

There remains considerable data deficiency for high resolution, in-situ GHG measurements in natural environments and in restored habitats during different stages of the restoration phases. The N_2O and CH_4 concentrations presented in this research address this deficiency and were applied to estimate emissions based on empirical models. This provides important spatial information for targeting high concentrations of dissolved GHG in surface waters, though a lack of in-situ gas flux measurements could be considered a limitation of this research. In future work, the estimated gas exchange velocity (k) of N_2O and CH_4, and therefore estimates of air-water gas fluxes, may be improved by taking direct hydrological measurements of river discharge, velocity, and depth, and meteorological measurements such as windspeed using a handheld anemometer at the time of sample collection.

However, including these extra measurements in the sampling regime would add considerably to the logistical challenges of delivering high-resolution monitoring across a river-to-coast transect. Time constraints are

a limiting factor in reaching a satisfactory number of representative sites across a catchment and therefore it may not be feasible to deliver accurate hydrological monitoring alongside biogeochemistry sampling. The sampled river sites in this thesis were selected based on existing water quality stations monitored by the Environment Agency. Future site selection could also target existing and active hydrological monitoring stations, such as Gunnislake, so that the environmental variables used in gas flux estimations are as representative of the sampled site conditions as possible.

There was a limit as to how far the biogeochemical processes relevant to N_2O and CH_4 concentrations could be constrained in this research. Future work could examine controls on hotspots of N_2O and CH_4 using stable isotopic signatures of 15N and 13C to trace dominant biogeochemical pathways (Ho *et al.,* 2024; McIlvin and Casciotti, 2010). It would be particularly interesting to identify terrestrial vs water sources of GHG to distinguish whether land runoff or in-situ production was a dominant driver of concentrations of N_2O and CH_4. Furthermore, this could be incorporated into studies of changing farmland practices under the development of Environmental Land Management schemes (ELMs) or during ecosystem restoration projects to identify the most effective interventions for reducing GHG from natural sources.

This research identified important relationships between GHG concentrations and river flows. This poses further questions around how the restoration of hydrological connectivity between aquatic ecosystems could impact spatial variability of GHG emissions along the LOAC, from river to coast. Over 1 million barriers fragment rivers in Europe (Belletti *et al.,* 2020) and only 1 % of UK rivers flow unobstructed from source to sea (Jones *et al.,* 2019). This is likely to be a conservative estimate due to the coarse availability of data. Instream barriers such as weirs, dams, and reservoirs, are known to have an impact on observations of N_2O and CH_4 (Bednařík *et al.,* 2017; Maavara *et al.,* 2020; Park *et al.,* 2023). There is increasing

interest in the removal of instream barriers, largely focused on the benefits of restoring hydrological connectivity and free flowing rivers (FFR) for vulnerable aquatic species such as migratory salmonid species (Barbarossa *et al.,* 2020; Buchanan *et al.,* 2022; Cortés-Espino *et al.,* 2023). A total of 391 in stream barriers exist in the Tamar and South Devon Catchments according to data collected by the AMBER Barrier Atlas (Figure 5.5) (AMBER Consortium, 2020; Jones *et al.,* 2019). The impact of these barriers on N_2O observations in this thesis was explored, but it was determined that there were not enough paired measurements above and below barriers, and of equal distance from barriers, to provide a statistically robust investigation. A study designed to sample above and below barriers could provide insight on how the removal of instream barriers may impact the transport of nutrients and GHG from river catchments to coastal seas. Such measurements alongside the high-resolution mapping of instream barriers would be highly beneficial to the scientific literature available to support the spatial planning of NbS for both climate change mitigation and biodiversity restoration across the LOAC.

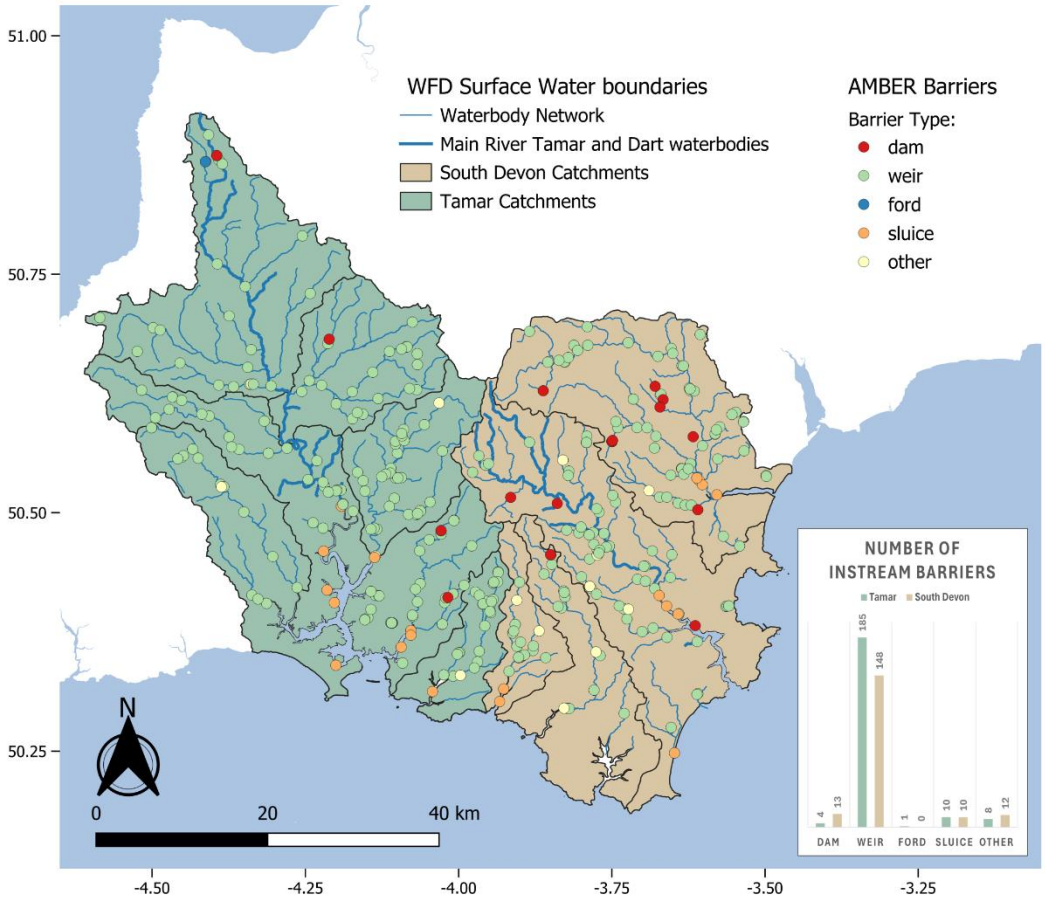

Figure 5.5. Location and type of instream barriers in the Tamar and South Devon Catchments. Data source: AMBER Barrier Atlas (AMBER Consortium, 2020)

5.5 Final conclusions

To conclude, NbS are a complimentary tool to, rather than a substitute for, other climate change mitigation practices, namely the rapid reduction of emissions from fossil fuels. Accounting for N_2O and CH_4 emissions can complicate assessments of the climate change mitigation potential of NbS. This work has demonstrated that restored wetlands can initially act as sources of N_2O and CH_4, highlighting the need for realistic expectations on short-term climate benefits of restoration projects. Caution is especially needed when assigning monetary values to the provision of ecosystem services during restoration projects, especially in the context of GHG

emission mitigation or offsetting. Standardizing methodologies in GHG flux estimations, strong interdisciplinary collaboration, and integrating long-term monitoring across ecosystem types is critical to reduce these uncertainties. Ultimately, our most effective climate change mitigation strategy remains halting further habitat degradation and removing reliance on fossil fuels, allowing natural recovery processes wherever possible.

Glossary

GHG – Greenhouse gas

CO_2 – Carbon dioxide

N_2O – Nitrous oxide

CH_4 – Methane

C – Carbon

N – Nitrogen

NbS – Nature-based Solutions

WCO – Western Channel Observatory

WEC – Western English Channel

LOAC – Land Ocean Aquatic Continuum

NDCs – Nationally Determined Contributions

List of references

Abril, G., Commarieu, M.-V., Guérin, F., 2007. Enhanced methane oxidation in an estuarine turbidity maximum. *Limnol. Oceanogr.* 52, 470–475. https://doi.org/10.4319/lo.2007.52.1.0470

Abril, G., Iversen, N., 2002. Methane dynamics in a shallow non-tidal estuary (Randers Fjord, Denmark). *Mar. Ecol. Prog. Ser.* 230, 171–181. https://doi.org/10.3354/meps230171

Abril, G., Riou, S.A., Etcheber, H., Frankignoulle, M., De Wit, R., Middelburg, J.J., 2000. Transient, Tidal Time-scale, Nitrogen Transformations in an Estuarine Turbidity Maximum—Fluid Mud System (The Gironde, South-west France). *Estuar. Coast. Shelf Sci.* 50, 703–715. https://doi.org/10.1006/ecss.1999.0598

Adams, C.A., Andrews, J.E., Jickells, T., 2012. Nitrous oxide and methane fluxes vs. carbon, nitrogen and phosphorous burial in new intertidal and saltmarsh sediments. *Sci. Total Environ.* 434, 240–251. https://doi.org/10.1016/j.scitotenv.2011.11.058

Aho, K.S., Maavara, T., Cawley, K.M., Raymond, P.A., 2023. Inland Waters can Act as Nitrous Oxide Sinks: Observation and Modeling Reveal that Nitrous Oxide Undersaturation May Partially Offset Emissions. *Geophys. Res. Lett.* 50, e2023GL104987. https://doi.org/10.1029/2023GL104987

Alin, S.R., Rasera, M.D.F.F.L., Salimon, C.I., Richey, J.E., Holtgrieve, G.W., Krusche, A.V., Snidvongs, A., 2011. Physical controls on carbon dioxide transfer velocity and flux in low-gradient river systems and implications for regional carbon budgets. *J. Geophys. Res.* 116, G01009. https://doi.org/10.1029/2010JG001398

AMBER Consortium, 2020. The AMBER Barrier Atlas. https://amber.international/european-barrier-atlas/

Anderson, C.M., DeFries, R.S., Litterman, R., Matson, P.A., Nepstad, D.C., Pacala, S., Schlesinger, W.H., Shaw, M.R., Smith, P., Weber, C., Field, C.B., 2019. Natural climate solutions are not enough. *Science* 363, 933–934. https://doi.org/10.1126/science.aaw2741

Arias-Ortiz, A., Oikawa, P.Y., Carlin, J., Masqué, P., Shahan, J., Kanneg, S., Paytan, A., Baldocchi, D.D., 2021. Tidal and Nontidal Marsh Restoration: A Trade-Off Between Carbon Sequestration, Methane Emissions, and Soil Accretion. *J. Geophys. Res. Biogeosciences* 126, e2021JG006573. https://doi.org/10.1029/2021JG006573

Armstrong McKay, D.I., Staal, A., Abrams, J.F., Winkelmann, R., Sakschewski, B., Loriani, S., Fetzer, I., Cornell, S.E., Rockström, J., Lenton, T.M., 2022. Exceeding 1.5°C global warming could trigger multiple climate tipping points. *Science* 377, eabn7950. https://doi.org/10.1126/science.abn7950

Bange, H.W., 2006. Nitrous oxide and methane in European coastal waters. *Estuar. Coast. Shelf Sci.* 70, 361–374. https://doi.org/10.1016/j.ecss.2006.05.042

Bange, H.W., Arevalo-Martinez, D.L., de la Paz, M., Farias, L., Kaiser, J., Kock, A., Law, C.S., Rees, A.P., Rehder, G., Tortell, P.D., Upstill-Goddard, R.C., Wilson, S.T., 2019a. A Harmonized Nitrous Oxide (N2O) Ocean Observation Network for the 21st Century. *Front. Mar. Sci.* 6, 157. https://doi.org/10.3389/fmars.2019.00157

Bange, H.W., Sim, C.H., Bastian, D., Kallert, J., Kock, A., Mujahid, A., Müller, M., 2019b. Nitrous oxide (N_2O) and methane (CH_4) in rivers and estuaries of northwestern Borneo. *Biogeosciences* 16, 4321–4335. https://doi.org/10.5194/bg-16-4321-2019

Barbarossa, V., Schmitt, R.J.P., Huijbregts, M.A.J., Zarfl, C., King, H., Schipper, A.M., 2020. Impacts of current and future large dams on the geographic range connectivity of freshwater fish worldwide. *Proc. Natl. Acad. Sci*. 117, 3648–3655. https://doi.org/10.1073/pnas.1912776117

Barnes, J., Upstill-Goddard, R.C., 2011. N_2 O seasonal distributions and air-sea exchange in UK estuaries: Implications for the tropospheric N_2 O source from European coastal waters. *J. Geophys. Res.* 116, G01006. https://doi.org/10.1029/2009JG001156

Bastviken, D., Tranvik, L.J., Downing, J.A., Crill, P.M., Enrich-Prast, A., 2011. Freshwater Methane Emissions Offset the Continental Carbon Sink. *Science* 331, 50–50. https://doi.org/10.1126/science.1196808

Beaulieu, J.J., DelSontro, T., Downing, J.A., 2019. Eutrophication will increase methane emissions from lakes and impoundments during the 21st century. *Nat. Commun.* 10, 1375. https://doi.org/10.1038/s41467-019-09100-5

Beaulieu, J.J., Tank, J.L., Hamilton, S.K., Wollheim, W.M., Hall, R.O., Mulholland, P.J., Peterson, B.J., Ashkenas, L.R., Cooper, L.W., Dahm, C.N., Dodds, W.K., Grimm, N.B., Johnson, S.L., McDowell, W.H., Poole, G.C., Valett, H.M., Arango, C.P., Bernot, M.J., Burgin, A.J., Crenshaw, C.L., Helton, A.M., Johnson, L.T., O'Brien, J.M., Potter, J.D., Sheibley, R.W., Sobota, D.J., Thomas, S.M., 2011. Nitrous oxide emission from denitrification in stream and river networks. *Proc. Natl. Acad. Sci.* 108, 214–219. https://doi.org/10.1073/pnas.1011464108

Bednařík, A., Blaser, M., Matoušů, A., Hekera, P., Rulík, M., 2017. Effect of weir impoundments on methane dynamics in a river. *Sci. Total Environ.* 584–585, 164–174. https://doi.org/10.1016/j.scitotenv.2017.01.163

Belletti, B., Garcia de Leaniz, C., Jones, J., Bizzi, S., Börger, L., Segura, G., Castelletti, A., van de Bund, W., Aarestrup, K., Barry, J., Belka, K.,

Berkhuysen, A., Birnie-Gauvin, K., Bussettini, M., Carolli, M., Consuegra, S., Dopico, E., Feierfeil, T., Fernández, S., Fernandez Garrido, P., Garcia-Vazquez, E., Garrido, S., Giannico, G., Gough, P., Jepsen, N., Jones, P.E., Kemp, P., Kerr, J., King, J., Łapińska, M., Lázaro, G., Lucas, M.C., Marcello, L., Martin, P., McGinnity, P., O'Hanley, J., Olivo del Amo, R., Parasiewicz, P., Pusch, M., Rincon, G., Rodriguez, C., Royte, J., Schneider, C.T., Tummers, J.S., Vallesi, S., Vowles, A., Verspoor, E., Wanningen, H., Wantzen, K.M., Wildman, L., Zalewski, M., 2020. More than one million barriers fragment Europe's rivers. *Nature* 588, 436–441. https://doi.org/10.1038/s41586-020-3005-2

Bertagnolli, A.D., Konstantinidis, K.T., Stewart, F.J., 2020. Non-denitrifier nitrous oxide reductases dominate marine biomes. *Environ. Microbiol. Rep*. 12, 681–692. https://doi.org/10.1111/1758-2229.12879

Beusen, A.H.W., Doelman, J.C., Van Beek, L.P.H., Van Puijenbroek, P.J.T.M., Mogollón, J.M., Van Grinsven, H.J.M., Stehfest, E., Van Vuuren, D.P., Bouwman, A.F., 2022. Exploring river nitrogen and phosphorus loading and export to global coastal waters in the Shared Socio-economic pathways. *Glob. Environ. Change* 72, 102426. https://doi.org/10.1016/j.gloenvcha.2021.102426

Bhushan, A., Goyal, V.C., Srivastav, A.L., 2024. Greenhouse gas emissions from inland water bodies and their rejuvenation: a review. *J. Water Clim. Change* 15, 5626–5644. https://doi.org/10.2166/wcc.2024.561

Bidlack, A., Bisbing, S., Buma, B., Diefenderfer, H., Fellman, J., Floyd, W., Giesbrecht, I., Lally, A., Lertzman, K., Perakis, S., Butman, D., D'Amore, D., Fleming, S., Hood, E., Hunt, B., Kiffney, P., McNicol, G., Menounos, B., Tank, S., 2021. Climate-Mediated Changes to Linked Terrestrial and Marine Ecosystems across the Northeast Pacific Coastal Temperate Rainforest Margin. *BioScience* 71. https://doi.org/10.1093/biosci/biaa171

Billett, M.F., Moore, T.R., 2008. Supersaturation and evasion of CO_2 and CH_4 in surface waters at Mer Bleue peatland, Canada. *Hydrol. Process.* 22, 2044–2054. https://doi.org/10.1002/hyp.6805

Borges, A., Vanderborght, J.-P., Schiettecatte, L.-S., Gazeau, F., Ferrón-Smith, S., Delille, B., Frankignoulle, M., 2004. Variability of gas transfer velocity of CO2 in a macrotidal estuary (The Scheldt). *Estuaries* 27, 593–603. https://doi.org/10.1007/BF02907647

Borges, A.V., Darchambeau, F., Lambert, T., Bouillon, S., Morana, C., Brouyère, S., Hakoun, V., Jurado, A., Tseng, H.-C., Descy, J.-P., Roland, F.A.E., 2018. Effects of agricultural land use on fluvial carbon dioxide, methane and nitrous oxide concentrations in a large European river, the Meuse (Belgium). *Sci. Total Environ*. 610–611, 342–355. https://doi.org/10.1016/j.scitotenv.2017.08.047

Borges, A.V., Darchambeau, F., Lambert, T., Morana, C., Allen, G.H., Tambwe, E., Toengaho Sembaito, A., Mambo, T., Nlandu Wabakhangazi, J., Descy, J.-P., Teodoru, C.R., Bouillon, S., 2019. Variations in dissolved greenhouse gases (CO2, CH4, N2O) in the Congo River network overwhelmingly driven by fluvial-wetland connectivity. *Biogeosciences* 16, 3801–3834. https://doi.org/10.5194/bg-16-3801-2019

Bouwman, A.F., Bierkens, M.F.P., Griffioen, J., Hefting, M.M., Middelburg, J.J., Middelkoop, H., Slomp, C.P., 2013. Nutrient dynamics, transfer and retention along the aquatic continuum from land to ocean: towards integration of ecological and biogeochemical models. *Biogeosciences* 10, 1–22. https://doi.org/10.5194/bg-10-1-2013

Branton, C., Robinson, D.T., 2020. Quantifying Topographic Characteristics of Wetlandscapes. *Wetlands* 40, 433–449. https://doi.org/10.1007/s13157-019-01187-2

Brazier, R.E., Puttock, A., Graham, H.A., Auster, R.E., Davies, K.H., Brown, C.M.L., 2021. Beaver: Nature's ecosystem engineers. *WIREs Water* 8, e1494. https://doi.org/10.1002/wat2.1494

Brewer, P.G., Riley, J.P., 1967. A study of some manual and automatic procedures for the determination of nitrate and silicate in ocean water. *Deep Sea Res. Oceanogr. Abstr*. 14, 475–477. https://doi.org/10.1016/0011-7471(67)90055-1

Brooks, T.M., Butchart, S.H.M., Cox, N.A., Heath, M., Hilton-Taylor, C., Hoffmann, M., Kingston, N., Rodríguez, J.P., Stuart, S.N., Smart, J., 2015. Harnessing biodiversity and conservation knowledge products to track the Aichi Targets and Sustainable Development Goals. *Biodiversity* 16, 157–174. https://doi.org/10.1080/14888386.2015.1075903

Brown, A.M., Bass, A.M., Pickard, A.E., 2022. Anthropogenic-estuarine interactions cause disproportionate greenhouse gas production: A review of the evidence base. *Mar. Pollut. Bull.* 174, 113240. https://doi.org/10.1016/j.marpolbul.2021.113240

Brown, A.M., Bass, A.M., Skiba, U., MacDonald, J.M., Pickard, A.E., 2023. Urban landscapes and legacy industry provide hotspots for riverine greenhouse gases: A source-to-sea study of the River Clyde. *Water Res*. 236, 119969. https://doi.org/10.1016/j.watres.2023.119969

Brown, A.M., Bass, A.M., White, S., Corr, M., Skiba, U., MacDonald, J.M., Pickard, A.E., 2024. The impact of estuarine flushing on greenhouse gases: A study of the stratified Clyde estuary. *Estuar. Coast. Shelf Sci.* 304, 108830. https://doi.org/10.1016/j.ecss.2024.108830

Buchanan, B.P., Sethi, S.A., Cuppett, S., Lung, M., Jackman, G., Zarri, L., Duvall, E., Dietrich, J., Sullivan, P., Dominitz, A., Archibald, J.A., Flecker, A., Rahm, B.G., 2022. A machine learning approach to identify barriers in stream networks demonstrates high prevalence of unmapped riverine

dams. *J. Environ. Manage.* 302, 113952. https://doi.org/10.1016/j.jenvman.2021.113952

Burns, F., Mordue, S., al Fulaij, N., Boersch-Supan, P.H., Boswell, J., Boyd, R.J., Bradfer-Lawrence, T., de Ornellas, P., de Palma, A., de Zylva, P., Dennis, E.B., Foster, S., Gilbert, G., Halliwell, L., Hawkins, K., Haysom, K.A., Holland, M.M., Hughes, J., Jackson, A.C., Mancini, F., Mathews, F., McQuatters-Gollop, A., Noble, D.G., O'Brien, D., Pescott, O.L., Purvis, A., Simkin, J., Smith, A., Stanbury, A.J., Villemot, J., Walker, K.J., Walton, P., Webb, T.J., Williams, J., Wilson, R., Gregory, R.D., 2023. State of Nature 2023. The State of Nature Partnership.

Bussmann, I., Koedel, U., Schütze, C., Kamjunke, N., Koschorreck, M., 2022. Spatial Variability and Hotspots of Methane Concentrations in a Large Temperate River. *Front. Environ. Sci.* 10.

Cadier, C., Waltham, N.J., Canning, A., Fry, S., Adame, M.F., 2023. Tidal restoration to reduce greenhouse gas emissions from freshwater impounded coastal wetlands. *Restor. Ecol*. 31, e13829. https://doi.org/10.1111/rec.13829

Calvin, K., Dasgupta, D., Krinner, G., Mukherji, A., Thorne, P.W., Trisos, C., Romero, J., Aldunce, P., Barrett, K., Blanco, G., Cheung, W.W.L., Connors, S., Denton, F., Diongue-Niang, A., Dodman, D., Garschagen, M., Geden, O., Hayward, B., Jones, C., Jotzo, F., Krug, T., Lasco, R., Lee, Y.-Y., Masson-Delmotte, V., Meinshausen, M., Mintenbeck, K., Mokssit, A., Otto, F.E.L., Pathak, M., Pirani, A., Poloczanska, E., Pörtner, H.-O., Revi, A., Roberts, D.C., Roy, J., Ruane, A.C., Skea, J., Shukla, P.R., Slade, R., Slangen, A., Sokona, Y., Sörensson, A.A., Tignor, M., Van Vuuren, D., Wei, Y.-M., Winkler, H., Zhai, P., Zommers, Z., Hourcade, J.-C., Johnson, F.X., Pachauri, S., Simpson, N.P., Singh, C., Thomas, A., Totin, E., Arias, P., Bustamante, M., Elgizouli, I., Flato, G.,

Howden, M., Méndez-Vallejo, C., Pereira, J.J., Pichs-Madruga, R., Rose, S.K., Saheb, Y., Sánchez Rodríguez, R., Ürge-Vorsatz, D., Xiao, C., Yassaa, N., Alegría, A., Armour, K., Bednar-Friedl, B., Blok, K., Cissé, G., Dentener, F., Eriksen, S., Fischer, E., Garner, G., Guivarch, C., Haasnoot, M., Hansen, G., Hauser, M., Hawkins, E., Hermans, T., Kopp, R., Leprince-Ringuet, N., Lewis, J., Ley, D., Ludden, C., Niamir, L., Nicholls, Z., Some, S., Szopa, S., Trewin, B., Van Der Wijst, K.-I., Winter, G., Witting, M., Birt, A., Ha, M., Romero, J., Kim, J., Haites, E.F., Jung, Y., Stavins, R., Birt, A., Ha, M., Orendain, D.J.A., Ignon, L., Park, S., Park, Y., Reisinger, A., Cammaramo, D., Fischlin, A., Fuglestvedt, J.S., Hansen, G., Ludden, C., Masson-Delmotte, V., Matthews, J.B.R., Mintenbeck, K., Pirani, A., Poloczanska, E., Leprince-Ringuet, N., Péan, C., 2023. IPCC, 2023: Climate Change 2023: Synthesis Report. Contribution of Working Groups I, II and III to the Sixth Assessment Report of the Intergovernmental Panel on Climate Change [Core Writing Team, H. Lee and J. Romero (eds.)]. IPCC, Geneva, Switzerland. Intergovernmental Panel on Climate Change (IPCC). https://doi.org/10.59327/IPCC/AR6-9789291691647

Campos, C.J.A., Kershaw, S., Lee, R.J., Morgan, O.C., Hargin, K., 2011. Rainfall and river flows are predictors for β-glucuronidase positive Escherichia coli accumulation in mussels and Pacific oysters from the Dart Estuary (England). *J. Water Health* 9, 368–381. https://doi.org/10.2166/wh.2011.136

Capelle, D., 2016. Temporal trends and biogeochemical controls on methane and nitrous-oxide distributions in coastal waters of the subarctic Pacific Ocean 202.

Casciotti, K.L., Buchwald, C., Santoro, A.E., Frame, C., 2011. Assessment of Nitrogen and Oxygen Isotopic Fractionation During Nitrification and Its

Expression in the Marine Environment, in: Methods in Enzymology. *Elsevier*, pp. 253–280. https://doi.org/10.1016/B978-0-12-381294-0.00011-0

Cicerone, R.J., Oremland, R.S., 1988. Biogeochemical aspects of atmospheric methane. *Glob. Biogeochem. Cycles* 2, 299–327. https://doi.org/10.1029/GB002i004p00299

Cirpka, O., Reichert, P., Wanner, O., Mueller, S., R., Schwarzenbach, R., P., 1993. Gas exchange at river cascades: field experiments and model calculations. *Environ. Sci. Technol.* 27, 2086–2097. https://doi.org/10.1021/es00047a014

Clark, J., Schlosser, P., Simpson, H., Stute, M., Wanninkhof, R., Ho, D., 1995. Relationship between Gas Transfer Velocities and Wind Speeds in The Tidal Hudson River Determined by the Dual Tracer Technique. *Air-Water Gas Transf.*

Collins, R., Johnson, D., Crilly, D., Rickard, A., Neal, L., Morse, A., Walker, M., Lear, R., Deasy, C., Paling, N., Anderton, S., Ryder, C., Bide, P., Holt, A., 2020. Collaborative water management across England – An overview of the Catchment Based Approach. *Environ. Sci. Policy* 112, 117–125. https://doi.org/10.1016/j.envsci.2020.06.001

Convention on Biological Diversity, 2022. 15/4. Kunming-Montreal Global Biodiversity Framework. URL https://www.cbd.int/doc/decisions/cop-15/cop-15-dec-04-en.pdf (accessed 6.3.25).

Cook-Patton, S.C., Drever, C.R., Griscom, B.W., Hamrick, K., Hardman, H., Kroeger, T., Pacheco, P., Raghav, S., Stevenson, M., Webb, C., Yeo, S., Ellis, P.W., 2021. Protect, manage and then restore lands for climate mitigation. *Nat. Clim. Change* 11, 1027–1034. https://doi.org/10.1038/s41558-021-01198-0

Cornejo-D'Ottone, M., Murillo, A., Farias, L., 2015. An Unaccounted for N2O Sink In The Surface Water of the Eastern Subtropical South Pacific: Physical Versus Biological Mechanisms. *Prog. Oceanogr.* 137. https://doi.org/10.1016/j.pocean.2014.12.016

Cortés-Espino, A., Langle-Flores, A., Gauna Ruíz De León, C., 2023. Valuing Free-Flowing Rivers: The Influence of Social Value on Willingness to Pay for Ecosystem Services Protection. *Water* 15, 1279. https://doi.org/10.3390/w15071279

Costanza, R., Anderson, S.J., Sutton, P., Mulder, K., Mulder, O., Kubiszewski, I., Wang, X., Liu, X., Pérez-Maqueo, O., Luisa Martinez, M., Jarvis, D., Dee, G., 2021. The global value of coastal wetlands for storm protection. *Glob. Environ. Change* 70, 102328. https://doi.org/10.1016/j.gloenvcha.2021.102328

Costanza, R., d'Arge, R., de Groot, R., Farber, S., Grasso, M., Hannon, B., Limburg, K., Naeem, S., O'Neill, R.V., Paruelo, J., Raskin, R.G., Sutton, P., van den Belt, M., 1997. The value of the world's ecosystem services and natural capital. *Nature* 387, 253–260. https://doi.org/10.1038/387253a0

Davidson, E.A., 2009. The contribution of manure and fertilizer nitrogen to atmospheric nitrous oxide since 1860. *Nat. Geosci*. 2, 659–662. https://doi.org/10.1038/ngeo608

de Angelis, M.A., Lee, C., 1994. Methane production during zooplankton grazing on marine phytoplankton. *Limnol. Oceanogr.* 39, 1298–1308. https://doi.org/10.4319/lo.1994.39.6.1298

De Notaris, C., Mortensen, E.Ø., Sørensen, P., Olesen, J.E., Rasmussen, J., 2021. Cover crop mixtures including legumes can self-regulate to optimize N2 fixation while reducing nitrate leaching. *Agric. Ecosyst. Environ*. 309, 107287. https://doi.org/10.1016/j.agee.2020.107287

DelSontro, T., Perez, K.K., Sollberger, S., Wehrli, B., 2016. Methane dynamics downstream of a temperate run-of-the-river reservoir. *Limnol. Oceanogr.* 61. https://doi.org/10.1002/lno.10387

Díaz, S., Settele, J., Brondízio, E.S., Ngo, H.T., Guèze, M., Agard, J., Arneth, A., Balvanera, P., Brauman, K.A., Butchart, S.H.M., Chan, K.M.A., Garibaldi, L.A., Ichii, K., Liu, J., Subramanian, S.M., Midgley, G.F., Miloslavich, P., Molnár, Z., Obura, D., Pfaff, A., Polasky, S., Purvis, A., Razzaque, J., Reyers, B., Roy Chowdhury, R., Shin, Y.J., Visseren-Hamakers, I.J., Willis, K.J., Zayas, C.N., Díaz, S., Settele, J., Brondízio, E.S., Ngo, H.T., Guèze, M., Agard, J., Arneth, A., Balvanera, P., Brauman, K.A., Butchart, S.H.M., Chan, K.M.A., Garibaldi, L.A., Ichii, K., Liu, J., Subramanian, S.M., Midgley, G.F., Miloslavich, P., Molnár, Z., Obura, D., Pfaff, A., Polasky, S., Purvis, A., Razzaque, J., Reyers, B., Roy Chowdhury, R., Shin, Y.J., Visseren-Hamakers, I.J., Willis, K.J., Zayas, C.N., 2019. Summary for policymakers of the global assessment report on biodiversity and ecosystem services of the Intergovernmental Science-Policy Platform on Biodiversity and Ecosystem Services. IPBES Secretariat, Bonn, Germany.

Dijkstra, F.A., Prior, S.A., Runion, G.B., Torbert, H.A., Tian, H., Lu, C., Venterea, R.T., 2012. Effects of elevated carbon dioxide and increased temperature on methane and nitrous oxide fluxes: evidence from field experiments. Front. Ecol. Environ. 10, 520–527. https://doi.org/10.1890/120059

Dlugokenck, E.J., Steele, L.P., Lang, P.M., Masarie, K.A., 1994. The growth rate and distribution of atmospheric methane. J. *Geophys. Res. Atmospheres* 99, 17021–17043. https://doi.org/10.1029/94JD01245

Dlugokencky, E.J., Masarie, K.A., Lang, P.M., Tans, P.P., 1998. Continuing decline in the growth rate of the atmospheric methane burden. *Nature* 393, 447–450. https://doi.org/10.1038/30934

Dong, L.F., Nedwell, D.B., Colbeck, I., Finch, J., 2005. Nitrous oxide emission from some English and Welsh rivers and estuaries. *Water Air Soil Pollut*. Focus 4, 127–134. https://doi.org/10.1007/s11267-005-3022-z

Drake, T.W., Raymond, P.A., Spencer, R.G.M., 2018. Terrestrial carbon inputs to inland waters: A current synthesis of estimates and uncertainty. *Limnol. Oceanogr. Lett.* 3, 132–142. https://doi.org/10.1002/lol2.10055

Dumont, E.L., Harrison, J., Kroeze, C., Bakker, E.-J., Seitzinger, S., 2005. Global distribution and sources of dissolved inorganic nitrogen export to the coastal zone: Results from a spatially explicit, global model.

Dunklin, P., Parry, J., Gegg, T., 2024. Should nature restoration projects be able to stack multiple revenue streams from ecosystem services? Full impact accounting as a clear way forward. *Nat.-Based Solut.* 5, 100141. https://doi.org/10.1016/j.nbsj.2024.100141

Entwistle, N.S., Heritage, G.L., Schofield, L.A., Williamson, R.J., 2019. Recent changes to floodplain character and functionality in England. CATENA 174, 490–498. https://doi.org/10.1016/j.catena.2018.11.018

Environment Agency, 2025a. Catchment Data Explorer: Tamar Management Catchment [WWW Document]. URL https://environment.data.gov.uk/catchment-planning/ManagementCatchment/3089/classifications (accessed 2.2.25).

Environment Agency, 2025b. Catchment Data Explorer: Dart Water Body [WWW Document]. URL https://environment.data.gov.uk/catchment-planning/WaterBody/GB108046008350

Environment Agency, 2022. River Habitat Survey in Britain and Ireland Field Survey Guidance Manual: 2003 Version (2022 Reprint).

Environment Agency, https://environment.data.gov.uk/hydrology/explore. Defra Hydrology Data Explorer [WWW Document].

https://environment.data.gov.uk/hydrology/explore. URL https://environment.data.gov.uk/hydrology/explore (accessed 5.14.24).

Etheridge, D.M., Pearman, G.I., Fraser, P.J., 1992. Changes in tropospheric methane between 1841 and 1978 from a high accumulation-rate Antarctic ice core. Tellus B 44, 282–294. https://doi.org/10.1034/j.1600-0889.1992.t01-3-00006.x

Evans, C.D., Cooper, D.M., Gannon, B., 2001. A Novel Method for Mapping Critical Loads Across a River Network: Application to the River Dart, Southwest England. *Water Air Soil Pollut.* Focus 1, 437–453. https://doi.org/10.1023/A:1011546930939

Evans, C.D., Peacock, M., Baird, A.J., Artz, R.R.E., Burden, A., Callaghan, N., Chapman, P.J., Cooper, H.M., Coyle, M., Craig, E., Cumming, A., Dixon, S., Gauci, V., Grayson, R.P., Helfter, C., Heppell, C.M., Holden, J., Jones, D.L., Kaduk, J., Levy, P., Matthews, R., McNamara, N.P., Misselbrook, T., Oakley, S., Page, S.E., Rayment, M., Ridley, L.M., Stanley, K.M., Williamson, J.L., Worrall, F., Morrison, R., 2021. Overriding water table control on managed peatland greenhouse gas emissions. *Nature* 593, 548–552. https://doi.org/10.1038/s41586-021-03523-1

Evans, P.N., Boyd, J.A., Leu, A.O., Woodcroft, B.J., Parks, D.H., Hugenholtz, P., Tyson, G.W., 2019. An evolving view of methane metabolism in the Archaea. *Nat. Rev. Microbiol.* 17, 219–232. https://doi.org/10.1038/s41579-018-0136-7

Ewing, J.M., Vepraskas, M.J., Broome, S.W., White, J.G., 2012. Changes in wetland soil morphological and chemical properties after 15, 20, and 30 years of agricultural production. *Geoderma* 179–180, 73–80. https://doi.org/10.1016/j.geoderma.2012.02.018

Fankhauser, S., Smith, S.M., Allen, M., Axelsson, K., Hale, T., Hepburn, C., Kendall, J.M., Khosla, R., Lezaun, J., Mitchell-Larson, E., Obersteiner, M.,

Rajamani, L., Rickaby, R., Seddon, N., Wetzer, T., 2022. The meaning of net zero and how to get it right. *Nat. Clim. Change* 12, 15–21. https://doi.org/10.1038/s41558-021-01245-w

Farías, L., Faúndez, J., Fernández, C., Cornejo, M., Sanhueza, S., Carrasco, C., 2013. Biological N2O Fixation in the Eastern South Pacific Ocean and Marine Cyanobacterial Cultures. *PLoS ONE* 8, e63956. https://doi.org/10.1371/journal.pone.0063956

Farquharson, R., 2016. Nitrification rates and associated nitrous oxide emissions from agricultural soils – a synopsis. *Soil Res.* 54, 469–480. https://doi.org/10.1071/SR15304

Fiorini, A., Maris, S.C., Abalos, D., Amaducci, S., Tabaglio, V., 2020. Combining no-till with rye (Secale cereale L.) cover crop mitigates nitrous oxide emissions without decreasing yield. *Soil Tillage Res.* 196, 104442. https://doi.org/10.1016/j.still.2019.104442

Fluet-Chouinard, E., Stocker, B.D., Zhang, Z., Malhotra, A., Melton, J.R., Poulter, B., Kaplan, J.O., Goldewijk, K.K., Siebert, S., Minayeva, T., Hugelius, G., Joosten, H., Barthelmes, A., Prigent, C., Aires, F., Hoyt, A.M., Davidson, N., Finlayson, C.M., Lehner, B., Jackson, R.B., McIntyre, P.B., 2023. Extensive global wetland loss over the past three centuries. *Nature* 614, 281–286. https://doi.org/10.1038/s41586-022-05572-6

Gauci, V., Pangala, S.R., Shenkin, A., Barba, J., Bastviken, D., Figueiredo, V., Gomez, C., Enrich-Prast, A., Sayer, E., Stauffer, T., Welch, B., Elias, D., McNamara, N., Allen, M., Malhi, Y., 2024. Global atmospheric methane uptake by upland tree woody surfaces. *Nature* 631, 796–800. https://doi.org/10.1038/s41586-024-07592-w

Girardin, C.A.J., Jenkins, S., Seddon, N., Allen, M., Lewis, S.L., Wheeler, C.E., Griscom, B.W., Malhi, Y., 2021. Nature-based solutions can help cool the planet — if we act now. *Nature*.

Graßhoff, K., 1976. Methods of seawater analysis. Verl. Chemie, Weinheim.

Grill, G., Lehner, B., Thieme, M., Geenen, B., Tickner, D., Antonelli, F., Babu, S., Borrelli, P., Cheng, L., Crochetiere, H., Ehalt Macedo, H., Filgueiras, R., Goichot, M., Higgins, J., Hogan, Z., Lip, B., McClain, M.E., Meng, J., Mulligan, M., Nilsson, C., Olden, J.D., Opperman, J.J., Petry, P., Reidy Liermann, C., Sáenz, L., Salinas-Rodríguez, S., Schelle, P., Schmitt, R.J.P., Snider, J., Tan, F., Tockner, K., Valdujo, P.H., van Soesbergen, A., Zarfl, C., 2019. Mapping the world's free-flowing rivers. *Nature* 569, 215–221. https://doi.org/10.1038/s41586-019-1111-9

Griscom, B.W., Adams, J., Ellis, P.W., Houghton, R.A., Lomax, G., Miteva, D.A., Schlesinger, W.H., Shoch, D., Siikamäki, J.V., Smith, P., Woodbury, P., Zganjar, C., Blackman, A., Campari, J., Conant, R.T., Delgado, C., Elias, P., Gopalakrishna, T., Hamsik, M.R., Herrero, M., Kiesecker, J., Landis, E., Laestadius, L., Leavitt, S.M., Minnemeyer, S., Polasky, S., Potapov, P., Putz, F.E., Sanderman, J., Silvius, M., Wollenberg, E., Fargione, J., 2017. Natural climate solutions. *Proc. Natl. Acad. Sci.* 114, 11645–11650. https://doi.org/10.1073/pnas.1710465114

Gruber, N., Galloway, J.N., 2008. An Earth-system perspective of the global nitrogen cycle. Nature 451, 293–296. https://doi.org/10.1038/nature06592

Grundle, D.S., Löscher, C.R., Krahmann, G., Altabet, M.A., Bange, H.W., Karstensen, J., Körtzinger, A., Fiedler, B., 2017. Low oxygen eddies in the eastern tropical North Atlantic: Implications for N2O cycling. *Sci. Rep*. 7, 4806. https://doi.org/10.1038/s41598-017-04745-y

Gupta, R., Bhattarai, R., Kalita, P.K., Dokoohaki, H., Coppess, J.W., Armstrong, S.D., 2023. Evaluation of long-term impact of cereal rye as a winter cover crop in Illinois. *Sci. Total Environ*. 877, 162956. https://doi.org/10.1016/j.scitotenv.2023.162956

Hale, T., Smith, S.M., Black, R., Cullen, K., Fay, B., Lang, J., Mahmood, S., 2022. Assessing the rapidly-emerging landscape of net zero targets. *Clim. Policy* 22, 18–29. https://doi.org/10.1080/14693062.2021.2013155

Hall Jr., R.O., Ulseth, A.J., 2020. Gas exchange in streams and rivers. WIREs *Water* 7, e1391. https://doi.org/10.1002/wat2.1391

Hanson, R.S., Hanson, T.E., 1996. Methanotrophic bacteria. *Microbiol. Rev*. 60, 439–471. https://doi.org/10.1128/mr.60.2.439-471.1996

Harley, J.F., Carvalho, L., Dudley, B., Heal, K.V., Rees, R.M., Skiba, U., 2015. Spatial and seasonal fluxes of the greenhouse gases N2O, CO2 and CH4 in a UK macrotidal estuary. *Estuar. Coast. Shelf Sci.* 153, 62–73. https://doi.org/10.1016/j.ecss.2014.12.004

He, S., Guo, X., Zhao, M., Chen, D., Fu, S., Tian, G., Xu, H., Liang, X., Wang, H., Li, G., Liu, X., 2025. Ecological restoration reduces greenhouse gas emissions by altering planktonic and sedimentary microbial communities in a shallow eutrophic lake. *Environ. Res.* 275, 121400. https://doi.org/10.1016/j.envres.2025.121400

He, T., Ding, W., Cheng, X., Cai, Y., Zhang, Y., Xia, H., Wang, X., Zhang, J., Zhang, K., Zhang, Q., 2024. Meta-analysis shows the impacts of ecological restoration on greenhouse gas emissions. *Nat. Commun*. 15, 2668. https://doi.org/10.1038/s41467-024-46991-5

Hessen, D.O., Kaartvedt, S., 2014. Top–down cascades in lakes and oceans: different perspectives but same story? *J. Plankton Res*. 36, 914–924. https://doi.org/10.1093/plankt/fbu040

Hink, L., Gubry-Rangin, C., Nicol, G.W., Prosser, J.I., 2018. The consequences of niche and physiological differentiation of archaeal and bacterial ammonia oxidisers for nitrous oxide emissions. *ISME* J. 12, 1084–1093. https://doi.org/10.1038/s41396-017-0025-5

Ho, L., Pham, K., Barthel, M., Harris, S., Bodé, S., De Vrieze, J., Vermeir, P., Six, J., Boeckx, P., Goethals, P., 2024. Unravelling CH4 and N2O dynamics in tidal wetlands using natural abundance isotopes and functional genes. *Soil Biol. Biochem.* 196, 109497. https://doi.org/10.1016/j.soilbio.2024.109497

Holmquist, J.R., Eagle, M., Molinari, R.L., Nick, S.K., Stachowicz, L.C., Kroeger, K.D., 2023. Mapping methane reduction potential of tidal wetland restoration in the United States. *Commun*. *Earth Environ*. 4, 353. https://doi.org/10.1038/s43247-023-00988-y

Hu, H.-W., Chen, D., He, J.-Z., 2015. Microbial regulation of terrestrial nitrous oxide formation: understanding the biological pathways for prediction of emission rates. *FEMS Microbiol. Rev.* 39, 729–749. https://doi.org/10.1093/femsre/fuv021

Hu, M., Chen, D., Dahlgren, R.A., 2016. Modeling nitrous oxide emission from rivers: a global assessment. *Glob. Change Biol.* 22, 3566–3582. https://doi.org/10.1111/gcb.13351

Huggett, R.D., Haigh, I.D., Purdie, D.A., 2021a. Modelling the impact of river flow, macronutrients and solar radiation on the eutrophication status of small shallow estuaries. *J. Mar. Syst.* 222, 103606. https://doi.org/10.1016/j.jmarsys.2021.103606

Huggett, R.D., Purdie, D.A., Haigh, I.D., 2021b. Modelling the Influence of Riverine Inputs on the Circulation and Flushing Times of Small Shallow Estuaries. *Estuaries Coasts* 44, 54–69. https://doi.org/10.1007/s12237-020-00776-3

Iram, N., Kavehei, E., Maher, D.T., Bunn, S.E., Rezaei Rashti, M., Farahani, B.S., Adame, M.F., 2021. Soil greenhouse gas fluxes from tropical coastal wetlands and alternative agricultural land uses. *Biogeosciences* 18, 5085–5096. https://doi.org/10.5194/bg-18-5085-2021

Jacobs, 2024. Haye Marsh Feasibility Study. National Trust.

Jähne, B., Haußecker, H., 1998. Air-Water Gas Exchange. Annu. Rev. Fluid Mech. 30, 443–468. https://doi.org/10.1146/annurev.fluid.30.1.443

Jeewani, P.H., Brown, R.W., Evans, C.D., Cook, J., Roberts, B.P., Fraser, M.D., Chadwick, D.R., Jones, D.L., 2025. Rewetting alongside biochar and sulphate addition mitigates greenhouse gas emissions and retain carbon in degraded upland peatlands. Soil Biol. Biochem. 207, 109814. https://doi.org/10.1016/j.soilbio.2025.109814

Ji, Q., Ward, B.B., 2017. Nitrous oxide production in surface waters of the mid-latitude N orth A tlantic O cean. J. Geophys. Res. Oceans 122, 2612–2621. https://doi.org/10.1002/2016JC012467

Jiang, H.-H., Sun, Z.-G., Wang, L., Mou, X.-J., Sun, W.-L., Song, H.-L., Sun, W.-G., 2012. Methane fluxes and controlling factors in the intertidal zone of the Yellow River estuary in autumn. Huan Jing Ke Xue Huanjing Kexue Bian Ji Zhongguo Ke Xue Yuan Huan Jing Ke Xue Wei Yuan Hui Huan Jing Ke Xue Bian Ji Wei Yuan Hui 33, 565–73.

Jickells, T.D., Andrews, J.E., Parkes, D.J., 2016. Direct and Indirect Effects of Estuarine Reclamation on Nutrient and Metal Fluxes in the Global Coastal Zone. Aquat. Geochem. 22, 337–348. https://doi.org/10.1007/s10498-015-9278-7

Jin, Q., Liu, H., Xu, X., Zhao, L., Chen, Liangang, Chen, Liming, Shi, R., Li, W., 2023. Emission dynamics of greenhouse gases regulated by fluctuation of water level in river-connected wetland. J. Environ. Manage. 329, 117091. https://doi.org/10.1016/j.jenvman.2022.117091

Jones, J., Börger, L., Tummers, J., Jones, P., Lucas, M., Kerr, J., Kemp, P., Bizzi, S., Consuegra, S., Marcello, L., Vowles, A., Belletti, B., Verspoor, E., Van de Bund, W., Gough, P., Garcia de Leaniz, C., 2019. A comprehensive

assessment of stream fragmentation in Great Britain. Sci. Total Environ. 673, 756–762. https://doi.org/10.1016/j.scitotenv.2019.04.125

Jonsson, A., Åberg, J., Lindroth, A., Jansson, M., 2008. Gas transfer rate and CO_2 flux between an unproductive lake and the atmosphere in northern Sweden. J. Geophys. Res. Biogeosciences 113, 2008JG000688. https://doi.org/10.1029/2008JG000688

Keenan, L.W., Lowe, E.F., 2001. Determining ecologically acceptable nutrient loads to natural wetlands for water quality improvement. Water Sci. Technol. 44, 289–294. https://doi.org/10.2166/wst.2001.0842

Kelly, C.L., Travis, N.M., Baya, P.A., Frey, C., Sun, X., Ward, B.B., Casciotti, K.L., 2024. Isotopomer labeling and oxygen dependence of hybrid nitrous oxide production. Biogeosciences 21, 3215–3238. https://doi.org/10.5194/bg-21-3215-2024

Khalil, M.A.K., Rasmussen, R.A., 1989. Climate-induced feedbacks for the global cycles of methane and nitrous oxide. Tellus B Chem. Phys. Meteorol. 41, 554. https://doi.org/10.3402/tellusb.v41i5.15111

Kirkwood, D., S., 1989. Simultaneous determination of selected nutrients in sea water (No. 29), International Council for the Exploration of the Sea (ICES) Annual Report. International Council for the Exploration of the Sea (ICES) Annual Report.

Kitidis, V., Upstill-Goddard, R., Anderson, L., 2010. Methane and Nitrous Oxide in surface water along the North-West Passage, Arctic Ocean. Mar. Chem. 80–86. https://doi.org/10.1016/j.marchem.2010.03.006

Klaus, M., Labasque, T., Botter, G., Durighetto, N., Schelker, J., 2022. Unraveling the Contribution of Turbulence and Bubbles to Air-Water Gas Exchange in Running Waters. J. Geophys. Res. Biogeosciences 127, e2021JG006520. https://doi.org/10.1029/2021JG006520

Kopf, R.K., Finlayson, C.M., Humphries, P., Sims, N.C., Hladyz, S., 2015. Anthropocene Baselines: Assessing Change and Managing Biodiversity in Human-Dominated Aquatic Ecosystems. BioScience 65, 798–811.

Kopittke, P.M., Dalal, R.C., McKenna, B.A., Smith, P., Wang, P., Weng, Z., van der Bom, F.J.T., Menzies, N.W., 2024. Soil is a major contributor to global greenhouse gas emissions and climate change. SOIL 10, 873–885. https://doi.org/10.5194/soil-10-873-2024

Kroeze, C., Seitzinger, S.P., 1998. Nitrogen inputs to rivers, estuaries and continental shelves and related nitrous oxide emissions in 1990 and 2050: a global model 18.

Kurek, M.R., Wickland, K.P., Nichols, N.A., McKenna, A.M., Anderson, S.M., Dornblaser, M.M., Koupaei-Abyazani, N., Poulin, B.A., Bansal, S., Fellman, J.B., Druschel, G.K., Bernhardt, E.S., Spencer, R.G.M., 2024. Linking Dissolved Organic Matter Composition to Landscape Properties in Wetlands Across the United States of America. Glob. Biogeochem. Cycles 38, e2023GB007917. https://doi.org/10.1029/2023GB007917

La, W., Han, X., Liu, C.-Q., Ding, H., Liu, M., Sun, F., Li, S., Lang, Y., 2022. Sulfate concentrations affect sulfate reduction pathways and methane consumption in coastal wetlands. Water Res. 217, 118441. https://doi.org/10.1016/j.watres.2022.118441

Lan, X., Thoning, K., Dlugokencky, E., NOAA Global Monitoring Laboratory, 2025. Trends in globally-averaged CH4, N2O, and SF6 determined from NOAA Global Monitoring Laboratory measurements. Version 2025-06. https://doi.org/10.15138/P8XG-AA10

Law, C.S., Rees, A.P., Owens, N.J.P., 1992. Nitrous oxide: Estuarine sources and atmospheric flux. Estuar. Coast. Shelf Sci. 35, 301–314. https://doi.org/10.1016/S0272-7714(05)80050-2

Law, C.S., Rees, A.P., Owens, N.J.P., 1991. Temporal Variability of Denitrification in Estuarine Sediments. Estuar. Coast. Shelf Sci. 37–56.

Leonardi, N., Carnacina, I., Donatelli, C., Ganju, N.K., Plater, A.J., Schuerch, M., Temmerman, S., 2018. Dynamic interactions between coastal storms and salt marshes: A review. Geomorphology 301, 92–107. https://doi.org/10.1016/j.geomorph.2017.11.001

Line, D.E., Osmond, D.L., Childres, W., 2016. Effectiveness of Livestock Exclusion in a Pasture of Central North Carolina. J. Environ. Qual. 45, 1926–1932. https://doi.org/10.2134/jeq2016.03.0089

Liu, N., Wu, Y., Liu, Z., 2025. Decline in global biodiversity intactness over the past two decades. Sci. Total Environ. 964, 178550. https://doi.org/10.1016/j.scitotenv.2025.178550

Logozzo, L.A., Soued, C., Bortolotti, L.E., Badiou, P., Kowal, P., Page, B., Bogard, M.J., 2025. Agricultural Land Use Impacts Aquatic Greenhouse Gas Emissions From Wetlands in the Canadian Prairie Pothole Region. Glob. Biogeochem. Cycles 39, e2024GB008209. https://doi.org/10.1029/2024GB008209

Lorke, A., Bodmer, P., Koca, K., Noss, C., 2019. Hydrodynamic control of gas-exchange velocity in small streams. https://doi.org/10.31223/OSF.IO/8U6VC

Lu, X., Harris, S.J., Fisher, R.E., France, J.L., Nisbet, E.G., Lowry, D., Röckmann, T., van der Veen, C., Menoud, M., Schwietzke, S., Kelly, B.F.J., 2021. Isotopic signatures of major methane sources in the coal seam gas fields and adjacent agricultural districts, Queensland, Australia. Atmospheric Chem. Phys. 21, 10527–10555. https://doi.org/10.5194/acp-21-10527-2021

Maavara, T., Chen, Q., Van Meter, K., Brown, L.E., Zhang, J., Ni, J., Zarfl, C., 2020. River dam impacts on biogeochemical cycling. Nat. Rev. Earth Environ. 1, 103–116. https://doi.org/10.1038/s43017-019-0019-0

Maavara, T., Lauerwald, R., Laruelle, G.G., Akbarzadeh, Z., Bouskill, N.J., Van Cappellen, P., Regnier, P., 2019. Nitrous oxide emissions from inland waters: Are IPCC estimates too high? Glob. Change Biol. 25, 473–488. https://doi.org/10.1111/gcb.14504

Maeck, A., DelSontro, T., McGinnis, D., Fischer, H., Flury, S., Schmidt, M., Fietzek, P., Lorke, A., 2013. Sediment Trapping by Dams Creates Methane Emission Hot Spots. Environ. Sci. Technol. 47. https://doi.org/10.1021/es4003907

Magazzino, C., Madaleno, M., Waqas, M., Leogrande, A., 2024. Exploring the determinants of methane emissions from a worldwide perspective using panel data and machine learning analyses. Environ. Pollut. 348, 123807. https://doi.org/10.1016/j.envpol.2024.123807

Mander, Ü., Espenberg, M., Melling, L., Kull, A., 2023. Peatland restoration pathways to mitigate greenhouse gas emissions and retain peat carbon. Biogeochemistry 167, 523–543. https://doi.org/10.1007/s10533-023-01103-1

Mander, Ü., Hayakawa, Y., Kuusemets, V., 2005. Purification processes, ecological functions, planning and design of riparian buffer zones in agricultural watersheds. Ecol. Eng., Riparian buffer zones in agricultural watersheds 24, 421–432. https://doi.org/10.1016/j.ecoleng.2005.01.015

Mantoura, R.F.C., Woodward, E.M.S., 1983. Optimization of the indophenol blue method for the automated determination of ammonia in estuarine waters. Estuar. Coast. Shelf Sci. 17, 219–224. https://doi.org/10.1016/0272-7714(83)90067-7

Marcé, R., Obrador, B., Gómez-Gener, L., Catalán, N., Koschorreck, M., Arce, M.I., Singer, G., von Schiller, D., 2019. Emissions from dry inland waters are a blind spot in the global carbon cycle. Earth-Sci. Rev. 188, 240–248. https://doi.org/10.1016/j.earscirev.2018.11.012

Martínez-Espinosa, C., Sauvage, S., Al Bitar, A., Green, P.A., Vörösmarty, C.J., Sánchez-Pérez, J.M., 2021. Denitrification in wetlands: A review towards a quantification at global scale. Sci. Total Environ. 754, 142398. https://doi.org/10.1016/j.scitotenv.2020.142398

Marzadri, A., Amatulli, G., Tonina, D., Bellin, A., Shen, L.Q., Allen, G.H., Raymond, P.A., 2021. Global riverine nitrous oxide emissions: The role of small streams and large rivers. Sci. Total Environ. 776, 145148. https://doi.org/10.1016/j.scitotenv.2021.145148

Mathews, R.E., Tengberg, A., Sjödin, J., Liss-Lymer, B., 2019. Implementing the source-to-sea approach: a guide for practitioners. SIWI, Stockholm.

Mayorga, E., Seitzinger, S.P., Harrison, J.A., Dumont, E., Beusen, A.H.W., Bouwman, A.F., Fekete, B.M., Kroeze, C., Van Drecht, G., 2010. Global Nutrient Export from WaterSheds 2 (NEWS 2): Model development and implementation. Environ. Model. Softw. 25, 837–853. https://doi.org/10.1016/j.envsoft.2010.01.007

McEvoy, A.J., Atkinson, A., Airs, R.L., Brittain, R., Brown, I., Fileman, E.S., Findlay, H.S., McNeill, C.L., Ostle, C., Smyth, T.J., Somerfield, P.J., Tait, K., Tarran, G.A., Thomas, S., Widdicombe, C.E., Woodward, E.M.S., Beesley, A., Conway, D.V.P., Fishwick, J., Haines, H., Harris, C., Harris, R., Hélaouët, P., Johns, D., Lindeque, P.K., Mesher, T., McQuatters-Gollop, A., Nunes, J., Perry, F., Queiros, A.M., Rees, A., Rühl, S., Sims, D., Torres, R., Widdicombe, S., 2023. The Western Channel Observatory: a century of physical, chemical and biological data compiled from pelagic

and benthic habitats in the western English Channel. Earth Syst. Sci. Data 15, 5701–5737. https://doi.org/10.5194/essd-15-5701-2023

McIlvin, M.R., Casciotti, K.L., 2010. Fully automated system for stable isotopic analyses of dissolved nitrous oxide at natural abundance levels. Limnol. Oceanogr. Methods 8, 54–66. https://doi.org/10.4319/lom.2010.8.54

Millennium Ecosystem Assessment, 2005. A Report of the Millennium Ecosystem Assessment: Ecosystems and Human Well-Being. Island Press, Washington, DC.

Minschwaner, K., Siskind, D.E., 1993. A new calculation of nitric oxide photolysis in the stratosphere, mesosphere, and lower thermosphere. J. Geophys. Res. 98, 20401. https://doi.org/10.1029/93JD02007

Moeslund, J.E., Andersen, D.K., Brunbjerg, A.K., Bruun, H.H., Fløjgaard, C., McQueen, S.N., Nygaard, B., Ejrnæs, R., 2023. High nutrient loads hinder successful restoration of natural habitats in freshwater wetlands. Restor. Ecol. 31, e13796. https://doi.org/10.1111/rec.13796

Morton, R.D., Marston, C.G., O'Neil, A.W., Rowland, C.S., 2024. Land Cover Map 2023 (10m classified pixels, GB). https://doi.org/10.5285/7727CE7D-531E-4D77-B756-5CC59FF016BD

Murray, N.J., Worthington, T.A., Bunting, P., Duce, S., Hagger, V., Lovelock, C.E., Lucas, R., Saunders, M.I., Sheaves, M., Spalding, M., Waltham, N.J., Lyons, M.B., 2022. High-resolution mapping of losses and gains of Earth's tidal wetlands. Science 376, 744–749. https://doi.org/10.1126/science.abm9583

Mwanake, R.M., Gettel, G.M., Wangari, E.G., Glaser, C., Houska, T., Breuer, L., Butterbach-Bahl, K., Kiese, R., 2023a. Anthropogenic activities significantly increase annual greenhouse gas (GHG) fluxes from temperate headwater streams in Germany. Biogeosciences 20, 3395–3422. https://doi.org/10.5194/bg-20-3395-2023

Mwanake, R.M., Gettel, G.M., Wangari, E.G., Glaser, C., Houska, T., Breuer, L., Butterbach-Bahl, K., Kiese, R., 2023b. Anthropogenic activities significantly increase annual greenhouse gas (GHG) fluxes from temperate headwater streams in Germany. Biogeosciences 20, 3395–3422. https://doi.org/10.5194/bg-20-3395-2023

National River Flow Archive, 2025a. National River Flow Archive: Station 47001 - Tamar at Gunnislake [WWW Document]. URL https://nrfa.ceh.ac.uk/data/station/meanflow/47001

National River Flow Archive, 2025b. National River Flow Archive: Station 46003 - Dart at Austins Bridge [WWW Document]. URL https://nrfa.ceh.ac.uk/data/station/meanflow/46003 (accessed 3.18.25).

Nature4Climate Coalition, 2024. A Guide for Including Nature in Nationally Determined Contributions: 2nd Edition.

Nedwell, D.B., Dong, L.F., Sage, A., Underwood, G.J.C., 2002. Variations of the Nutrients Loads to the Mainland U.K. Estuaries: Correlation with Catchment Areas, Urbanization and Coastal Eutrophication. Estuar. Coast. Shelf Sci. 54, 951–970. https://doi.org/10.1006/ecss.2001.0867

Needelman, B.A., Emmer, I.M., Emmett-Mattox, S., Crooks, S., Megonigal, J.P., Myers, D., Oreska, M.P.J., McGlathery, K., 2018. The Science and Policy of the Verified Carbon Standard Methodology for Tidal Wetland and Seagrass Restoration. Estuaries Coasts 41, 2159–2171. https://doi.org/10.1007/s12237-018-0429-0

Nesshöver, C., Assmuth, T., Irvine, K.N., Rusch, G.M., Waylen, K.A., Delbaere, B., Haase, D., Jones-Walters, L., Keune, H., Kovacs, E., Krauze, K., Külvik, M., Rey, F., van Dijk, J., Vistad, O.I., Wilkinson, M.E., Wittmer, H., 2017. The science, policy and practice of nature-based solutions: An interdisciplinary perspective. Sci. Total Environ. 579, 1215–1227. https://doi.org/10.1016/j.scitotenv.2016.11.106

Nightingale, P.D., Malin, G., Law, C.S., Watson, A.J., Liss, P.S., Liddicoat, M.I., Boutin, J., Upstill-Goddard, R.C., 2000. In situ evaluation of air-sea gas exchange parameterizations using novel conservative and volatile tracers. Glob. Biogeochem. Cycles 14, 373–387. https://doi.org/10.1029/1999GB900091

Nisbet, E.G., Dlugokencky, E.J., Manning, M.R., Lowry, D., Fisher, R.E., France, J.L., Michel, S.E., Miller, J.B., White, J.W.C., Vaughn, B., Bousquet, P., Pyle, J.A., Warwick, N.J., Cain, M., Brownlow, R., Zazzeri, G., Lanoisellé, M., Manning, A.C., Gloor, E., Worthy, D.E.J., Brunke, E.-G., Labuschagne, C., Wolff, E.W., Ganesan, A.L., 2016. Rising atmospheric methane: 2007–2014 growth and isotopic shift. Glob. Biogeochem. Cycles 30, 1356–1370. https://doi.org/10.1002/2016GB005406

NOAA, G.W., https://gml.noaa.gov/data/data.php. NOAA Global Monitoring Laboratory [WWW Document]. URL https://gml.noaa.gov/data/data.php (accessed 2.14.25).

Nummi, P., Vehkaoja, M., Pumpanen, J., Ojala, A., 2018. Beavers affect carbon biogeochemistry: both short-term and long-term processes are involved. Mammal Rev. 48, 298–311. https://doi.org/10.1111/mam.12134

Odebiri, O., Archbold, J., Glen, J., Macreadie, P.I., Malerba, M.E., 2024. Excluding livestock access to farm dams reduces methane emissions and boosts water quality. Sci. Total Environ. 951, 175420. https://doi.org/10.1016/j.scitotenv.2024.175420

O'Neill, P., 1998. Environmental Chemistry, 3rd ed. Blackie Academic & Professional, Thomson Science.

Oremland, R.S., 1979. Methanogenic activity in plankton samples and fish intestines A mechanism for in situ methanogenesis in oceanic surface waters. Limnol. Oceanogr. 24, 1136–1141. https://doi.org/10.4319/lo.1979.24.6.1136

Pal, S., Singha, P., 2023. Linking river flow modification with wetland hydrological instability, habitat condition, and ecological responses. Environ. Sci. Pollut. Res. 30, 11634–11660. https://doi.org/10.1007/s11356-022-22761-y

Paranaíba, J.R., Kosten, S., 2024. Mitigating inland waters' greenhouse gas emissions: current insights and prospects: Kilham Memorial Lecture on occasion of the 37th SIL Congress, Iguazu Falls, Brazil, 2024. Inland Waters 14, 97–110. https://doi.org/10.1080/20442041.2024.2372229

Park, J.-H., Lee, H., Zhumabieke, M., Kim, S.-H., Shin, K.-H., Khim, B.-K., 2023. Basin-specific pollution and impoundment effects on greenhouse gas distributions in three rivers and estuaries. Water Res. 236, 119982. https://doi.org/10.1016/j.watres.2023.119982

Pickard, A.E., Brown, I., Burden, A., Callaghan, N., Evans, C.D., Kitidis, V., Mayor, D., Olszewska, J., Pereira, G., Spears, B.M., Williamson, J., Woodward, M., Rees, A.P., 2022. Greenhouse gas and nutrient data measured across estuaries in the UK, 2017-2018. https://doi.org/10.5285/328CACCA-C33B-450A-A39C-302B4EED07A2

Poff, N.L., Allan, J.D., Bain, M.B., Karr, J.R., Prestegaard, K.L., Richter, B.D., Sparks, R.E., Stromberg, J.C., 1997. The Natural Flow Regime. BioScience 47, 769–784. https://doi.org/10.2307/1313099

Poffenbarger, H., Needelman, B., Megonigal, P., 2011. Salinity Influence on Methane Emissions from Tidal Marshes. Wetlands 31, 831–842. https://doi.org/10.1007/s13157-011-0197-0

Prather, M.J., Holmes, C.D., Hsu, J., 2012. Reactive greenhouse gas scenarios: Systematic exploration of uncertainties and the role of atmospheric chemistry. Geophys. Res. Lett. 39. https://doi.org/10.1029/2012GL051440

Prather, M.J., Hsu, J., DeLuca, N.M., Jackman, C.H., Oman, L.D., Douglass, A.R., Fleming, E.L., Strahan, S.E., Steenrod, S.D., Søvde, O.A., Isaksen,

I.S.A., Froidevaux, L., Funke, B., 2015. Measuring and modeling the lifetime of nitrous oxide including its variability. J. Geophys. Res. Atmospheres 120, 5693–5705. https://doi.org/10.1002/2015JD023267

Price, G., D., 2002. The distribution of trace metal pollutants within intertidal sediments of the Tamar Estuary, SW England. Geosci. South-West Engl. 10, 319–322.

Pringle, C., 2003. What is hydrologic connectivity and why is it ecologically important? Hydrol. Process. 17, 2685–2689. https://doi.org/10.1002/hyp.5145

Probst, B.S., Toetzke, M., Kontoleon, A., Díaz Anadón, L., Minx, J.C., Haya, B.K., Schneider, L., Trotter, P.A., West, T.A.P., Gill-Wiehl, A., Hoffmann, V.H., 2024. Systematic assessment of the achieved emission reductions of carbon crediting projects. Nat. Commun. 15, 9562. https://doi.org/10.1038/s41467-024-53645-z

Prosser, J.I., Hink, L., Gubry-Rangin, C., Nicol, G.W., 2020. Nitrous oxide production by ammonia oxidizers: Physiological diversity, niche differentiation and potential mitigation strategies. Glob. Change Biol. 26, 103–118. https://doi.org/10.1111/gcb.14877

Puttock, A., Graham, H.A., Ashe, J., Luscombe, D.J., Brazier, R.E., 2021. Beaver dams attenuate flow: A multi-site study. Hydrol. Process. 35, e14017. https://doi.org/10.1002/hyp.14017

Puttock, A., Graham, H.A., Carless, D., Brazier, R.E., 2018. Sediment and nutrient storage in a beaver engineered wetland. Earth Surf. Process. Landf. 43, 2358–2370. https://doi.org/10.1002/esp.4398

Que, Z., Wang, X., Liu, T., Wu, S., He, Y., Zhou, T., Yu, L., Qing, Z., Chen, H., Yuan, X., 2023. Watershed land use change indirectly dominated the spatial variations of CH4 and N2O emissions from two small suburban

rivers. J. Hydrol. 619, 129357. https://doi.org/10.1016/j.jhydrol.2023.129357

Raes, E.J., Bodrossy, L., Van De Kamp, J., Holmes, B., Hardman-Mountford, N., Thompson, P.A., McInnes, A.S., Waite, A.M., 2016. Reduction of the Powerful Greenhouse Gas N2O in the South-Eastern Indian Ocean. PLOS ONE 11, e0145996. https://doi.org/10.1371/journal.pone.0145996

Rame Head NCI, https://www.nci-ramehead.org.uk/index.html. Rame Head NCI [WWW Document]. URL https://www.nci-ramehead.org.uk/index.html (accessed 2.14.25).

Ramsar Convention on Wetlands, 2018. Global Wetland Outlook: State of the World's Wetlands and their Services to People. Ramsar Convention Secretariat, Gland, Switzerland.

Ravishankara, A.R., Daniel, J.S., Portmann, R.W., 2009. Nitrous Oxide (N2O): The Dominant Ozone-Depleting Substance Emitted in the 21st Century. Science 326, 123–125. https://doi.org/10.1126/science.1176985

Rawlins, B.G., O'Donnell, K., Ingham, M., 2003. Geochemical survey of the Tamar catchment (south-west England) (No. CR/03/027), British Geological Survey Report. Nottingham, UK, British Geological Survey.

Raymond, P.A., Cole, J.J., 2001. Gas exchange in rivers and estuaries: Choosing a gas transfer velocity. Estuaries 24, 312–317. https://doi.org/10.2307/1352954

Raymond, P.A., Zappa, C.J., Butman, D., Bott, T.L., Potter, J., Mulholland, P., Laursen, A.E., McDowell, W.H., Newbold, D., 2012. Scaling the gas transfer velocity and hydraulic geometry in streams and small rivers. Limnol. Oceanogr. Fluids Environ. 2, 41–53. https://doi.org/10.1215/21573689-1597669

Reed, D., Van Wesenbeeck, B., Herman, P.M.J., Meselhe, E., 2018. Tidal flat-wetland systems as flood defenses: Understanding biogeomorphic

controls. Estuar. Coast. Shelf Sci. 213, 269–282. https://doi.org/10.1016/j.ecss.2018.08.017

Rees, A., Gilbert, J., Kelly-Gerreyn, B., 2009. Nitrogen fixation in the western English Channel (NE Atlantic Ocean). Mar. Ecol. Prog. Ser. 374, 7–12. https://doi.org/10.3354/meps07771

Rees, A.P., Bange, H.W., Arévalo-Martínez, D.L., Artioli, Y., Ashby, D.M., Brown, I., Campen, H.I., Clark, D.R., Kitidis, V., Lessin, G., Tarran, G.A., Turley, C., 2022. Nitrous oxide and methane in a changing Arctic Ocean. Ambio 51, 398–410. https://doi.org/10.1007/s13280-021-01633-8

Rees, A.P., Brown, I.J., Jayakumar, A., Lessin, G., Somerfield, P.J., Ward, B.B., 2021. Biological nitrous oxide consumption in oxygenated waters of the high latitude Atlantic Ocean. Commun. Earth Environ. 2, 1–8. https://doi.org/10.1038/s43247-021-00104-y

Regnier, P., Friedlingstein, P., Ciais, P., Mackenzie, F.T., Gruber, N., Janssens, I.A., Laruelle, G.G., Lauerwald, R., Luyssaert, S., Andersson, A.J., Arndt, S., Arnosti, C., Borges, A.V., Dale, A.W., Gallego-Sala, A., Goddéris, Y., Goossens, N., Hartmann, J., Heinze, C., Ilyina, T., Joos, F., LaRowe, D.E., Leifeld, J., Meysman, F.J.R., Munhoven, G., Raymond, P.A., Spahni, R., Suntharalingam, P., Thullner, M., 2013. Anthropogenic perturbation of the carbon fluxes from land to ocean. Nat. Geosci. 6, 597–607. https://doi.org/10.1038/ngeo1830

Regnier, P., Resplandy, L., Najjar, R.G., Ciais, P., 2022. The land-to-ocean loops of the global carbon cycle. Nature 603, 401–410. https://doi.org/10.1038/s41586-021-04339-9

Rocher-Ros, G., Stanley, E.H., Loken, L.C., Casson, N.J., Raymond, P.A., Liu, S., Amatulli, G., Sponseller, R.A., 2023. Global methane emissions from rivers and streams. Nature 621, 530–535. https://doi.org/10.1038/s41586-023-06344-6

Rosentreter, J.A., Al-Haj, A.N., Fulweiler, R.W., Williamson, P., 2021a. Methane and Nitrous Oxide Emissions Complicate Coastal Blue Carbon Assessments. Glob. Biogeochem. Cycles 35, e2020GB006858. https://doi.org/10.1029/2020GB006858

Rosentreter, J.A., Borges, A.V., Deemer, B.R., Holgerson, M.A., Liu, S., Song, C., Melack, J., Raymond, P.A., Duarte, C.M., Allen, G.H., Olefeldt, D., Poulter, B., Battin, T.I., Eyre, B.D., 2021b. Half of global methane emissions come from highly variable aquatic ecosystem sources. Nat. Geosci. 14, 225–230. https://doi.org/10.1038/s41561-021-00715-2

Rosentreter, J.A., Laruelle, G.G., Bange, H.W., Bianchi, T.S., Busecke, J.J.M., Cai, W.-J., Eyre, B.D., Forbrich, I., Kwon, E.Y., Maavara, T., Moosdorf, N., Najjar, R.G., Sarma, V.V.S.S., Van Dam, B., Regnier, P., 2023. Coastal vegetation and estuaries are collectively a greenhouse gas sink. Nat. Clim. Change 13, 579–587. https://doi.org/10.1038/s41558-023-01682-9

Saunois, M., Martinez, A., Poulter, B., Zhang, Z., Raymond, P., Regnier, P., Canadell, J.G., Jackson, R.B., Patra, P.K., Bousquet, P., Ciais, P., Dlugokencky, E.J., Lan, X., Allen, G.H., Bastviken, D., Beerling, D.J., Belikov, D.A., Blake, D.R., Castaldi, S., Crippa, M., Deemer, B.R., Dennison, F., Etiope, G., Gedney, N., Höglund-Isaksson, L., Holgerson, M.A., Hopcroft, P.O., Hugelius, G., Ito, A., Jain, A.K., Janardanan, R., Johnson, M.S., Kleinen, T., Krummel, P., Lauerwald, R., Li, T., Liu, X., McDonald, K.C., Melton, J.R., Mühle, J., Müller, J., Murguia-Flores, F., Niwa, Y., Noce, S., Pan, S., Parker, R.J., Peng, C., Ramonet, M., Riley, W.J., Rocher-Ros, G., Rosentreter, J.A., Sasakawa, M., Segers, A., Smith, S.J., Stanley, E.H., Thanwerdas, J., Tian, H., Tsuruta, A., Tubiello, F.N., Weber, T.S., van der Werf, G., Worthy, D.E., Xi, Y., Yoshida, Y., Zhang, W., Zheng, B., Zhu, Qing, Zhu, Qiuan, Zhuang, Q., 2024a. Global

Methane Budget 2000-2020. Earth Syst. Sci. Data Discuss. 1–147. https://doi.org/10.5194/essd-2024-115

Saunois, M., Martinez, A., Poulter, B., Zhang, Z., Raymond, P., Regnier, P., Canadell, J.G., Jackson, R.B., Patra, P.K., Bousquet, P., Ciais, P., Dlugokencky, E.J., Lan, X., Allen, G.H., Bastviken, D., Beerling, D.J., Belikov, D.A., Blake, D.R., Castaldi, S., Crippa, M., Deemer, B.R., Dennison, F., Etiope, G., Gedney, N., Höglund-Isaksson, L., Holgerson, M.A., Hopcroft, P.O., Hugelius, G., Ito, A., Jain, A.K., Janardanan, R., Johnson, M.S., Kleinen, T., Krummel, P., Lauerwald, R., Li, T., Liu, X., McDonald, K.C., Melton, J.R., Mühle, J., Müller, J., Murguia-Flores, F., Niwa, Y., Noce, S., Pan, S., Parker, R.J., Peng, C., Ramonet, M., Riley, W.J., Rocher-Ros, G., Rosentreter, J.A., Sasakawa, M., Segers, A., Smith, S.J., Stanley, E.H., Thanwerdas, J., Tian, H., Tsuruta, A., Tubiello, F.N., Weber, T.S., Van Der Werf, G., Worthy, D.E., Xi, Y., Yoshida, Y., Zhang, W., Zheng, B., Zhu, Qing, Zhu, Qiuan, Zhuang, Q., 2024b. Global Methane Budget 2000–2020. https://doi.org/10.5194/essd-2024-115

Saunois, M., Stavert, A.R., Poulter, B., Bousquet, P., Canadell, J.G., Jackson, R.B., Raymond, P.A., Dlugokencky, E.J., Houweling, S., Patra, P.K., Ciais, P., Arora, V.K., Bastviken, D., Bergamaschi, P., Blake, D.R., Brailsford, G., Bruhwiler, L., Carlson, K.M., Carrol, M., Castaldi, S., Chandra, N., Crevoisier, C., Crill, P.M., Covey, K., Curry, C.L., Etiope, G., Frankenberg, C., Gedney, N., Hegglin, M.I., Höglund-Isaksson, L., Hugelius, G., Ishizawa, M., Ito, A., Janssens-Maenhout, G., Jensen, K.M., Joos, F., Kleinen, T., Krummel, P.B., Langenfelds, R.L., Laruelle, G.G., Liu, L., Machida, T., Maksyutov, S., McDonald, K.C., McNorton, J., Miller, P.A., Melton, J.R., Morino, I., Müller, J., Murguia-Flores, F., Naik, V., Niwa, Y., Noce, S., O'Doherty, S., Parker, R.J., Peng, C., Peng, S., Peters, G.P., Prigent, C., Prinn, R., Ramonet, M., Regnier, P., Riley, W.J.,

Rosentreter, J.A., Segers, A., Simpson, I.J., Shi, H., Smith, S.J., Steele, L.P., Thornton, B.F., Tian, H., Tohjima, Y., Tubiello, F.N., Tsuruta, A., Viovy, N., Voulgarakis, A., Weber, T.S., van Weele, M., van der Werf, G.R., Weiss, R.F., Worthy, D., Wunch, D., Yin, Y., Yoshida, Y., Zhang, W., Zhang, Z., Zhao, Y., Zheng, B., Zhu, Qing, Zhu, Qiuan, Zhuang, Q., 2020a. The Global Methane Budget 2000–2017. Earth Syst. Sci. Data 12, 1561–1623. https://doi.org/10.5194/essd-12-1561-2020

Saunois, M., Stavert, A.R., Poulter, B., Bousquet, P., Canadell, J.G., Jackson, R.B., Raymond, P.A., Dlugokencky, E.J., Houweling, S., Patra, P.K., Ciais, P., Arora, V.K., Bastviken, D., Bergamaschi, P., Blake, D.R., Brailsford, G., Bruhwiler, L., Carlson, K.M., Carrol, M., Castaldi, S., Chandra, N., Crevoisier, C., Crill, P.M., Covey, K., Curry, C.L., Etiope, G., Frankenberg, C., Gedney, N., Hegglin, M.I., Höglund-Isaksson, L., Hugelius, G., Ishizawa, M., Ito, A., Janssens-Maenhout, G., Jensen, K.M., Joos, F., Kleinen, T., Krummel, P.B., Langenfelds, R.L., Laruelle, G.G., Liu, L., Machida, T., Maksyutov, S., McDonald, K.C., McNorton, J., Miller, P.A., Melton, J.R., Morino, I., Müller, J., Murguia-Flores, F., Naik, V., Niwa, Y., Noce, S., O'Doherty, S., Parker, R.J., Peng, C., Peng, S., Peters, G.P., Prigent, C., Prinn, R., Ramonet, M., Regnier, P., Riley, W.J., Rosentreter, J.A., Segers, A., Simpson, I.J., Shi, H., Smith, S.J., Steele, L.P., Thornton, B.F., Tian, H., Tohjima, Y., Tubiello, F.N., Tsuruta, A., Viovy, N., Voulgarakis, A., Weber, T.S., van Weele, M., van der Werf, G.R., Weiss, R.F., Worthy, D., Wunch, D., Yin, Y., Yoshida, Y., Zhang, W., Zhang, Z., Zhao, Y., Zheng, B., Zhu, Qing, Zhu, Qiuan, Zhuang, Q., 2020b. The Global Methane Budget 2000–2017. Earth Syst. Sci. Data 12, 1561–1623. https://doi.org/10.5194/essd-12-1561-2020

Schuwerack, P.-M.M., Neal, M., Neal, C., 2007. The Dart estuary, Devon, UK: a case study of chemical dynamics and pollutant mobility. Hydrol. Earth Syst. Sci. 11, 382–398. https://doi.org/10.5194/hess-11-382-2007

Seddon, N., Daniels, E., Davis, R., Chausson, A., Harris, R., Hou-Jones, X., Huq, S., Kapos, V., Mace, G.M., Rizvi, A.R., Reid, H., Roe, D., Turner, B., Wicander, S., 2020. Global recognition of the importance of nature-based solutions to the impacts of climate change. Glob. Sustain. 3, e15. https://doi.org/10.1017/sus.2020.8

Seitzinger, S.P., Mayorga, E., Bouwman, A.F., Kroeze, C., Beusen, A.H.W., Billen, G., Van Drecht, G., Dumont, E., Fekete, B.M., Garnier, J., Harrison, J.A., 2010. Global river nutrient export: A scenario analysis of past and future trends. Glob. Biogeochem. Cycles 24. https://doi.org/10.1029/2009GB003587

Sela-Adler, M., Ronen, Z., Herut, B., Antler, G., Vigderovich, H., Eckert, W., Sivan, O., 2017. Co-existence of Methanogenesis and Sulfate Reduction with Common Substrates in Sulfate-Rich Estuarine Sediments. Front. Microbiol. 8, 766. https://doi.org/10.3389/fmicb.2017.00766

Shakhova, N., Semiletov, I., Chuvilin, E., 2019. Understanding the Permafrost–Hydrate System and Associated Methane Releases in the East Siberian Arctic Shelf. Geosciences 9, 251. https://doi.org/10.3390/geosciences9060251

Shakhova, N., Semiletov, I., Salyuk, A., Yusupov, V., Kosmach, D., Gustafsson, O., 2010. Extensive methane venting to the atmosphere from sediments of the East Siberian Arctic Shelf. Science 327, 1246–1250. https://doi.org/10.1126/science.1182221

Shindell, D., Kuylenstierna, J.C.I., Vignati, E., van Dingenen, R., Amann, M., Klimont, Z., Anenberg, S.C., Muller, N., Janssens-Maenhout, G., Raes, F., Schwartz, J., Faluvegi, G., Pozzoli, L., Kupiainen, K., Höglund-Isaksson,

L., Emberson, L., Streets, D., Ramanathan, V., Hicks, K., Oanh, N.T.K., Milly, G., Williams, M., Demkine, V., Fowler, D., 2012. Simultaneously Mitigating Near-Term Climate Change and Improving Human Health and Food Security. Science 335, 183–189. https://doi.org/10.1126/science.1210026

Shukla, P.R., Skea, J., Calvo Buendia, E., Masson-Delmotte, V., Pörtner, H.-O., Roberts, D.C., Zhai, P., Slade, R., Connors, S., van Diemen, R., Ferrat, M., Haughey, E., Luz, S., Neogi, S., Pathak, M., Petzold, J., Portugal Pereira, J., Vyas, P., Huntley, E., Kissick, K., Belkacemi, M., Malley, J. (Eds.), 2019. Climate Change and Land: an IPCC special report on climate change, desertification, land degradation, sustainable land management, food security, and greenhouse gas fluxes in terrestrial ecosystems. Intergovernmental Panel on Climate Change (IPCC).

Simenstad, C., Reed, D., Ford, M., 2006. When is restoration not? Ecol. Eng. 26, 27–39. https://doi.org/10.1016/j.ecoleng.2005.09.007

Sivan, O., Shusta, S.S., Valentine, D.L., 2016. Methanogens rapidly transition from methane production to iron reduction. Geobiology 14, 190–203. https://doi.org/10.1111/gbi.12172

Smith, C.S., Serra, L., Li, Y., Inglett, P., Inglett, K., 2011. Restoration of Disturbed Lands: The Hole-in-the-Donut Restoration in the Everglades. Crit. Rev. Environ. Sci. Technol. 41, 723–739. https://doi.org/10.1080/10643389.2010.530913

Smith, H.B., Vaughan, N.E., Forster, J., 2024. Residual emissions in long-term national climate strategies show limited climate ambition. One Earth 7, 867–884. https://doi.org/10.1016/j.oneear.2024.04.009

Smith, H.B., Vaughan, N.E., Forster, J., 2022. Long-term national climate strategies bet on forests and soils to reach net-zero. Commun. Earth Environ. 3, 305. https://doi.org/10.1038/s43247-022-00636-x

Smith, H.G., Blake, W.H., 2014. Sediment fingerprinting in agricultural catchments: A critical re-examination of source discrimination and data corrections. Geomorphology 204, 177–191. https://doi.org/10.1016/j.geomorph.2013.08.003

Smith, P., Adams, J., Beerling, D.J., Beringer, T., Calvin, K.V., Fuss, S., Griscom, B., Hagemann, N., Kammann, C., Kraxner, F., Minx, J.C., Popp, A., Renforth, P., Vicente Vicente, J.L., Keesstra, S., 2019. Land-Management Options for Greenhouse Gas Removal and Their Impacts on Ecosystem Services and the Sustainable Development Goals. Annu. Rev. Environ. Resour. 44, 255–286. https://doi.org/10.1146/annurev-environ-101718-033129

Soued, C., Bogard, M.J., Finlay, K., Bortolotti, L.E., Leavitt, P.R., Badiou, P., Knox, S.H., Jensen, S., Mueller, P., Lee, S.C., Ng, D., Wissel, B., Chan, C.N., Page, B., Kowal, P., 2024. Salinity causes widespread restriction of methane emissions from small inland waters. Nat. Commun. 15, 717. https://doi.org/10.1038/s41467-024-44715-3

South West Water, 2023. Tamar exc Wider Plymouth Level 2 Drainage and Wastewater Management Plan.

Stafford, R., Chamberlain, B., Clavey, L., Gillingham, P.K., McKain, S., Morecroft, M.D., Morrison-Bell, C., Watts, O. (Eds.), 2021. Nature-based Solutions for Climate Change in the UK: A Report by the British Ecological Society. British Ecological Society, London, UK.

Stanley, E.H., Casson, N.J., Christel, S.T., Crawford, J.T., Loken, L.C., Oliver, S.K., 2016. The ecology of methane in streams and rivers: patterns, controls, and global significance. Ecol. Monogr. 86, 146–171. https://doi.org/10.1890/15-1027

Stanley, E.H., Casson, N.J., Christel, S.T., Crawford, J.T., Loken, L.C., Oliver, S.K., 2015. The ecology of methane in streams and rivers: patterns,

controls, and global significance. Ecol. Monogr. 86, 146–171. https://doi.org/10.1890/15-1027

Stein, L.Y., Klotz, M.G., 2016. The nitrogen cycle. Curr. Biol. 26, R94–R98. https://doi.org/10.1016/j.cub.2015.12.021

Storch, L.C., Schulz, K., Kraft, J.M., Prochnow, A., Ruess, L., Trost, B., Theuerl, S., 2023. Nitrifier denitrification potentially dominates N_2 O production in a sandy soil – results from different fertilization and irigation regimes in potato cropping in Germany. https://doi.org/10.5194/egusphere-2023-2277

Stutter, M.I., Graeber, D., Evans, C.D., Wade, A.J., Withers, P.J.A., 2018. Balancing macronutrient stoichiometry to alleviate eutrophication. Sci. Total Environ. 634, 439–447. https://doi.org/10.1016/j.scitotenv.2018.03.298

Syakila, A., Kroeze, C., 2011. The global nitrous oxide budget revisited. Greenh. Gas Meas. Manag. 1, 17–26. https://doi.org/10.3763/ghgmm.2010.0007

Taillardat, P., Thompson, B.S., Garneau, M., Trottier, K., Friess, D.A., 2020. Climate change mitigation potential of wetlands and the cost-effectiveness of their restoration. Interface Focus 10, 20190129. https://doi.org/10.1098/rsfs.2019.0129

Tamar Valley National Landscape, 2024. Tamar Valley Nature Recovery Plan 2023–2030. Tamar Valley National Landscape, Devon & Cornwall, United Kingdom.

Tan, L., Ge, Z., Ji, Y., Lai, D.Y.F., Temmerman, S., Li, S., Li, X., Tang, J., 2022. Land use and land cover changes in coastal and inland wetlands cause soil carbon and nitrogen loss. Glob. Ecol. Biogeogr. 31, 2541–2563. https://doi.org/10.1111/geb.13597

Tan, L., Ge, Z., Zhou, X., Li, S., Li, X., Tang, J., 2020. Conversion of coastal wetlands, riparian wetlands, and peatlands increases greenhouse gas

emissions: A global meta-analysis. Glob. Change Biol. 26, 1638–1653. https://doi.org/10.1111/gcb.14933

Temmink, R.J.M., Lamers, L.P.M., Angelini, C., Bouma, T.J., Fritz, C., van de Koppel, J., Lexmond, R., Rietkerk, M., Silliman, B.R., Joosten, H., van der Heide, T., 2022. Recovering wetland biogeomorphic feedbacks to restore the world's biotic carbon hotspots. Science 376, eabn1479. https://doi.org/10.1126/science.abn1479

Thom, T.J., Doar, N., 2021. Quantifying the Potential Impact of Nature Based Solutions on Greenhouse Gas Emissions from UK Habitats. The Wildlife Trusts, Newark, UK.

Tian, H., Pan, N., Thompson, R.L., Canadell, J.G., Suntharalingam, P., Regnier, P., Davidson, E.A., Prather, M., Ciais, P., Muntean, M., Pan, S., Winiwarter, W., Zaehle, S., Zhou, F., Jackson, R.B., Bange, H.W., Berthet, S., Bian, Z., Bianchi, D., Bouwman, A.F., Buitenhuis, E.T., Dutton, G., Hu, M., Ito, A., Jain, A.K., Jeltsch-Thömmes, A., Joos, F., Kou-Giesbrecht, S., Krummel, P.B., Lan, X., Landolfi, A., Lauerwald, R., Li, Y., Lu, C., Maavara, T., Manizza, M., Millet, D.B., Mühle, J., Patra, P.K., Peters, G.P., Qin, X., Raymond, P., Resplandy, L., Rosentreter, J.A., Shi, H., Sun, Q., Tonina, D., Tubiello, F.N., van der Werf, G.R., Vuichard, N., Wang, J., Wells, K.C., Western, L.M., Wilson, C., Yang, J., Yao, Y., You, Y., Zhu, Q., 2024. Global nitrous oxide budget (1980–2020). Earth Syst. Sci. Data 16, 2543–2604. https://doi.org/10.5194/essd-16-2543-2024

Tian, H., Xu, R., Canadell, J.G., Thompson, R.L., Winiwarter, W., Suntharalingam, P., Davidson, E.A., Ciais, P., Jackson, R.B., Janssens-Maenhout, G., Prather, M.J., Regnier, P., Pan, N., Pan, S., Peters, G.P., Shi, H., Tubiello, F.N., Zaehle, S., Zhou, F., Arneth, A., Battaglia, G., Berthet, S., Bopp, L., Bouwman, A.F., Buitenhuis, E.T., Chang, J., Chipperfield, M.P., Dangal, S.R.S., Dlugokencky, E., Elkins, J.W., Eyre,

B.D., Fu, B., Hall, B., Ito, A., Joos, F., Krummel, P.B., Landolfi, A., Laruelle, G.G., Lauerwald, R., Li, W., Lienert, S., Maavara, T., MacLeod, M., Millet, D.B., Olin, S., Patra, P.K., Prinn, R.G., Raymond, P.A., Ruiz, D.J., van der Werf, G.R., Vuichard, N., Wang, J., Weiss, R.F., Wells, K.C., Wilson, C., Yang, J., Yao, Y., 2020. A comprehensive quantification of global nitrous oxide sources and sinks. Nature 586, 248–256. https://doi.org/10.1038/s41586-020-2780-0

Tian, L., Cai, Y., Akiyama, H., 2019. A review of indirect N2O emission factors from agricultural nitrogen leaching and runoff to update of the default IPCC values. Environ. Pollut. 245, 300–306. https://doi.org/10.1016/j.envpol.2018.11.016

Tian, W., Wu, X., Zhao, X., Ma, R., Zhang, B., 2019. Quantifying global CH4 and N2O footprints. J. Environ. Manage. 251, 109566. https://doi.org/10.1016/j.jenvman.2019.109566

Tong, C., Wang, W.-Q., Zeng, C.-S., Marrs, R., 2010. Methane (CH4) emission from a tidal marsh in the Min River estuary, southeast China. J. Environ. Sci. Health Part A 45, 506–516. https://doi.org/10.1080/10934520903542261

Treby, S., Carnell, P., 2023. Impacts of feral grazers and unseasonal summer flooding on floodplain carbon dynamics: A case study. Ecohydrol. Hydrobiol. 23, 186–197. https://doi.org/10.1016/j.ecohyd.2022.12.007

Trimmer, M., Chronopoulou, P.-M., Maanoja, S.T., Upstill-Goddard, R.C., Kitidis, V., Purdy, K.J., 2016. Nitrous oxide as a function of oxygen and archaeal gene abundance in the North Pacific. Nat. Commun. 7, 13451. https://doi.org/10.1038/ncomms13451

Tye, A., Balfour, C., Bowes, M., Brown, I., Evans, C., Farr, G., Felgate, S., Hargreaves, G., Kitidis, V., Lapworth, D.J., Martin, A., Mayor, D.J., Mounteney, I., Nightingale, P., Pickard, A., Sanders, R., Spears, B.,

Stephens, J., Stinchcombe, M., Torres, R., Williams, P., Williamson, J., Woodward, M., Boothroyd, I., Breimann, S., Burden, A., Callaghan, N., Gilbert, P., Ives, S., Juergens, M., Keenan, P., Hughes, L., Lichtschlag, A., Mack, S., Mallin Martin, D., Mawji, E., McDonald, R., Olszewska, J., Parkes, D., Pearce, C., Peel, K., Perreira, G., Pugh, J., Rees, A., White, D., Worrall, F., Yarrow, D., 2020. Monthly sampling of riverine chemistry and organic matter for 41 rivers in Great Britain in 2017 as part of the LOCATE project. https://doi.org/10.5285/08223CDD-5E01-43AD-840D-15FF81E58ACF

Tye, A.M., Jarvie, H.P., Spears, B.M., Dise, N.B., Williamson, J.L., Lapworth, D.J., Monteith, D., Sanders, R., Mayor, D.J., Bowes, M.J., Bowes, M., Burden, A., Callaghan, N., Farr, G., Felgate, S., Gibb, S., Gilbert, P., Hargreaves, G., Humphrey, O.S., Keenan, P., Kitidis, V., Jürgens, M.D., Martin, A., Pearson, M., Nightingale, P.D., Gloria Pereira, M., Olszewska, J., Pickard, A., Rees, A.P., Stinchcombe, M., Worrall, F., Evans, C.D., 2024. Riverine concentrations and export of dissolved silicon, and potential controls on nutrient stoichiometry, across the land–ocean continuum in Great Britain. J. Hydrol. 640, 131738. https://doi.org/10.1016/j.jhydrol.2024.131738

UK Gov, 2024. The Nature Recovery Network - GOV.UK [WWW Document]. URL https://www.gov.uk/government/publications/nature-recovery-network/nature-recovery-network (accessed 6.3.25).

UK Government, 2025. United Kingdom of Great Britain and Northern Ireland's 2035 Nationally Determined Contribution (NDC). HH Associates Ltd.

UK National Ecosystem Assessment, 2011. The UK National Ecosystem Assessment: Synthesis of the Key Findings. UNEP-WCMC, Cambridge.

UKGOV, 2025. New world-leading nature finance standards launched to encourage green investment - GOV.UK [WWW Document]. URL

https://www.gov.uk/government/news/new-world-leading-nature-finance-standards-launched-to-encourage-green-investment (accessed 3.28.25).

Uncles, R.J., Bale, A.J., Brinsley, M.D., Frickers, P.E., Harris, C., Lewis, R.E., Pope, N.D., Staff, F.J., Stephens, J.A., Turley, C.M., Widdows, J., 2003. Intertidal mudflat properties, currents and sediment erosion in the partially mixed Tamar Estuary, UK. Ocean Dyn. 53, 239–251. https://doi.org/10.1007/s10236-003-0047-6

Uncles, R.J., Fraser, A.I., Butterfield, D., Johnes, P., Harrod, T.R., 2002. The prediction of nutrients into estuaries and their subsequent behaviour: application to the Tamar and comparison with the Tweed, U.K., in: Orive, E., Elliott, M., de Jonge, V.N. (Eds.), Nutrients and Eutrophication in Estuaries and Coastal Waters: Proceedings of the 31st Symposium of the Estuarine and Coastal Sciences Association (ECSA), Held in Bilbao, Spain, 3–7 July 2000. Springer Netherlands, Dordrecht, pp. 239–250. https://doi.org/10.1007/978-94-017-2464-7_21

Uncles, R.J., Stephens, J.A., 2010. Turbidity and sediment transport in a muddy sub-estuary. Estuar. Coast. Shelf Sci., MECHANISMS OF SEDIMENT RETENTION IN ESTUARIES 87, 213–224. https://doi.org/10.1016/j.ecss.2009.03.041

Uncles, R.J., Stephens, J.A., 1993. Nature of the Turbidity Maximum in the Tamar Estuary, U.K. Estuar. Coast. Shelf Sci. 36, 413–431. https://doi.org/10.1006/ecss.1993.1025

Uncles, R.J., Torres, R., 2013. Estimating dispersion and flushing time-scales in a coastal zone: Application to the Plymouth area. Ocean Coast. Manag. 72, 3–12. https://doi.org/10.1016/j.ocecoaman.2011.09.013

Upadhyay, P., Prajapati, S.K., Kumar, A., 2023. Impacts of riverine pollution on greenhouse gas emissions: A comprehensive review. Ecol. Indic. 154, 110649. https://doi.org/10.1016/j.ecolind.2023.110649

Upstill-Goddard, R., Barnes, J., Frost, T., Punshon, S., Owens, N., 2000. Methane in the Southern North Sea: Low salinity inputs, estuarine removal and atmospheric flux. Glob. Biogeochem. Cycles 14, 1205–1217. https://doi.org/10.1029/1999GB001236

Upstill-Goddard, R.C., Barnes, J., 2016. Methane emissions from UK estuaries: Re-evaluating the estuarine source of tropospheric methane from Europe. Mar. Chem. 180, 14–23. https://doi.org/10.1016/j.marchem.2016.01.010

Upstill-Goddard, R.C., Rees, A.P., Owens, N.J.P., 1996. Simultaneous high-precision measurements of methane and nitrous oxide in water and seawater by single phase equilibration gas chromatography. Deep Sea Res. Part Oceanogr. Res. Pap. 43, 1669–1682. https://doi.org/10.1016/S0967-0637(96)00074-X

Verstraete, W., Philips, S., 1998. Nitrification–denitrification processes and technologies in new contexts, in: Van der Hoek, K.W., Erisman, J.W., Smeulders, S., Wisniewski, J.R., Wisniewski, J. (Eds.), Nitrogen, the Confer-N-s. Elsevier, Amsterdam, pp. 717–726. https://doi.org/10.1016/B978-0-08-043201-4.50102-7

Vymazal, J., 2010. Constructed Wetlands for Wastewater Treatment. Water 2, 530–549. https://doi.org/10.3390/w2030530

Wallin, M.B., Öquist, M.G., Buffam, I., Billett, M.F., Nisell, J., Bishop, K.H., 2011. Spatiotemporal variability of the gas transfer coefficient (K_{CO2}) in boreal streams: Implications for large scale estimates of CO_2 evasion: VARIABILITY OF K_{CO2} IN BOREAL STREAMS. Glob. Biogeochem. Cycles 25, n/a-n/a. https://doi.org/10.1029/2010GB003975

Wang, Z., Chan, F.K.S., Feng, M., Johnson, M.F., 2024. Greenhouse gas emissions from hydropower reservoirs: emission processes and management approaches. Environ. Res. Lett. 19, 073002. https://doi.org/10.1088/1748-9326/ad560c

Wang, Z., Sadat-Noori, M., Glamore, W., 2022. Groundwater discharge drives water quality and greenhouse gas emissions in a tidal wetland. Water Sci. Eng. 15, 141–151. https://doi.org/10.1016/j.wse.2022.02.005

Wanninkhof, R., 2014. Relationship between wind speed and gas exchange over the ocean revisited. Limnol. Oceanogr. Methods 12, 351–362. https://doi.org/10.4319/lom.2014.12.351

Wanninkhof, R., Asher, W.E., Ho, D.T., Sweeney, C., McGillis, W.R., 2009. Advances in Quantifying Air-Sea Gas Exchange and Environmental Forcing. Annu. Rev. Mar. Sci. 1, 213–244. https://doi.org/10.1146/annurev.marine.010908.163742

Ward, N.D., Bianchi, T.S., Medeiros, P.M., Seidel, M., Richey, J.E., Keil, R.G., Sawakuchi, H.O., 2017. Where Carbon Goes When Water Flows: Carbon Cycling across the Aquatic Continuum. Front. Mar. Sci. 4. https://doi.org/10.3389/fmars.2017.00007

Webb, J.R., Hayes, N.M., Simpson, G.L., Leavitt, P.R., Baulch, H.M., Finlay, K., 2019. Widespread nitrous oxide undersaturation in farm waterbodies creates an unexpected greenhouse gas sink. Proc. Natl. Acad. Sci. U. S. A. 116, 9814–9819. https://doi.org/10.1073/pnas.1820389116

Weiss, R.F., Price, B.A., 1980. Nitrous oxide solubility in water and seawater. Mar. Chem. 8, 347–359. https://doi.org/10.1016/0304-4203(80)90024-9

Wickham, H., Averick, M., Bryan, J., Chang, W., McGowan, L., François, R., Grolemund, G., Hayes, A., Henry, L., Hester, J., Kuhn, M., Pedersen, T., Miller, E., Bache, S., Müller, K., Ooms, J., Robinson, D., Seidel, D., Spinu, V., Takahashi, K., Vaughan, D., Wilke, C., Woo, K., Yutani, H., 2019. Welcome to the Tidyverse. J. Open Source Softw. 4, 1686. https://doi.org/10.21105/joss.01686

Wiesenburg, D.A., Guinasso, N.L.Jr., 1979. Equilibrium solubilities of methane, carbon monoxide, and hydrogen in water and sea water. J. Chem. Eng. Data 24, 356–360. https://doi.org/10.1021/je60083a006

Williams, P., Biggs, J., Stoate, C., Szczur, J., Brown, C., Bonney, S., 2020. Nature based measures increase freshwater biodiversity in agricultural catchments. Biol. Conserv. 244, 108515. https://doi.org/10.1016/j.biocon.2020.108515

Winslow, L.A., Zwart, J.A., Batt, R.D., Dugan, H.A., Woolway, R.I., Corman, J.R., Hanson, P.C., Read, J.S., 2016. LakeMetabolizer: an R package for estimating lake metabolism from free-water oxygen using diverse statistical models. Inland Waters 6, 622–636. https://doi.org/10.1080/IW-6.4.883

Wood, K.A., Jupe, L.L., Aguiar, F.C., Collins, A.M., Davidson, S.J., Freeman, W., Kirkpatrick, L., Lobato-de Magalhães, T., McKinley, E., Nuno, A., Pagès, J.F., Petruzzella, A., Pritchard, D., Reeves, J.P., Thomaz, S.M., Thornton, S.A., Yamashita, H., Newth, J.L., 2024. A global systematic review of the cultural ecosystem services provided by wetlands. Ecosyst. Serv. 70, 101673. https://doi.org/10.1016/j.ecoser.2024.101673

Woodrow, R., White, S., 2023. Enhanced stream greenhouse gas emissions at night and during flood events. https://doi.org/10.6084/M9.FIGSHARE.24439210.V1

Wrage-Mönnig, N., Horn, M.A., Well, R., Müller, C., Velthof, G., Oenema, O., 2018. The role of nitrifier denitrification in the production of nitrous oxide revisited. Soil Biol. Biochem. 123, A3–A16. https://doi.org/10.1016/j.soilbio.2018.03.020

Wu, H., Zhang, J., Ngo, H.H., Guo, W., Hu, Z., Liang, S., Fan, J., Liu, H., 2015. A review on the sustainability of constructed wetlands for wastewater

treatment: Design and operation. Bioresour. Technol. 175, 594–601. https://doi.org/10.1016/j.biortech.2014.10.068

Wu, S., Wang, X., Liu, T., He, Y., Que, Z., Wang, J., Li, H., Yu, L., Zhang, Y., Yuan, X., 2021. Spatiotemporal Variability of the Nitrous Oxide Concentrations and Fluxes From a Cascaded Dammed River. Front. Environ. Sci. 9. https://doi.org/10.3389/fenvs.2021.728489

Wu, Y., Sun, J., Hu, B., Zhang, G., Rousseau, A.N., 2023. Wetland-based solutions against extreme flood and severe drought: Efficiency evaluation of risk mitigation. Clim. Risk Manag. 40, 100505. https://doi.org/10.1016/j.crm.2023.100505

Wurtsbaugh, W.A., Paerl, H.W., Dodds, W.K., 2019. Nutrients, eutrophication and harmful algal blooms along the freshwater to marine continuum. WIREs Water 6, e1373. https://doi.org/10.1002/wat2.1373

Xenopoulos, M.A., Downing, J.A., Kumar, M.D., Menden-Deuer, S., Voss, M., 2017. Headwaters to oceans: Ecological and biogeochemical contrasts across the aquatic continuum. Limnol. Oceanogr. 62, S3–S14. https://doi.org/10.1002/lno.10721

Xing, C.-Y., Li, H., Li, Q., Lu, L.-H., Li, Z., 2023. Shifts in composition and function of bacterial communities reveal the effect of small barriers on nitrous oxide and methane accumulation in fragmented rivers. Front. Microbiol. 14, 1110025. https://doi.org/10.3389/fmicb.2023.1110025

Yan, W., Yang, L., Wang, F., Wang, J., Ma, P., 2012. Riverine N2O concentrations, exports to estuary and emissions to atmosphere from the Changjiang River in response to increasing nitrogen loads. Glob. Biogeochem. Cycles 26. https://doi.org/10.1029/2010GB003984

Yang, H., Tang, J., Zhang, C., Dai, Y., Zhou, C., Xu, P., Perry, D.C., Chen, X., 2020. Enhanced Carbon Uptake and Reduced Methane Emissions in a

Newly Restored Wetland. J. Geophys. Res. Biogeosciences 125, e2019JG005222. https://doi.org/10.1029/2019JG005222

Yang, M., Bell, T.G., Hopkins, F.E., Kitidis, V., Cazenave, P.W., Nightingale, P.D., Yelland, M.J., Pascal, R.W., Prytherch, J., Brooks, I.M., Smyth, T.J., 2016. Air–sea fluxes of CO_2 and CH_4 from the Penlee Point Atmospheric Observatory on the south-west coast of the UK. Atmospheric Chem. Phys. 16, 5745–5761. https://doi.org/10.5194/acp-16-5745-2016

Yang, W., Hall, S., McNicol, G., 2021. Global gases. pp. 557–579. https://doi.org/10.1016/B978-0-12-820202-9.00020-4

Yi, Q., Huixin, G., Yaomin, Z., Jinlian, S., Xingyu, Z., Huize, Y., Jiaxin, W., Zhenguo, N., Liping, L., Shudong, W., Tianjie, Z., Yue, C., Zongming, W., Dehua, M., Mingming, J., Ke, G., Peng, G., Guofa, C., Xiankai, H., 2024. Global conservation priorities for wetlands and setting post-2025 targets. Commun. Earth Environ. 5, 4. https://doi.org/10.1038/s43247-023-01195-5

Yoshida, T., Alexander, M., 1970. Nitrous Oxide Formation by Nitrosomonas Europaea and Heterotrophie Microorganisms. Soil Sci. Soc. Am. J. 34, 880–882. https://doi.org/10.2136/sssaj1970.03615995003400060020x

Zedler, J.B., Callaway, J.C., 1999. Tracking Wetland Restoration: Do Mitigation Sites Follow Desired Trajectories? Restor. Ecol. 7, 69–73. https://doi.org/10.1046/j.1526-100X.1999.07108.x

Zhang, J.-Z., Chi, J., 2002. Automated Analysis of Nanomolar Concentrations of Phosphate in Natural Waters with Liquid Waveguide. Environ. Sci. Technol. 36, 1048–1053. https://doi.org/10.1021/es011094v

Zhang, X., Ward, B.B., Sigman, D.M., 2020. Global Nitrogen Cycle: Critical Enzymes, Organisms, and Processes for Nitrogen Budgets and Dynamics. Chem. Rev. 120, 5308–5351. https://doi.org/10.1021/acs.chemrev.9b00613

Zhao, M., Han, G., Li, J., Song, W., Qu, W., Eller, F., Wang, J., Jiang, C., 2020. Responses of soil CO2 and CH4 emissions to changing water table level in a coastal wetland. J. Clean. Prod. 269, 122316. https://doi.org/10.1016/j.jclepro.2020.122316

Zhao, Y., Saunois, M., Bousquet, P., Lin, X., Berchet, A., Hegglin, M.I., Canadell, J.G., Jackson, R.B., Hauglustaine, D.A., Szopa, S., Stavert, A.R., Abraham, N.L., Archibald, A.T., Bekki, S., Deushi, M., Jöckel, P., Josse, B., Kinnison, D., Kirner, O., Marécal, V., O'Connor, F.M., Plummer, D.A., Revell, L.E., Rozanov, E., Stenke, A., Strode, S., Tilmes, S., Dlugokencky, E.J., Zheng, B., 2019. Inter-model comparison of global hydroxyl radical (OH) distributions and their impact on atmospheric methane over the 2000–2016 period. Atmospheric Chem. Phys. 19, 13701–13723. https://doi.org/10.5194/acp-19-13701-2019

Zhu, L., Wang, Z., Shu, Q., Takala, J., Hiltunen, E., Feng, P., Yuan, Z., 2013. Nutrient removal and biodiesel production by integration of freshwater algae cultivation with piggery wastewater treatment. Water Res. 47, 4294–4302. https://doi.org/10.1016/j.watres.2013.05.004

Zou, J., Ziegler, A.D., Chen, D., McNicol, G., Ciais, P., Jiang, X., Zheng, C., Wu, Jie, Wu, Jin, Lin, Z., He, X., Brown, L.E., Holden, J., Zhang, Z., Ramchunder, S.J., Chen, A., Zeng, Z., 2022. Rewetting global wetlands effectively reduces major greenhouse gas emissions. Nat. Geosci. 15, 627–632. https://doi.org/10.1038/s41561-022-00989-0

Zu Ermgassen, S.O.S.E., Hawkins, I., Lundhede, T., Liu, Q., Thorsen, B.J., Bull, J.W., 2025. The current state, opportunities and challenges for upscaling private investment in biodiversity in Europe. Nat. Ecol. Evol. 9, 515–524. https://doi.org/10.1038/s41559-024-02632-0

Appendix A: Chapter 1 Supplementary Information

Web of Science search criteria for Figure 1.2:

CH_4

Query link: https://www.webofscience.com/wos/alldb/summary/3a440ee0-6212-4f72-b31e-a4ea66e90f5f-01695957d1/relevance/1

Query text: (methane OR CH4) AND (concentration* OR emission* OR flux* OR efflux) AND (river* OR stream* OR lake* OR wetland* OR soil* OR estuary* OR freshwater* OR coastal* OR forest* OR grassland*) NOT ("fossil fuel" OR landfill OR combustion OR "natural gas" OR oil OR wastewater)

N_2O

Query link: https://www.webofscience.com/wos/alldb/summary/a9e05ada-b8f7-4bb2-8ef2-3d53f502e662-0169595d94/relevance/1

Query text: (nitrous oxide OR N2O) AND (concentration* OR emission* OR flux* OR efflux) AND (river* OR stream* OR lake* OR wetland* OR soil* OR estuary* OR freshwater* OR coastal* OR forest* OR grassland*) NOT ("fossil fuel" OR landfill OR combustion OR "natural gas" OR oil OR wastewater)

Appendix B: Chapter 4 Supplementary Information

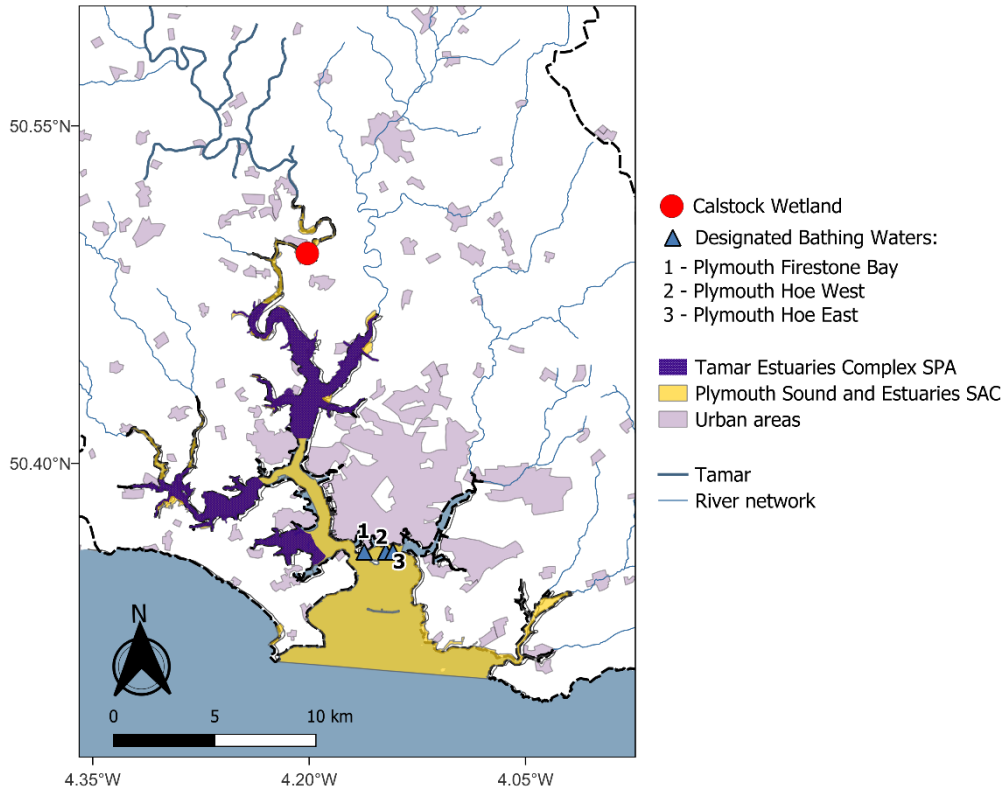

Figure S1. Location of protected areas in Tamar Estuary, downstream of Calstock Wetland

Appendix C: Research dissemination

I am grateful to have had the opportunity to share my research through a rich experience of summer schools, conferences, workshops and placements throughout my PhD.

Awards:

PlyMSEF travel bursary

Summer Schools:

2022 DARE-UK & CLASS International Summer School on Global Greenhouse Gases, Southampton

2022 River Collective Students for Rivers Camp, Austria

Conferences:

PlyMSEF 2022 ‘Greenhouse Gases in River Catchments to Coastal Seas’ (Oral presentation)

ASLO 2023 ‘A meeting of waters: river to coast biogeochemical controls of climate told from the hydrological perspective of a greenhouse gas’ (Poster)

ASLO 2024 ‘Monitoring biogeochemical and hydrological dynamics in a newly created intertidal wetland: implications for greenhouse gas fluxes and mitigation strategies’ (Oral presentation)

Challenger Society 2024 ‘Nitrous Oxide (N_2O) and Methane (CH_4) Dynamics in the Tamar and Dart Estuaries (Poster)

Workshops:

PML Science to Impact Challenge Areas (StIC): ‘Monitoring the effectiveness of intertidal wetland restoration for climate change mitigation’ (Oral presentation)

Educational outreach and media:

Contribution to The Box Museum ‘Marine Citizens of Plymouth’s National Marine Park’ Climate Change Teachers Learning Resource

Mentored MSc student undertaking research on beaver wetland dynamics at Plymouth Marine Laboratory

Directed the River Collective Students for Rivers Camp focusing on river-to-coast environmental pressures facing the River Dart

Production of public newsletter on Calstock environmental monitoring